RATE-DECLINE RELATIONS FOR UNCONVENTIONAL RESERVOIRS AND DEVELOPMENT OF PARAMETRIC CORRELATIONS FOR ESTIMATION OF RESERVOIR PROPERTIES

A Thesis

by

YOHANES AKLILU ASKABE

Submitted to the Office of Graduate Studies of
Texas A&M University
in partial fulfillment of the requirements for the degree of

MASTER OF SCIENCE

Approved by:

Chair of Committee,	Thomas A. Blasingame
Committee Members,	Maria A. Barrufet
	Walter B. Ayers, Jr.
Head of Department,	Daniel Hill

December 2012

Major Subject: Petroleum Engineering

ABSTRACT

Time-rate analysis and time-rate-pressure analysis methods are available to estimate reserves and study flow performance of wells in unconventional gas reservoirs. However, these tools are often incorrectly used or the analysis can become difficult because of the complex nature of the reservoir system. Conventional methods (*e.g.,* Arps' time-rate relations) are often used incorrectly to estimate reserves from such reservoirs. It was only recently that a serious study was conducted to outline the limitations of these relations and to set guidelines for their correct application. New time-rate relations, particularly the Duong and logistic growth model, were introduced to estimate reserves and forecast production from unconventional reservoirs. These new models are being used with limited understanding of their characteristics and limitations. Moreover, well performance analyses using analytical/semi-analytical solutions (time-rate-pressure) are often complicated from non-uniqueness that arises when estimating well/formation properties.

In this work, we present a detailed study of the Duong model and logistic growth model to investigate the behaviors and limitations of these models when analyzing production data from unconventional reservoirs. We consider production data generated from numerical simulation cases and data obtained from unconventional gas reservoirs to study the quality of match to specific flow regimes and compare accuracy of the reserve estimates. We use the power-law exponential model (PLE), which has been shown to model transient, transition and boundary-dominated flow regimes reliably, as a benchmark to study performance of Duong and logistic growth models. Moreover, we use the "continuous *EUR*" approach to compare these models during reserve estimation. Finally, we develop four new time-rate relations, based on characteristics of the time-rate data on diagnostic plots. Using diagnostic plots we show that the new time-rate relations provide a quality match to the production data across all flow regimes, leading to a reliable reserve estimate.

In a preliminary study, we integrated time-rate model parameters with fundamental reservoir properties (*i.e.*, fracture conductivity (F_c) and 30 year *EUR* (EUR_{30yr})), by studying 15 numerical simulation cases to yield parametric correlations. We have demonstrated a methodology to integrate time-rate model parameters and reservoir properties. This method avoids the non-uniqueness issues often associated with model-based production data analysis. This study provides theoretical basis for further demonstration of the methodology using field cases.

DEDICATION

I dedicate this work to my family.

ACKNOWLEDGEMENTS

I would like to thank, Dr. Blasingame, chair of my committee, for his constant support and guidance to perfection, Dave Symmons for his unyielding technical assistance, Dilhan Ilk for his crucial suggestions and advice, Viannet Okouma for his encouragement and guidance and Dr. Ayers and Dr. Barrufet for their support and for their service as committee members.

TABLE OF CONTENTS

LIST OF FIGURES

FIGURE Page

FIGURE Page

FIGURE Page

LIST OF TABLES

CHAPTER I

INTRODUCTION

1.1 Statement of the Problem

The discovery of significant unconventional gas reserves and the advent of new technologies, specifically, horizontal completion and hydraulic fracturing, have opened up vast natural gas resources for economic development. Unconventional gas resources currently account for about 40 percent (7.5 Tcf per year) of the total U.S natural gas production, and its contribution is expected to grow to more than half of the total U.S natural gas production by 2030 (8.0 Tcf per year) (EIA, 2007). The increasing interest in these unconventional gas resources (tight gas, coal bed methane (CBM), and shale gas) requires careful consideration in order to produces these resources successfully and economically.

Analytical production analysis techniques have been developed to study flow performance of wells in unconventional reservoirs. From rigorous analysis of rate and pressure data, it is possible to estimate reservoir properties and fracture characteristics. However these analyses are often difficult because of the non-uniqueness of the well and formation estimates. On the other hand, simple empirical relations are used widely to estimate reserves from oil and gas reservoirs. Specifically Arps' time-rate relations have been adapted to estimate reserves from unconventional reservoirs. However, incorrect application of Arps' rate decline models to match the long transient flow regime that is observed from unconventional reservoirs result in reserve estimates exceeding 100 percent (Rushing et al. 2007). Modern time-rate relations (Ilk et al. 2008b; Valko 2009) have been shown to model the long transient flow regimes accurately.

In this work, we consider modern time-rate models including the power law exponential (PLE), Duong and the logistic growth model to study their performance in modeling production data obtained from unconventional reservoirs. We present a study of field data as well as numerical simulation cases. Also, we demonstrate their performance in reserve estimation using the "continuous *EUR*" (Currie et al. 2010) approach. Finally we develop new time-rate relations based on the Duong and logistic growth models and show that the new models are superior at matching the transient, transition and boundary-dominated flow regimes.

In addition, we present a preliminary study to integrate time-rate model parameters with fundamental reservoir properties (*i.e.*, fracture conductivity (F_c) and 30 year *EUR* (EUR_{30yr})) using parametric correlations. Previously, Ilk et al. (2011) have shown that it is possible to correlate reservoir/well properties that are estimated using model-based production data analysis with parameters of the power-law

exponential (PLE) time-rate relation by using a limited number of wells from tight/shale gas reservoirs. From that study it was apparent that synthetic data cases are required to obtain a more rigorous (perhaps semi-analytical) correlation for the estimation of well/reservoir properties. We present production data analysis of 15 numerical simulation cases using power law exponential model, Duong and logistic growth models. This analysis provides theoretical basis to the work done by Ilk et al. (2011). Then, we demonstrate the relationship between the reservoir parameters and the time-rate model parameters using simple parametric functions. Finally, we show that reservoir properties (F_c and EUR_{30yr}) can be estimated from time-rate model parameters using parametric correlations. The ease of use of the time-rate relations helps reduce the amount of time required during model based production data analysis. Also, this method avoids the non-uniqueness issue often associated with model based production data analysis.

1.2 Objectives

The objectives of this work are to:

- Perform a diagnostic plot analysis of Duong and logistic growth model to investigate the short-term and long-term behavior of these models.
- Compare the match quality and reliability of reserve estimates using the PLE model as a benchmark.
- Develop new time-rate relations based on diagnostic behavior of the time-rate data to improve the quality of match and reliability of reserve estimates of Duong and logistic growth models.
- Develop a methodology for integration of reservoir/well properties — specifically, to demonstrate the correlation of fracture conductivity and 30 year *EUR* estimate (EUR_{30yr}) with time-rate model parameters, using production data generated from numerical simulation models.

1.3 Importance

This work outlines advantages and limitations of logistic growth and Duong models when used to analyze production data from unconventional reservoirs. We showed that these models misrepresented characteristics of the time-rate data observed on diagnostic plots (*i.e. D*-, *b*-parameter and $\not\beta$-derivative versus time plots). We have used the PLE model as a benchmark to compare the performance of these models when matching the transient, transition and boundary-dominated flow regimes.

Moreover, we have demonstrated application of the "continuous *EUR*" approach to investigate reliability of the reserve estimates obtained from Duong and logistic growth models. We have also compared the rate of convergence of *EUR* estimated using these models.

We have demonstrated that diagnostic functions are valuable to emphasize characteristics of the time-rate data that are not evident otherwise. Based on diagnostic properties of the time-rate data we have modified the Duong and logistic growth model to develop four new relations that conform to the observed diagnostic behaviors of the time-rate data. We have shown that these new models have a superior match quality across all flow regimes and provide a reliable reserve estimate compared to the Duong and logistic growth models.

Our methodology to estimate fundamental reservoir properties using the time-rate model parameters is an attempt to connect results from time-rate analysis with results from model-based production data analysis as a possible correlation mechanism to estimate reservoir properties. Using simulated data cases, this study provides a theoretical basis for further demonstration of the methodology using field cases.

1.4 Validation and Application

Here, we demonstrate a performance analysis of Duong, logistic growth, PLE as well as the newly derived models using a numerical simulation case. We perform a model match on a diagnostic plot and compare the *EUR* estimated using these models. Finally we will introduce the parametric correlation study.

1.4.1 Numerical Simulation Case: East Texas Tight Gas Well

We are considering a numerical simulation of a vertical well model producing through a single vertical fracture with finite conductivity in a tight gas reservoir. The model input parameters are provided in **Table 1.1.** The historical flow rate and cumulative production data is shown in **Fig. 1.1.**

Table 1.1 — Reservoir and fluid properties for numerical simulation case (vertical tight gas well with hydraulic fractures).

Reservoir Properties:		
Wellbore radius, r_w	=	0.333 ft
Net pay thickness, h	=	170 ft
Average porosity, ϕ	=	0.088 (fraction)
Permeability, k	=	0.005 md
Fluid Properties:		
Gas viscosity at p_i, μ_g	=	0.0361 cp
Gas compressibility at p_i, c_{gi}	=	5×10^{-5} psi^{-1}
Production Parameters:		
Initial reservoir pressure, p_i	=	9,330 psia
Gas production after 30 years, $G_{p,30\,yr}$	=	2.42 BSCF
Original gas in place, *OGIP*	=	2.65 BSCF

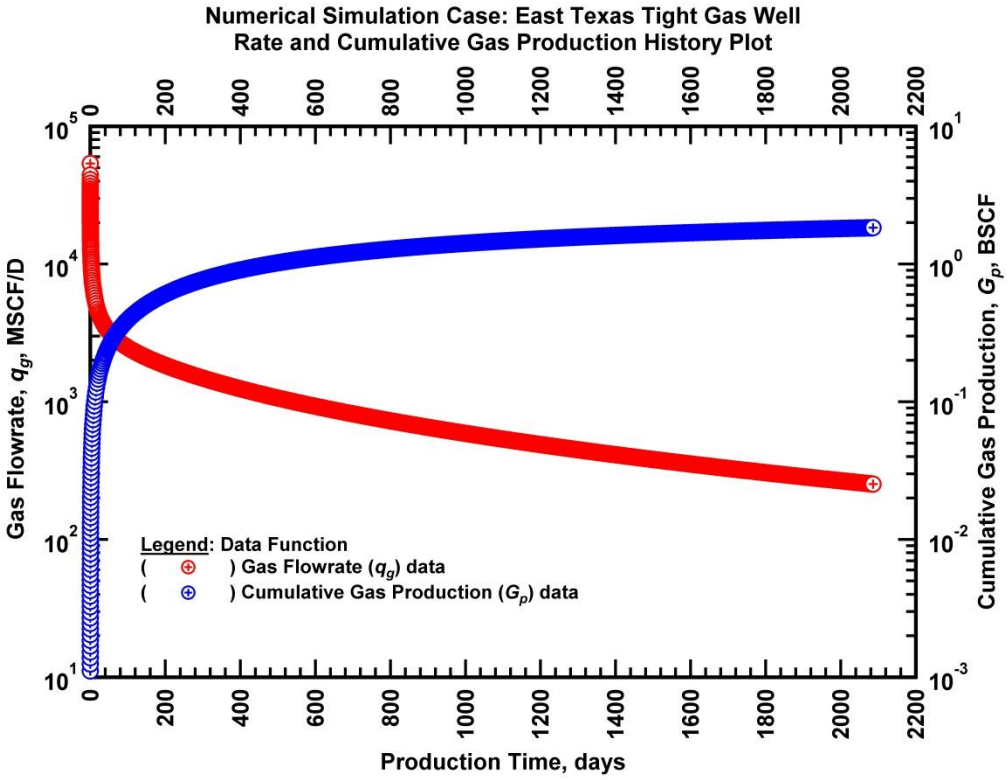

Figure 1.1 — (Semi-log Plot): Production history plot for numerical simulation case – flow rate (q_g) and cumulative production (G_p) versus production time (East Tx tight gas well numerical simulation model).

We use the *D*-, *b*-parameter and β-derivative of the data to diagnose and match all flow regimes as accurately as possible. These diagnostic functions are defined as follows:

$$D = -\frac{1}{q(t)}\frac{dq(t)}{dt} \qquad (D\text{-parameter}) \ldots\ldots (1.1)$$

$$b = -\frac{d}{dt}\left[\frac{q(t)}{dq(t)/dt}\right] \qquad (b\text{-parameter}) \ldots\ldots (1.2)$$

$$\beta = -\frac{t}{q(t)}\frac{dq(t)}{dt} \qquad (\beta\text{-derivative}) \ldots\ldots (1.3)$$

Table 1.2 summarizes the time-rate models studied in this work. The table also shows the newly derived time-rate relations.

Table 1.2 — PLE, Duong, logistic growth model and newly derived time-rate relations.

Time-Rate Relations	*Models*
Power-Law Exponential Model	$q(t) = \hat{q}_{gi} \exp[-D_{\infty} t - \hat{D}_i t^n]$
Duong Model	$q(t) = q_1 t^{-m} \exp\left[\frac{a}{1-m}(t^{1-m} - 1)\right]$, q_1 at $t = 1$
Logistic Growth Model	$q(t) = \frac{\hat{a}K\hat{n}t^{\hat{n}-1}}{(\hat{a} + t^{\hat{n}})^2}$
New Time-Rate Relations	***Models***
Modified Duong Model – 1 (MDNG – 1)	$q(t) = q_{t_1}\left(\frac{t_1}{t}\right)^m \exp[\frac{a}{1-m}(t^{1-m} - t_1^{1-m}) - D_{DNG}(t - t_1)]$
Modified Duong Model – 2 (MDNG – 2)	$q(t) = q_{t_1}\left(\frac{t_1}{t^m}\right)^m \exp\left[\frac{D_{DNG}(t_1 - t) + aD_{DNG}^{m-1}}{\left(\Gamma[1-m, D_{DNG}t_1] - \Gamma[1-m, D_{DNG}t]\right)}\right]$
Modified Logistic Growth Model – 1 (MLGM – 1)	$q(t) = \frac{\hat{a}K\hat{n}t^{(\hat{n}-1)}}{(\hat{a} + t^{\hat{n}})^2}\exp[-D_{LGM}t]$
Modified Logistic Growth Model – 2 (MLGM – 2)	$q(t) = \frac{\hat{a}\exp[D_{LGM}t]Kt^{\hat{n}-1}(\hat{n} + D_{LGM}t)}{\left(\hat{a} + (1+R)\exp[D_{LGM}t]t^{\hat{n}}\right)^2}$

First we consider MDNG – 1 and MLGM – 1 cases since these both rely on the *D*-parameter diagnostic plot for their derivation. First, the linear flow regime is matched by setting the constant decline parameters (D_{DNG} and D_{LGM}) to zero. After matching the observed transient flow regime, the constant decline parameters are adjusted to match the boundary-dominated flow regime. However, this boundary characteristic is not available in Duong and logistic growth models. **Table 1.3** shows the model match parameters for MDNG – 1 and MLGM – 1.

Table 1.3 — MDNG – 1 and MLGM – 1 model parameters for numerical simulation case (East Tx tight gas well).

Modified Duong Model (MDNG – 1)

q_{t1}=0.0042 day (MSCFD)	a	m	D_{Dng} (D^{-1})
49,277	0.72	1.03	0.0004

Modified Logistic Growth Model (MLGM – 1)

K (MSCF)	$\hat{a}$	$\hat{n}$	D_{LGM} (D^{-1})
4,075,259	230.24	0.7	0.00015

Next we match the data using MDNG – 2 model. In this analysis, the model parameters are determined on a *q/Gp* versus production time log-log plot. On this plot, the transient flow regime is indicated by a straight line with a negative slope whereas the boundary-dominated flow regime shows a sharper decline deviating from the straight line trend. **Fig. 1.2** shows *q/Gp* versus time diagnostic plot. The transient flow regime is matched first by adjusting the "*a*" and "*m*" parameters of Duong and MDNG – 2 models. Then, the boundary-dominated flow regime is matched by adjusting the "D_{DNG}" parameter of MDNG – 2. As mentioned earlier Duong model lacks this boundary characteristic.

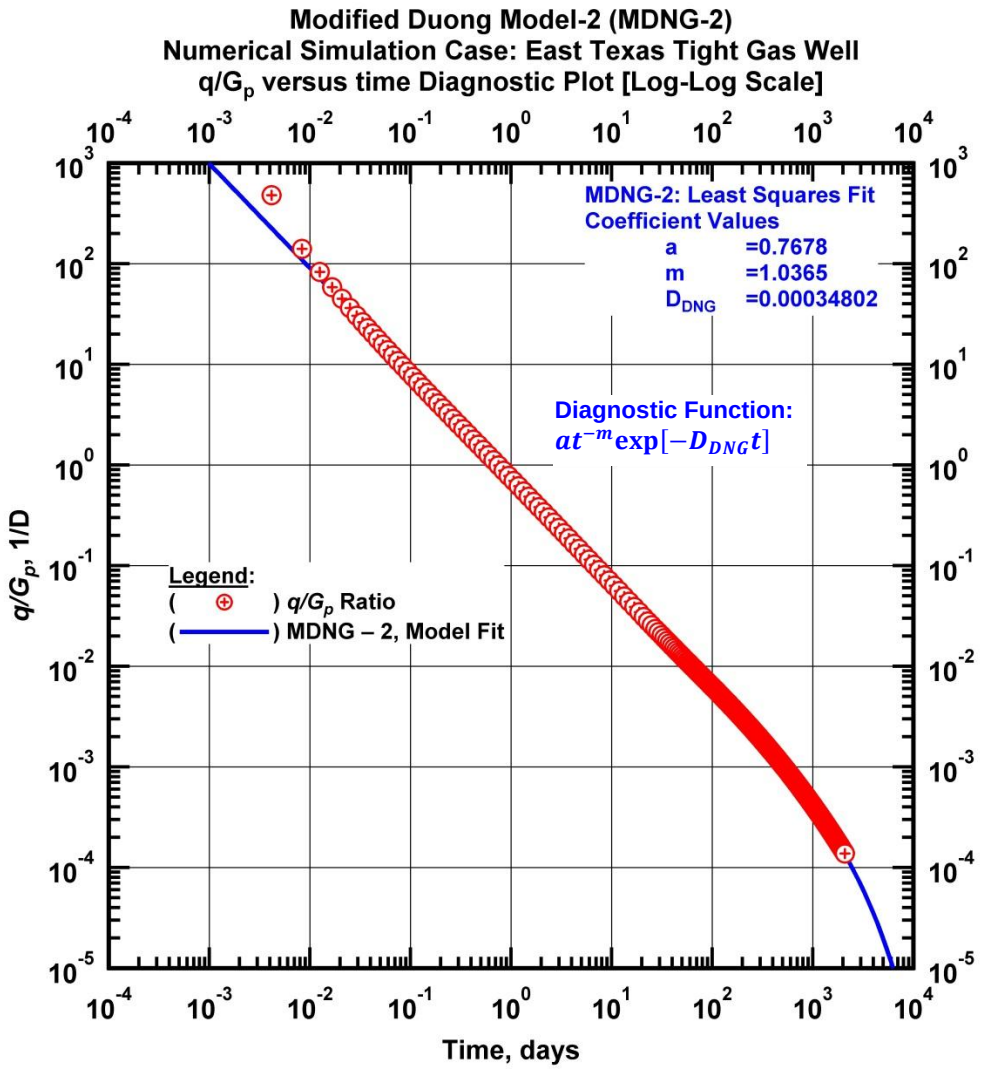

Figure 1.2 — (Log-log Plot): q/G_p versus production time. Duong model and Modified Duong Model (MDNG – 2) matches for numerical simulation case (East Tx tight gas well).

Table 1.4 — MDNG – 2 model parameters for numerical simulation case (East Tx tight gas well).

Modified Duong Model (MDNG – 2)			
$q_{t1=0.0042\ day}$ (MSCFD)	a	m	D_{Dng} (D^{-1})
49,277	0.768	1.04	0.00036

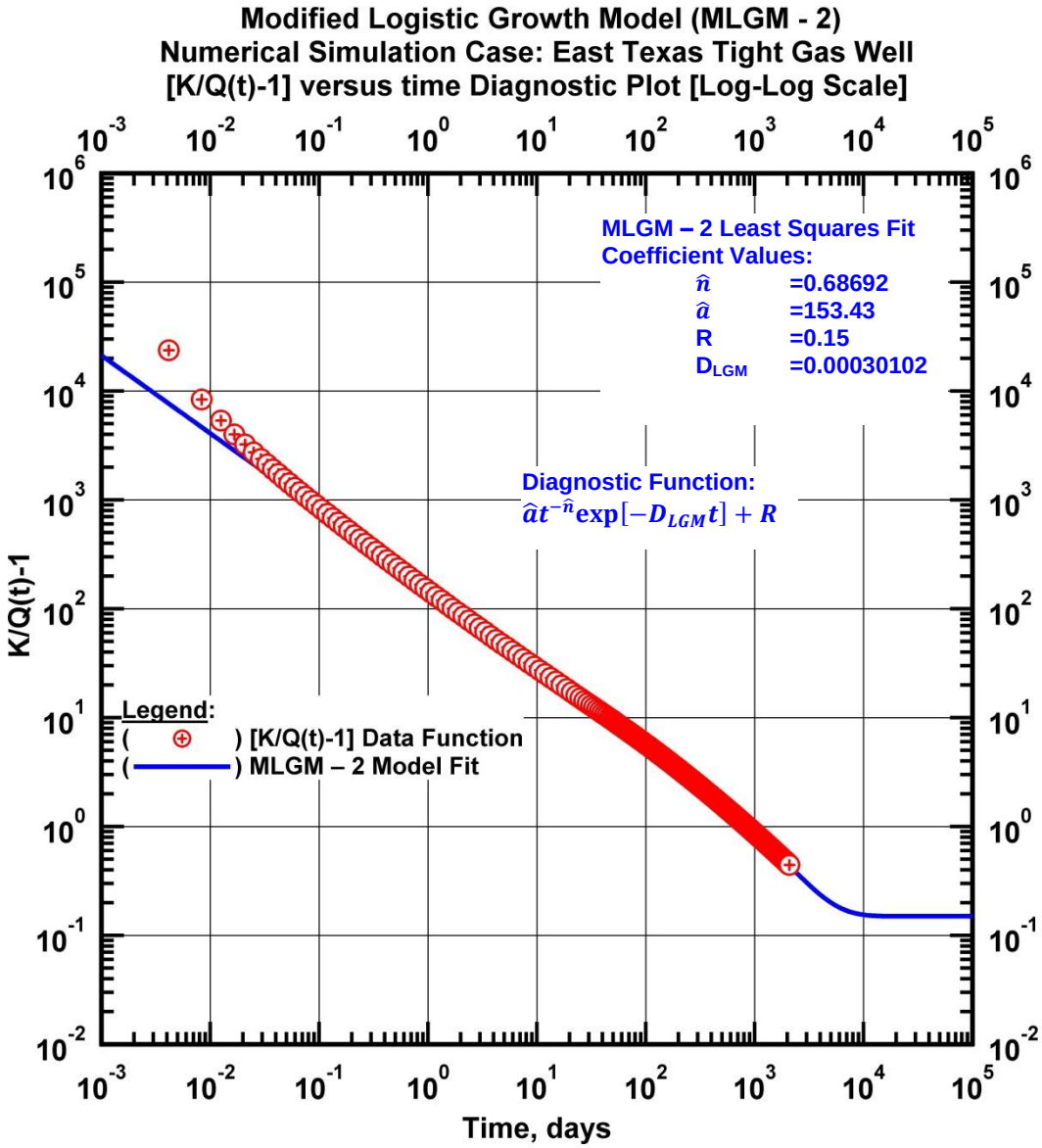

Figure 1.3 — (Log-log Plot): K/G_p – 1 versus production time. Modified Logistic Growth Model (MLGM – 2) matches for numerical simulation case (East Tx tight gas well).

The model parameter q_{t1} is then estimated by fixing the remaining parameters and matching the data manually or through regression to obtain a fit to the time-rate data. In this case q_{t1} is estimated at t_1=0.0043 days. This approach is the simplest way to obtain the model parameters. It is also possible to estimate the model parameters of MDNG – 2 using the time-rate relation shown in Table 1.2, if advanced computation tools are available. The model parameters are summarized in **Table 1.4.**

Next we match the data using MLGM – 2. In this case, the model parameters are estimated on plot of *K/Q* – 1 versus *time* plot. In this case prior estimate of *K* (initial gas in place) was available from volumetric calculations. **Fig. 1.3** shows the diagnostic plot necessary to evaluate the model parameters.

If the initial gas in place is known with confidence, all the unknown parameters can be estimated from the *K/Q* – 1 versus *time* diagnostic plot. The model parameters for MLGM – 2 are summarized in **Table 1.5**.

Table 1.5 — MLGM – 2 model parameters for numerical simulation case (East Tx tight gas well).

Modified Duong Model (MLGM – 2)

K *MSCF*	$\hat{a}$	$\hat{n}$	D_{LGM} (D^{-1})
2.65E+06	153.4	0.68	0.00030

Fig. 1.4 shows model matches for all the models on a flowrate, *D*-, *b*- parameter and β-derivative plot. The PLE and the newly derived relations were able to provide a quality match across all flow regimes. Duong and logistic growth model failed to match the later flow periods. The diagnostic functions clearly indicate that these models lack the characteristics to model boundary conditions.

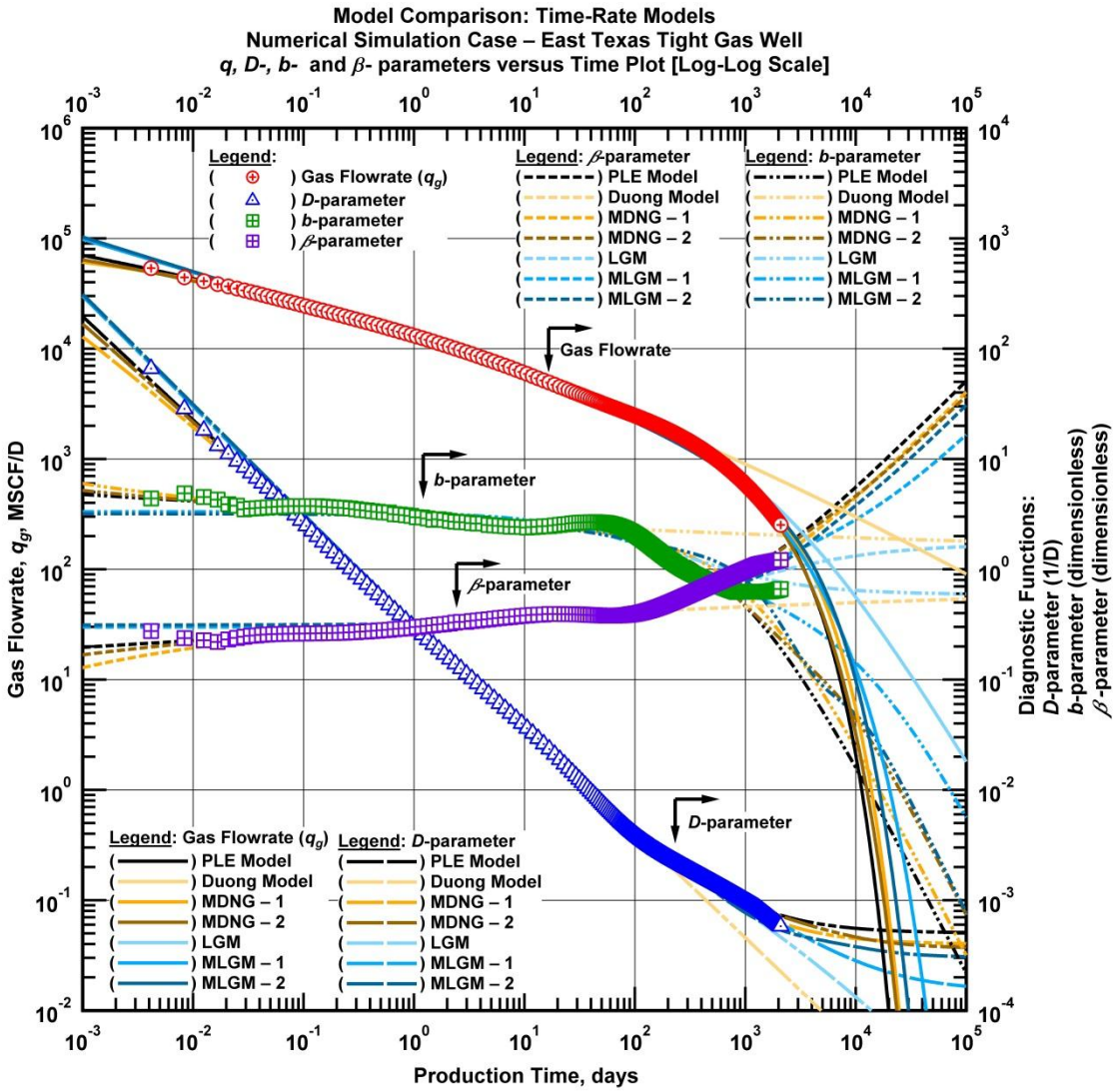

Figure 1.4 — (Log-log Plot): Flow rate (q_g), *D*-, *b*-parameter and β-derivative versus production time. PLE, logistic growth, Duong, MLGM – 1, MLGM – 2, MDNG – 1, and MDNG – 2 time-rate model matches for numerical simulation case (East Texas tight gas well).

Fig. 1.5 shows model match on the historical rate and cumulative production data. The modified relations were able to match the early time data as well as late time boundary-dominated flow regimes successfully. However; both Duong and logistic growth models are not constrained. As a result, reserves are overestimated.

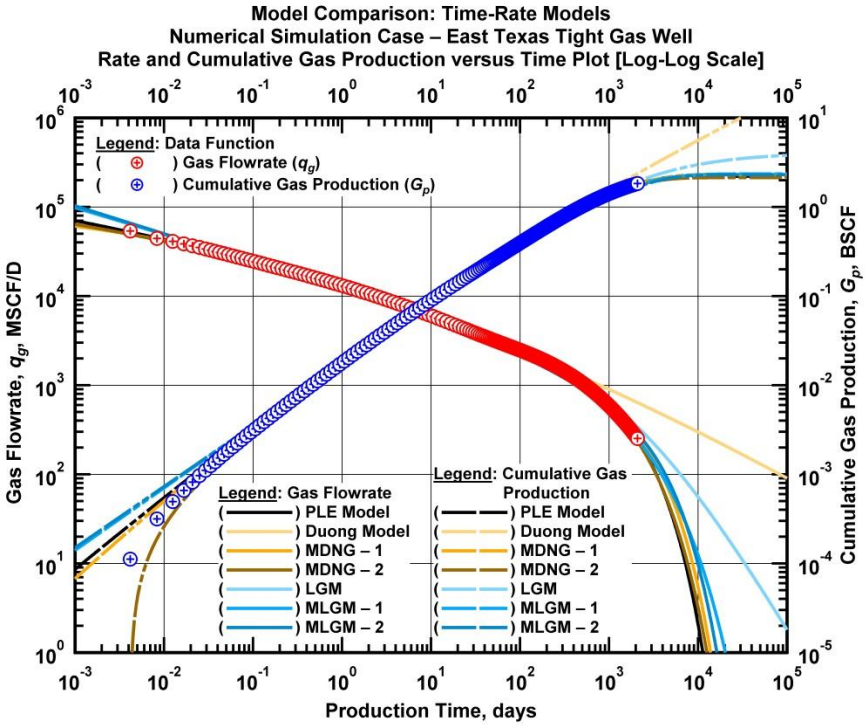

Figure 1.5 — (Log-log Plot): Rate and cumulative production versus time plot. PLE, logistic growth, Duong, MLGM – 1, MLGM – 2, MDNG – 1, and MDNG – 2 time-rate models matches for numerical simulation case (East Tx tight gas well).

Table 1.6 shows the cumulative production calculated at the end of the 6 years of production. Duong and logistic growth models have significantly overestimated the cumulative production. PLE and the modified relations have provided a reliable estimate of the cumulative production at the end of the flow period.

Table 1.6 — Comparison of calculated cumulative production values for East Texas tight gas well numerical simulation model. ($G_{p,max}$ = 1.82 BSCF from numerical simulation.)

Time-rate models	$G_{p,max}$
Duong model	2.37 BSCF
Logistic growth model	1.95 BSCF
Power-law exponential model (PLE)	1.84 BSCF
Modified Duong Model – 1 (MDNG – 1)	1.80 BSCF
Modified Duong Model – 2 (MDNG – 2)	1.79 BSCF
Modified Logistic Growth Model – 1 (MLGM – 1)	1.77 BSCF
Modified Logistic Growth Model – 2 (MLGM – 2)	1.78 BSCF

The performance of the time-rate models in estimating reserves was further investigated using the "continuous *EUR*" approach. **Fig. 1.6** shows results of the calculated *EUR* values versus production time based on the model matches obtained using PLE, Duong and logistic growth models. The *EUR* values calculated using the PLE model decrease significantly during early time and approach the maximum cumulative production faster than the other models. As expected, the Duong and logistic growth models overestimate the cumulative production.

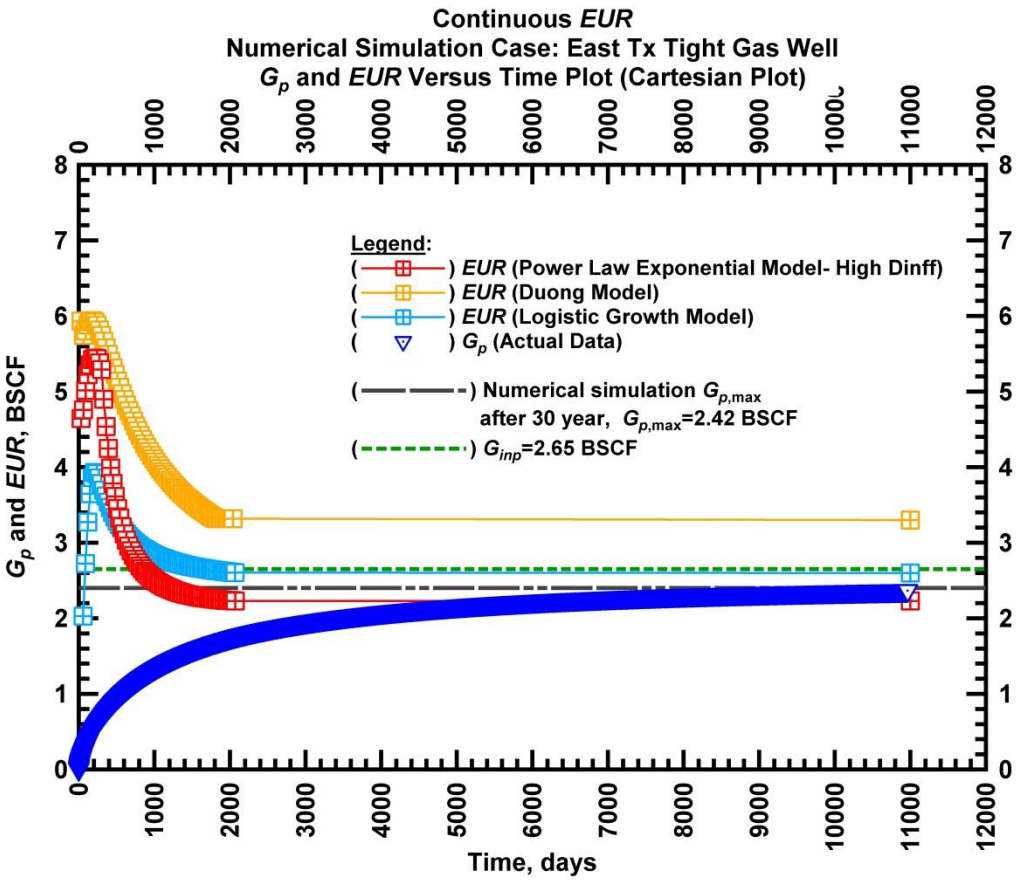

Figure 1.6 — (Cartesian Plot): *EUR* estimates from PLE, logistic growth, and Duong model matches and $G_{p,max}$ projected from numerical simulation case (East Texas tight gas well).

1.4.2 A Parametric Correlation Study

Here, we present a theoretical consideration to integrate time-rate model parameters with fundamental reservoir properties through parametric correlations. Our first task is to identify the relationship between each of the model parameters with reservoir properties. In this study, we considered only fracture

conductivity (F_c) and 30 year *EUR* estimates. Once we identified the relationship between the time-rate model parameters and the reservoir properties, we developed a parametric correlation to estimate the reservoir properties directly from the time-rate model parameters. **Fig. 1.7** shows result of parametric correlation study developed to estimate fracture conductivity from time-rate model parameters. The correlating function given by:

$$F_C = 1E-07 n^{1.7} \hat{D}_i^{4E-08} \hat{q}_i^{1.6} \quad \text{.....(1.4)}$$

Using this correlation, we can estimate fracture conductivity of wells that are producing with similar bottomhole pressure and production constrains from the time-rate model parameters obtained after matching the production data using the PLE model.

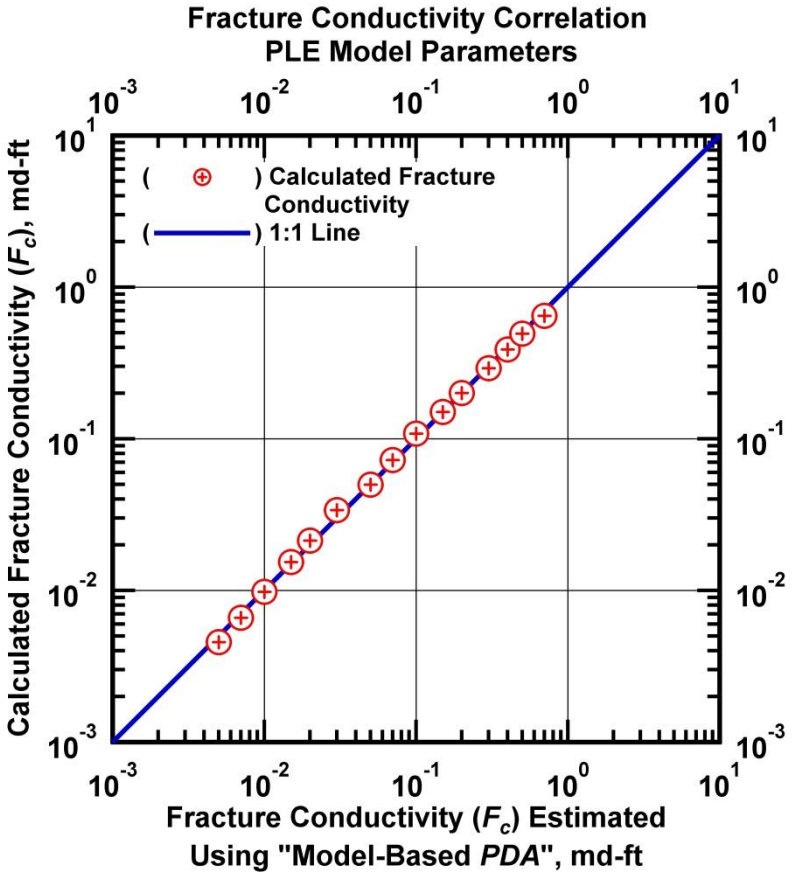

Figure 1.7 — (Log-log Plot): Comparison of fracture conductivity calculated using the fracture conductivity correlation using PLE model parameters versus fracture conductivity of numerical simulation models.

CHAPTER II

LITERATURE REVIEW

In the past several years, many advances have been made to analyze production data (time-rate-pressure) obtained from oil and gas wells. The methods provided engineers important tools with which to understand reservoir properties and to estimate reserves of oil and gas reservoirs. Since our aim is to investigate modern production analysis tools and their application to unconventional gas reservoirs, we present a literature review of important works done to analyze production data from these reservoirs. The literature review covers the following:

- Empirical, semi-analytical, and analytical production data analysis;
- Production data analysis of unconventional gas reservoirs.

2.1 Empirical, Semi-Analytical and Analytical Production Data Analysis

Lewis and Beal (1918) described the production data using percentage decline of rate and cumulative percentage curves to project the performance of the well to future time. The authors have also shown that the average percentage rate decline when plotted on a log-log plot exhibits a power-law behavior. They have shown that the straight line behavior on the log-log plot allows a simple and accurate projection of future performance. Cutler (1924) presented an overview of oil reserve estimation techniques in the 1920's. The author showed that percentage decline of production data is variable, and not constant as previously thought, and on a log-log plot the rate shows a hyperbolic behavior. Johnson and Bollens (1927) introduced a new way of visualizing the data using the "loss-ratio" and "loss-ratio" derivatives given by Eq. 2.1 and Eq. 2.2 respectively.

$$\frac{1}{D} = -\frac{q_g}{dq_g / dt} \quad \text{.....(2.1)}$$

$$b = \frac{d}{dt}\left[\frac{1}{D}\right] = -\frac{d}{dt}\left[\frac{q_g}{dq_g / dt}\right] \quad \text{.....(2.2)}$$

Arps (1945) derived the exponential and hyperbolic rate decline empirical relations. The exponential time-rate relation can be derived directly from the "loss-ratio" relation whereas the hyperbolic time-rate relation is derived from the "loss-ratio" derivative term. The hyperbolic rate decline is a generalization of the exponential decline behavior observed from wells exhibiting boundary conditions.

For reference Arps' exponential and hyperbolic relations are given by:

$$q(t) = q_i \exp[-Dt] \quad \text{.....(2.3)}$$

$$q(t) = \frac{q_i}{(1+bD_it)^{1/b}} \quad \text{.....(2.4)}$$

In Arps' definition the *b*-parameter varies between 0 and 1. As a result, Arps' exponential and hyperbolic relations are only applicable during boundary-dominated flow regimes. When the *b*-parameter in Arps' hyperbolic model approaches zero we obtain the exponential model (Eq. 2.3). During transient and transition flow regimes, application of Arps' hyperbolic model results in a *b*-parameter that is greater than 1 leading to an overestimation of future production. Rushing et al. (2007) have shown that application of Arps hyperbolic model during transient and transition flow regimes causes reserve estimate errors exceeding 100 percent.

This is not to say that hyperbolic models cannot be used for wells exhibiting transition and transient flow regimes. The authors have shown that reasonable reserve estimates can be obtained if care is taken to apply the Arps' hyperbolic model during transition and boundary-dominated flow regimes. Maley (1985) showed that Arps' hyperbolic model with a *b*-parameter greater than one can be used to match tight gas well data having long transient flow regimes. Robertson (1988) modified Arps' hyperbolic model by applying a constant percentage decline value at a specified time to represent the boundary-dominated flow regime with an exponential decline relation, thereby constraining the reserve estimate. The "modified hyperbolic model" matches early transient and transitional flow regimes with *b*-parameter between 0 and 1 and switches to exponential decline model with a constant decline parameter during late time boundary-dominated flow regimes.

In the past decade, several new time-rate relations have been developed with improvements over traditional Arps' rate decline models. This new models result in superior matches for wells flowing in transient and transition flow regimes for very long durations. Ilk et al.(2008b) presented the power-law exponential rate decline relation based on the inverse of the "loss-ratio" (*D*-parameter) behavior of the time-rate data. Through continuous evaluation of the *D*-parameter of production data, it is observed that the *D*-parameter exhibits a power-law behavior for early time data, characterized by a straight line on a log-log plot. The straight line characteristic is particularly true for wells in low/ultra-low permeability reservoirs. During the late-time period the *D*-parameter of the power-law exponential model is characterized by a constant decline parameter. As a result this model can match transient, transition and boundary-dominated flow regimes.

Valko (2009) independently introduced the stretched exponential decline model to describe observed decline behavior of a database of rate data obtained from unconventional reservoirs. Valko's aim was to perform a statistical investigation of producing wells in unconventional reservoirs. The stretched exponential model is similar to the power-law exponential model in matching the early time data, but it lacks the boundary conditions necessary to match long-time boundary conditions.

Duong (2011) proposed a time-rate relation to analyze production data obtained from low/ultra-low permeability reservoirs where the dominant flow path is through induced hydraulic fractures. The author showed that a log-log plot of rate divided by cumulative production (q/G_p) verus *time* yields a straight line trend. The author indicated that the slope and intercept of the straight line are characteristics of the reservoir. A range of values of the slope and intercept describe the type of rock or fracture stimulation practices.

Clark et al.(2011) adapted a type of logistic growth model to propose a new time-rate model to match production data of oil and gas wells. The logistic growth model is capable of modeling long transient behaviors of unconventional reservoirs as well as boundary conditions (to some extent). Ilk et al.(2010) have developed a set of new time-rate relations based on PLE, stretched exponential, and Arps' hyperbolic and exponential time-rate models to characterize the long transient flow regime and boundary-dominated flow regimes.

The idea of using time-rate relations to forecast future performance assumes prevailing reservoir characteristics remain unchanged in the future. One advantage of time-rate decline analysis technique is that we do *not* need to know values of fundamental reservoir properties that are often not readily available. The only data required for analysis is the time-rate data; as a result, the model parameters are purely mathematical results. If current operating conditions are not affecting future performance of the wells; then projection of the best fit line through the current data should describe future production trends. The analysis also assumes constant bottomhole flowing pressure (Rushing et al. 2007). These assumptions indicate that time-rate models have purely empirical basis.

There have been attempts aimed at assigning reservoir properties to rate decline model parameters. Fetkovich (1980) showed that analytical transient rate solutions for bounded reservoirs producing at a constant bottomhole pressure can be shown on a type curve together with Arps' empirical relations. The author showed that material balance relations can be combined with pseudosteady-state relations to provide a rate equation with a form identical to Arps' rate decline relations. This provides theoretical basis to Arps' empirical relations. Carter (1985) developed new set of type curves for analysis of gas rate data by taking into account real gas behaviors. Camacho and Raghavan (1989) investigated solution-gas drive

reservoirs in boundary-dominated flow and showed that Arps' *D*- and *b*-parameters depend on rock and fluid properties of the reservoir, reservoir dimensions and wellbore conditions.

Ilk et al.(2011) have shown that it is possible to correlate reservoir/well properties that are estimated using model-based production data analysis with parameters of the power-law exponential (PLE) time-rate relation. From that study it was apparent that synthetic data cases are required to obtain a more rigorous (perhaps semi-analytical) correlation for the estimation of well/reservoir properties. Chapter 5 of this work provides a theoretical basis using production data generated from numerical simulation cases.

2.2 Production Data Analysis of Unconventional Gas Resources

Van Kruysdijk and Dullaert (1989) described the major flow regimes identified during production data analysis of unconventional reservoirs. Freeman et al. (2009) presented a numerical simulation study of tight\shale gas reservoirs to determine factors that affects behavior of observed flow regimes. The major flow regimes observed from unconventional reservoirs are:

- **Linear flow regime:** occurs during early flow periods when the dominant flow is linear and perpendicular to the fracture face. Extreme pressure gradients cause sharp decline rates. In this flow regime, flow occurs only from fractures. This flow occurs as long as there is no interference to the pressure transients. This flow regime is characterized by a half-slope on a log-log plot of flow rate versus time.

- **Compound formation linear flow:** is characterized by a substantial drop in flow rate. It indicates that the pressure transients are experiencing fracture interference. The matrix contributes to the production during this flow regime.

- **Boundary-dominated flow regime:** occurs when the pressure transient reach the reservoir boundaries. During this period the entire reservoir has been contacted as a result flow-rate declines.

CHAPTER III

ANALYSIS OF TIME-RATE RELATIONS

In this chapter a detailed analysis of Duong and logistic growth model is presented. We have used the power-law exponential model (PLE) as a benchmark from which we can study the match quality and reliability of reserve estimates calculated using these models. We have focused the analysis by considering production data obtained from unconventional gas resources. We have used production data generated from a numerical simulation as well as data obtained from a tight gas reservoir.

We compare the quality of match to specific flow regimes observed from such reservoirs. The data match is conducted by taking full advantage of the characteristics of diagnostic functions including *D*-, *b*-, parameters, β-derivative as well as the flow rate data. We have used the Bourdet et al. (1989) algorithm to perform the numerical differentiation required to calculate the diagnostic functions. Moreover, we use the "continuous *EUR*" approach, where *EUR* is estimated dynamically, to investigate the reliability of the reserve estimates and rate of convergence of *EUR* when using these models. The time–rate empirical models considered in this research include:

- The Power Law Exponential model (PLE) (Ilk et al. 2008b),
- The Duong model (Duong 2011), and
- The Logistic Growth Model (LGM) (Clark et al. 2011).

Following we provide a short description of the time–rate models.

3.1 Power Law Exponential Model

The power–law exponential model was derived by observing the "loss-ratio" behavior of wells producing from low/ultra–low permeability reservoirs producing through fracture stimulation. Ilk et al.(2008b) demonstrated that by describing the "loss–ratio" of the data using a power–law function, it is possible to match the dominant transient and transition flow regimes observed from unconventional reservoirs. Moreover, they showed that boundary-dominated flow regimes are represented by adding a constant decline parameter (D_∞) to the power law relation. The PLE model inverse "loss-ratio" relation is given by:

$$D(t) = D_\infty + \hat{D}_i n t^{n-1} \quad \text{..... (3.1)}$$

During boundary-dominated flow regimes, the power-law term becomes less significant and $D(t)$ approaches a constant term (D_∞) similar to the case in Arps exponential decline model. Furthermore, the

authors observed that the derivative of the "loss-ratio" is not constant as was the case in Arps' rate decline relations (*i.e.*, exponential, hyperbolic and harmonic equations), but instead it is a function of time. The "loss-ratio" derivative (*b*-parameter) is given by:

$$b(t) = \frac{-\hat{D}_i (n-1) n t^n}{(D_\infty t + \hat{D}_i n t^n)^2} \quad \text{..... (3.2)}$$

And the PLE "β" relation is given by:

$$\beta(t) = D_\infty + \hat{D}_i n t^n \quad \text{..... (3.3)}$$

And the power-law exponential rate relation is given by:

$$q = \hat{q}_{gi} \exp[-D_\infty t - \hat{D}_i t^n] \quad \text{..... (3.4)}$$

As mentioned earlier a diagnostic plot of $D(t)$,$b(t)$ and $\beta(t)$ vs. *time* helps diagnose the time-rate data matching process.

The PLE model provides excellent match to the transient, transition and boundary-dominated flow regimes and in this study we use the PLE model as a benchmark to study the performance of Duong and logistic growth models.

3.2 Duong Model

Duong (2011) presented a new empirical rate decline model based on the long-term linear or bilinear flow regimes observed in hydraulically fractured low/ultra-low permeability reservoirs. On a log-log plot of rate versus time, the early time data shows half slope for linear flow and quarter slope for bilinear flow regimes. A log-log plot of rate over cumulative production versus *time* results in a straight line for wells producing from unconventional reservoirs. This straight line behavior is described by a power-law relation given by:

$$\frac{q}{G_p} = a t^{-m} \quad \text{..... (3.5)}$$

Where a is the straight line intercept and m is negative slope of straight line on log-log plot of q/G_p vs. time.

The slope and intercept parameters of Duong model show narrow ranges for wells producing from similar rock-types and similar fracture stimulation practices and operational conditions (Duong 2011). The parameters can be directly estimated from q/G_p versus *time* diagnostic plot.

The Duong rate and cumulative relations are given by:

$$\frac{q}{q_1} = t^{-m} \exp\left[\frac{a}{1-m}(t^{1-m}-1)\right] \quad \text{..... (3.6)}$$

$$G_p = \frac{q_1}{a} \exp\left[\frac{a}{1-m}(t^{1-m}-1)\right] \quad \text{..... (3.7)}$$

Where q_1 is the flow rate estimated during the first day (t=1 day).

In addition to q/G_p versus *time* log-log diagnostic plot, we use the "loss-ratio" and the "loss-ratio" derivative definitions to estimate the model parameters and guide the data matching process. The *b*-, *D*-parameters and the β-derivative of Duong model are given by:

$$D(t) = mt^{-1} - at^{-m} \quad \text{..... (3.8)}$$

$$b(t) = \frac{mt^m(t^m - at)}{(at - mt^m)^2} \quad \text{..... (3.9)}$$

$$\beta(t) = m - at^{-m} \quad \text{..... (3.10)}$$

We can also estimate the Duong m – parameter independently using the following diagnostic relation:

$$m = t\frac{G_p}{q}\frac{d}{dt}\left[\frac{q}{G_p}\right] \quad \text{..... (3.11)}$$

3.3 Logistic Growth Model

Yet another model, the logistic growth model, is adapted to model time-rate data from oil/gas reservoirs. The logistic growth model is used to model growth trends of various population sizes in nature. A form of the logistic growth model has been used to model growth of yeast and to study market penetration of new products and technologies (Martinez et al. 2008). Tsoularis and Wallace (2002) have provided a detailed study of logistic growth models and they have also presented a summary of different forms of logistic growth models.

Clark (2011) adapted the hyperbolic form of the logistic growth model to match time-rate data of oil/gas reservoirs. The hyperbolic form was suggested by Blumberg (1968) to study regenerative growth in nature. Eq. 3.12 shows the hyperbolic form of the logistic growth model.

$$N(t) = \frac{K(t+b)^{\hat{n}}}{\hat{a} + (t+b)^{\hat{n}}} \quad \text{..... (3.12)}$$

The model was used to study several oil and gas wells. After modifications the cumulative production form of the hyperbolic logistic growth model is given by:

$$Q(t) = \frac{Kt^{\hat{n}}}{\hat{a} + t^{\hat{n}}} \quad \text{..... (3.13)}$$

The rate relation is given by:

$$q(t) = \frac{\hat{a}K\hat{n}t^{\hat{n}-1}}{(\hat{a} + t^{\hat{n}})^2} \quad \text{..... (3.14)}$$

Similarly the *D*-, *b*-parameters and the β-derivative diagnostic functions are used to perform diagnostic match of time-rate data. Logistic growth model *b*-, *D*- and β- parameters are given by:

$$D(t) = \frac{\hat{a} - \hat{a}\hat{n} + (1+\hat{n})t^{\hat{n}}}{t(\hat{a} + t^{\hat{n}})} \quad \text{..... (3.15)}$$

$$b(t) = \frac{-\hat{a}^2(\hat{n}-1) - 2\hat{a}(\hat{n}^2-1)t^{\hat{n}} + (\hat{n}+1)t^{2\hat{n}}}{(\hat{a} - \hat{a}\hat{n} + (\hat{n}+1)t^{\hat{n}})^2} \quad \text{..... (3.16)}$$

$$\beta(t) = \frac{\hat{a} - \hat{a}\hat{n} + (1+\hat{n})t^{\hat{n}}}{(\hat{a} + t^{\hat{n}})} \quad \text{..... (3.17)}$$

The q/G_p formulation of logistic growth model is given by:

$$\frac{q}{G_p} = t\left(\frac{\hat{a} + t^{\hat{n}}}{\hat{a}\hat{n}}\right) \quad \text{..... (3.18)}$$

If the initial gas-in-place is known (*K*), we can rewrite the rate relation to find a diagnostic relation that allows a diagnostic plot estimation of the remaining model parameters (Clark et al. 2011).

$$\frac{K}{Q_g(t)} - 1 = \hat{a}t^{-\hat{n}} \quad \text{..... (3.19)}$$

3.4 Comparison of Time-Rate Models

In this section, analysis of PLE, logistic growth and Duong models is presented. We perform a quality analysis of the resulting model match using *D*-, *b*- parameters and β–derivative of the production data. We

also show a "continuous *EUR*" (Currie et al. 2010) analysis of the models to determine how fast a reliable *EUR* is estimated when production data is available at specific time intervals.

3.4.1 Numerical Simulation Case

In this case we consider a multi-fractured horizontal well model with finite conductivity producing from a low permeability reservoir. We have modeled a homogeneous reservoir with a rectangular boundary where a single phase gas is flowing. **Table 3.1** shows reservoir and well parameters used to generate production data for this numerical simulation case.

Table 3.1 — Reservoir and fluid properties for numerical simulation case (multi-fractured horizontal well model with multiple fractures).

Reservoir Properties		
Net pay thickness, h	=	160 ft
Formation permeability, k	=	2µD
Wellbore Radius, r_w	=	0.66 ft
Formation compressibility, c_f	=	3×10^{-6} psi^{-1}
Porosity, ϕ	=	0.05 (fraction)
Initial reservoir pressure, p_i	=	5000 psi
Gas saturation, s_g	=	1.0 fraction
Skin factor, s	=	0 (dimensionless)
Reservoir temperature, T_r	=	212 °F
Fluid properties:		
Gas specific gravity, γ_g	=	0.65 (air = 1)
Hydraulically fractured well model parameters:		
Fracture half-length, x_f	=	164.0 ft
Number of fractures	=	15
Horizontal well length	=	6561.7 ft
Production parameters:		
Flowing pressure, p_{wf}	=	500 psia
Production time, t	=	10,958 days (30 years)

Fig. 3.1 shows a history plot of the resulting rate and cumulative production data.

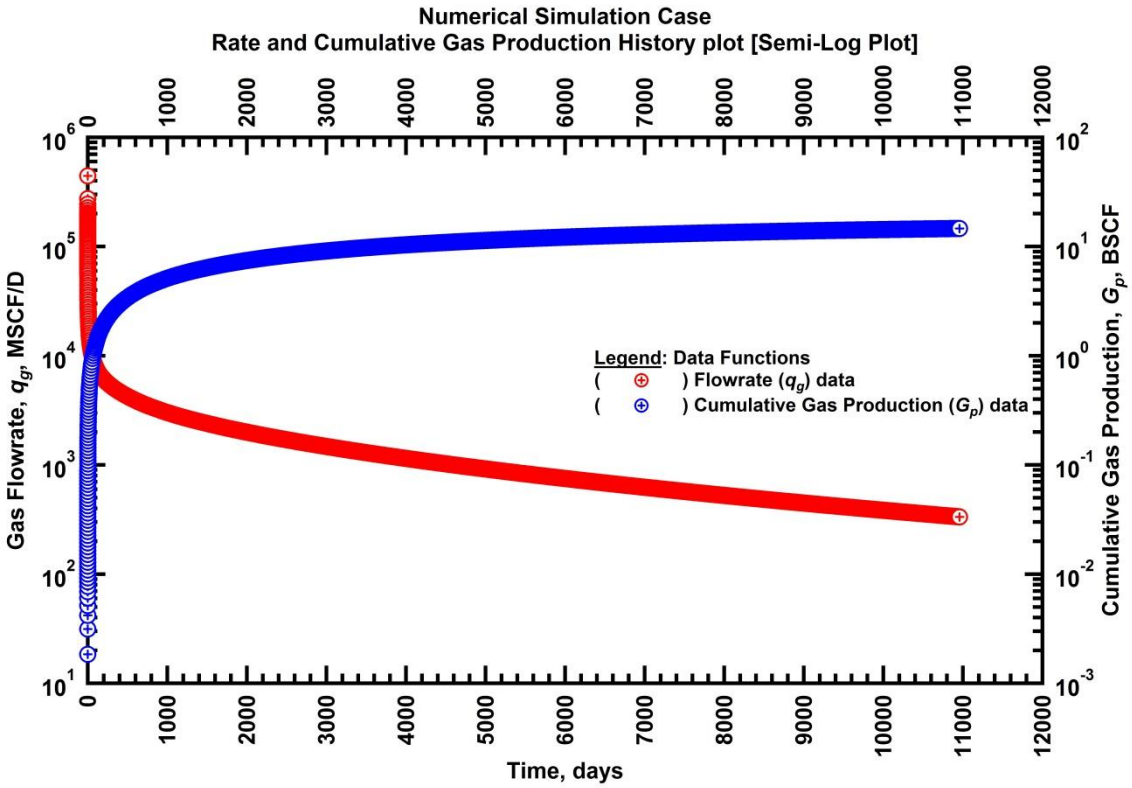

Figure 3.1 — (Semi-log Plot): Production history plot for numerical simulation case – flow rate (q_g) and cumulative production (G_p) versus production time (horizontal well model with multiple transverse fractures).

Fig. 3.2 shows the production data along with *D*-, *b*-and $\not\beta$- parameters. The production data indicates a long transient flow regime lasting for more than 3 years followed by a boundary-dominated flow regime. The transient flow is indicated by a constant value of 2 on the *b*-parameter data. The $\not\beta$-derivative indicates a constant value of 0.5 during the transient flow regime. The *D*-parameter shows a straight line behavior during transient flow periods. After 3 years we notice beginning of transition and boundary-dominated flow regimes. During this period, we notice that the data parameters start deviating from their transient behaviors. When matching the data, we aimed to obtain a quality fit across all flow regimes by using these diagnostic parameters.

When transient and boundary-dominated flow regimes are observed, the transient flow period is matched before matching the boundary-dominated flow regime. In this example, all the model matches show excellent fit to the data during transient flow periods. If *EUR* is estimated during this flow period, all

models result in accurate reserve estimates. However, we notice that logistic growth and Duong models fail to match the boundary-dominated flow regime. The PLE model excels at matching transient, transition and boundary-dominated flow regimes. The D_∞ parameter of PLE model is used to obtain a match for the production data profile during this flow period. Attempts to match the boundary-dominated flow regime using the logistic growth and Duong models results in low-quality match across all flow regimes.

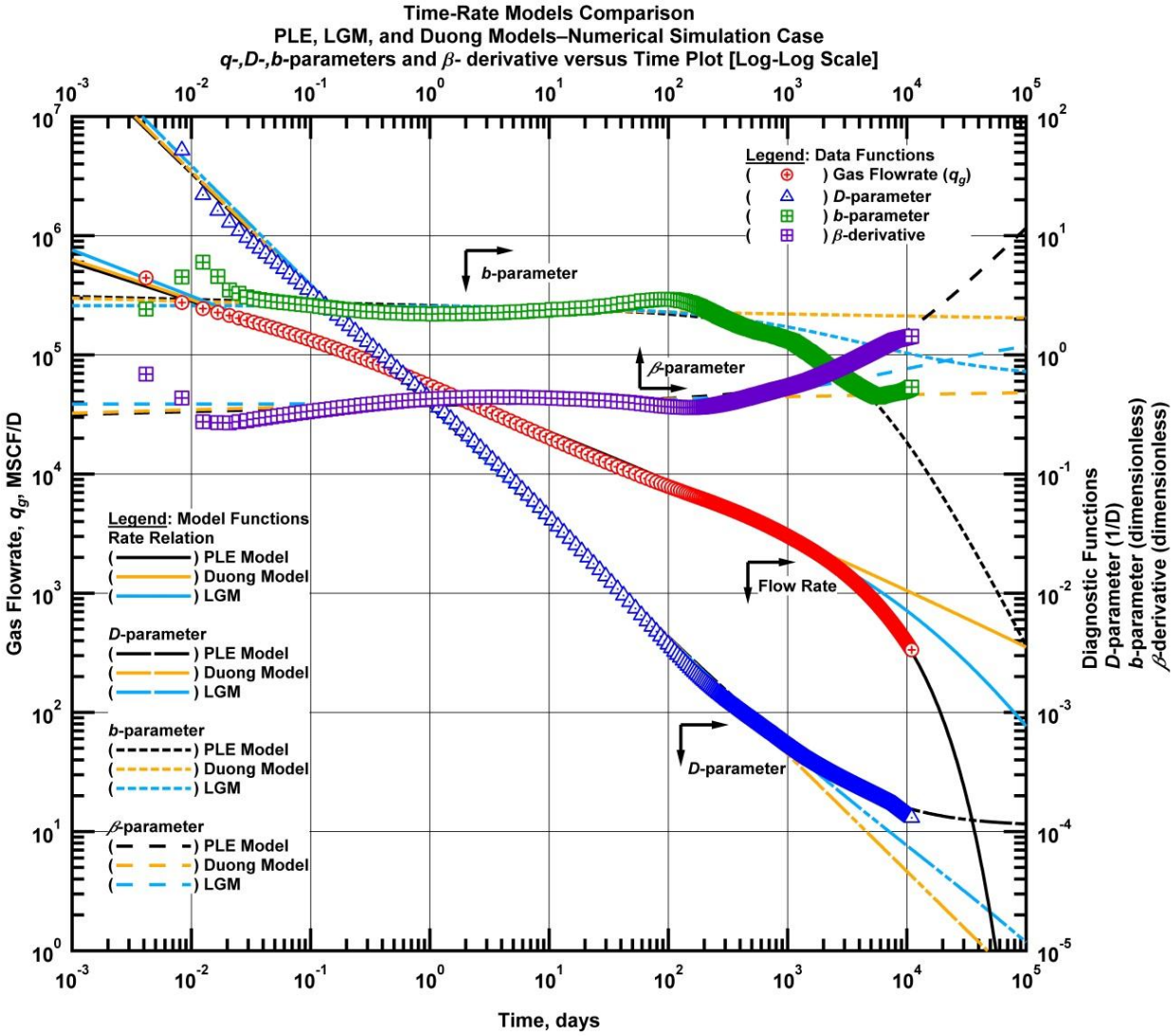

Figure 3.2 — (Log-log Plot): Flow rate (q_g), *D*-, *b*-parameter and β-derivative versus production time. PLE, logistic growth, and Duong model matches for numerical simulation case.

As a result, logistic growth and Duong models overestimate reserves at the end of the flow period. The reserve estimates obtained from the models are shown in **Table 3.2.**

Table 3.2 — 30 year reserve estimate obtained using PLE, Duong and logistic growth models for numerical simulation model ($G_{p,max}$=14.2 BSCF from numerical simulation.)

Time-rate models		*Reserve Estimate*
PLE Model	=	14.7 BSCF (3.5%)
Duong Model	=	19.5 BSCF (37.3%)
Logistic Growth Model	=	17.5 BSCF (23.2%)

The reserve estimates (Table 3.2) indicate that Duong model overestimated the reserve by 37.3 percent while logistic growth model overestimated reserve by 23.2 percent. The boundary conditions present in PLE model result in a more reliable match to transient, transition and boundary-dominated flow regimes resulting in a reliable estimate of the *EUR*.

Next, we perform a "continuous *EUR*" analysis to determine the rate of convergence of *EUR* estimated using the time-rate models to the "true" *EUR* value obtained from the numerical simulation model. The process is automated to evaluate *EUR* at specified time-steps. Although the process is automated, we have calibrated the matching procedures manually when it was necessary to do so. In addition to matching the production data, the match quality of the diagnostic functions (*D*-, *b*-, parameters and β-derivative) were used to check the quality of match during specific flow periods. Moreover, we were mindful of when a particular flow regime began in order to control the model parameters whenever it was possible to do so.

First, we perform the "continuous *EUR*" analysis using the PLE model. A set of production data extracted at successive time steps is matched using the PLE model. A computer program was created to automate the data matching procedure. **Fig. 3.3** show the flow rate, *D*-, *b*-, parameters and β-derivative of the data matched using the PLE model. The D_∞ parameter of the PLE model was initiated only after boundary-dominated flow regime effects were observed. The PLE model resulted in excellent matches for all flow regimes during each successive time step.

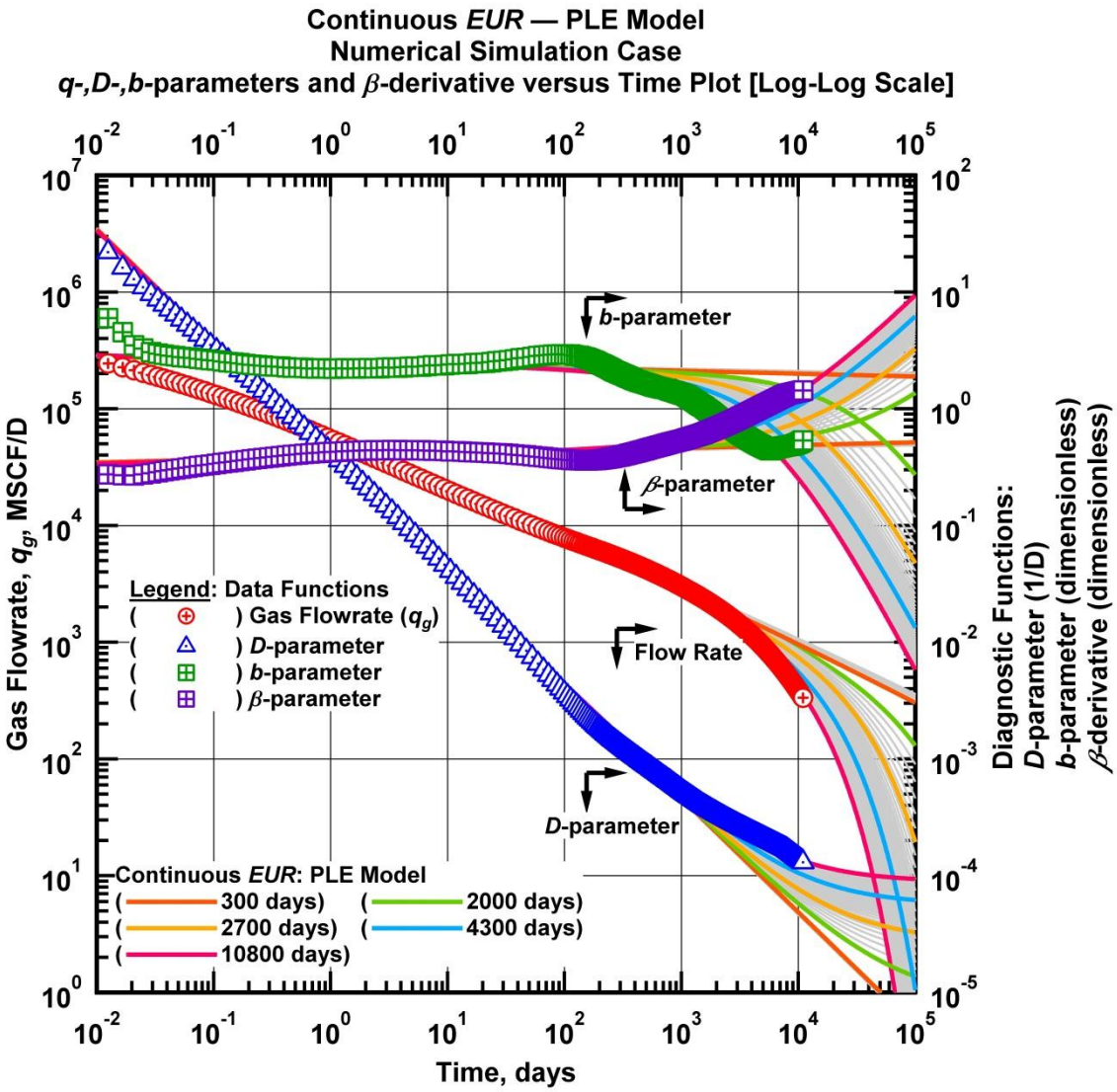

Figure 3.3 — (Log-log Plot): Continuous *EUR* analysis. Flow rate (q_g), *D*-, *b*-parameter and β-derivative versus production time. PLE model matches for numerical simulation case.

Fig. 3.4 shows the resulting model matches of Duong model plotted on the flow rate, *D*-, *b*-, parameters and β-derivative of the data. The Duong model shows excellent matches during the long transient flow regime. However, when transition and boundary-dominated flow regime effects are felt, the Duong model starts deviating from the match of the transient flow regime. *This implies that the Duong model should only be used to match transient flow behavior.* As a criteria, we require that a given model yield an excellent match across all observed flow regimes. We should not compromise the match quality to force a

match to the boundary-dominated flow regime. Since boundary-dominated flow regimes are not modeled, Duong model overestimate reserves.

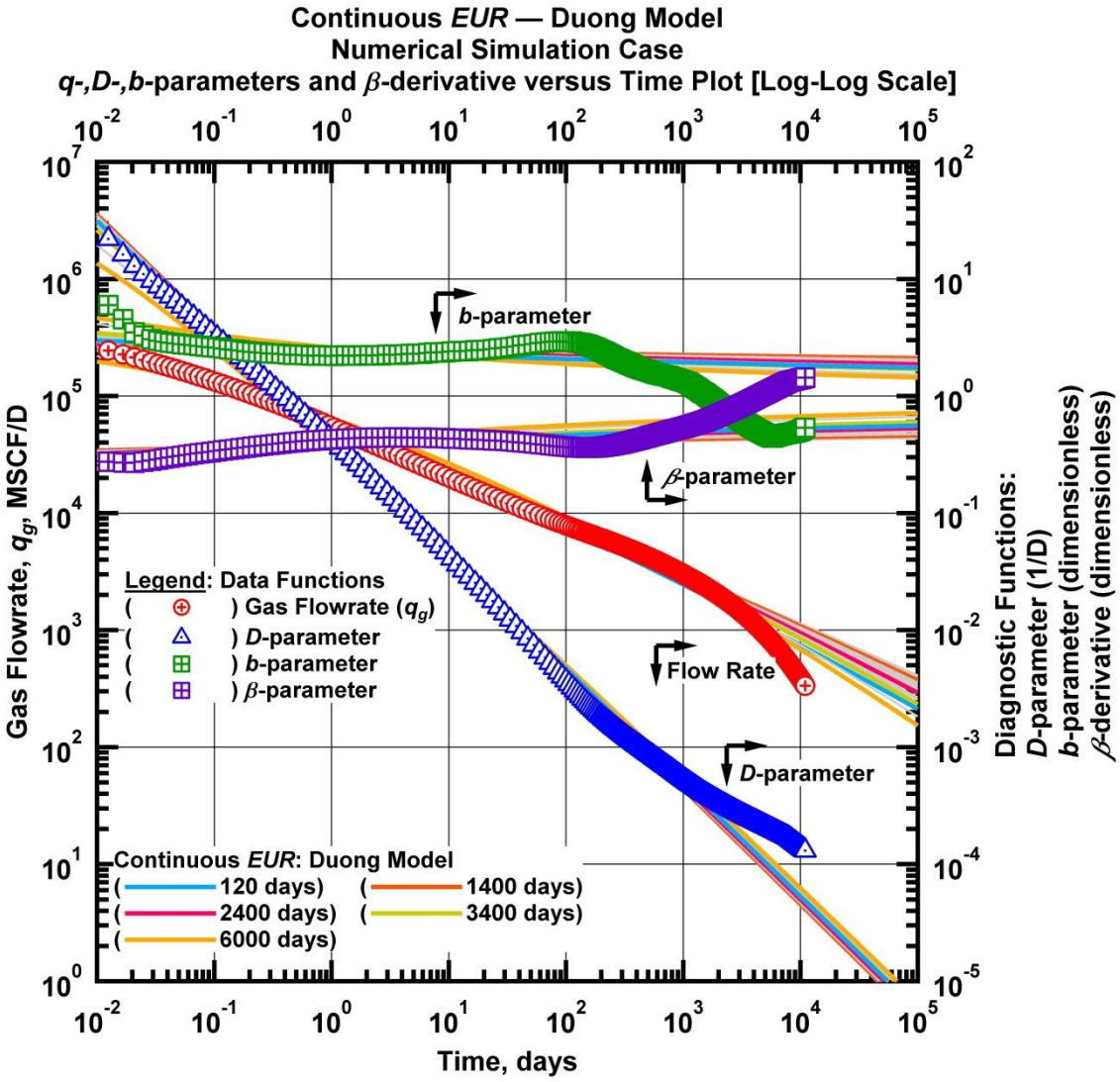

Figure 3.4 — (Log-log Plot): Continuous *EUR* analysis. Flow rate (q_g), *D*-, *b*-parameter and β-derivative versus production time. Duong model matches for numerical simulation case.

Fig. 3.5 shows the resulting model matches of logistic growth model imposed on the flow rate, *D*-, *b*-, parameters and β-derivative of the data. The model shows excellent match during the time steps in the transient and transition flow regimes. However boundary-dominated flow regimes are not modeled very

well. We observe a slight deviation from the transient/transitions model match at late times when boundary effects begin. As can be seen in Fig. 3.5, the logistic growth model *EUR* estimates converges at a higher *EUR* value. When true boundary-dominated flow regimes are observed, the logistic growth model lacks the character to match this flow regime accurately.

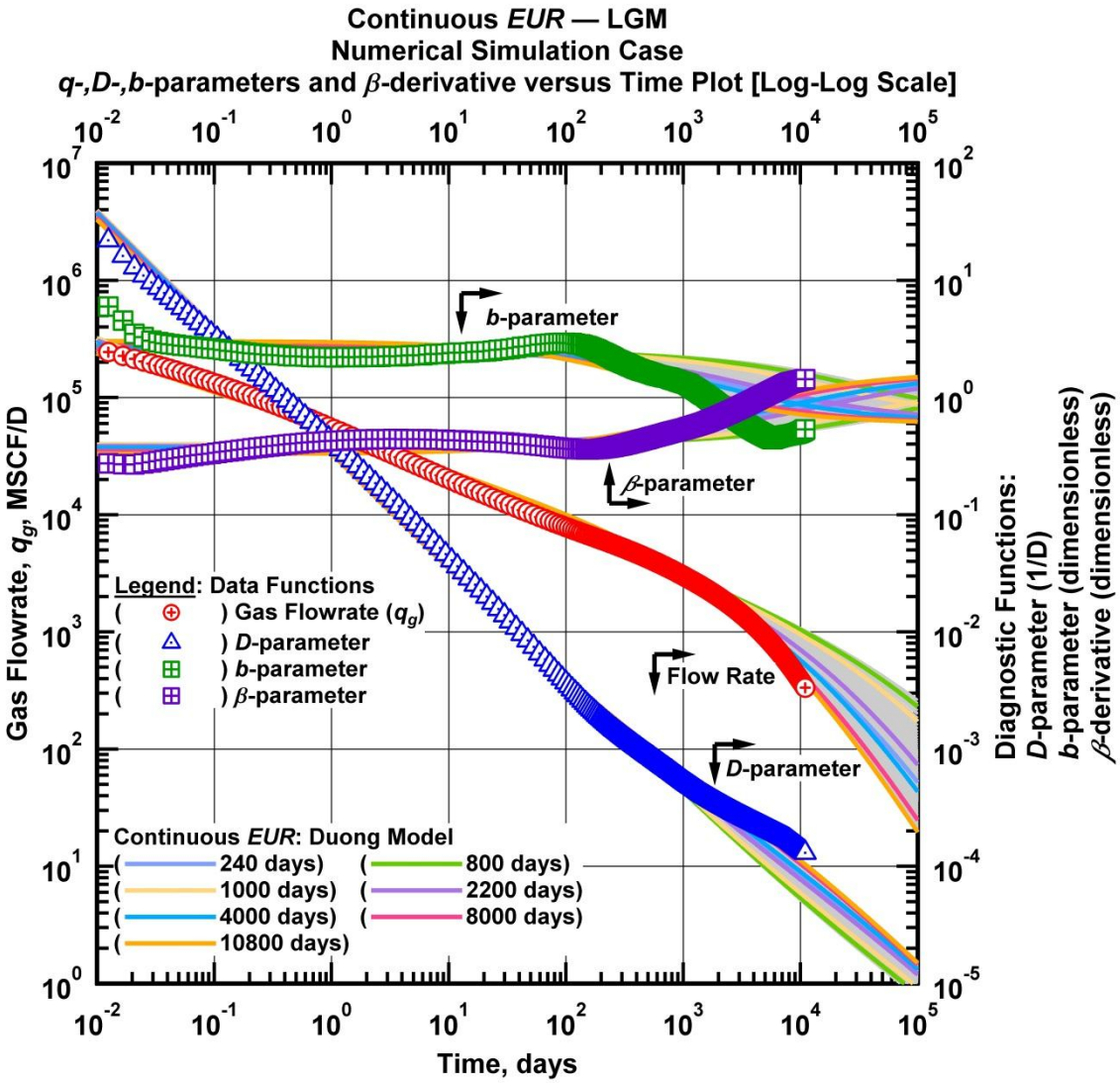

Figure 3.5 — (Log-log Plot): Continuous *EUR* analysis. Flow rate (q_g), *D*-, *b*-parameter and β-derivative versus production time. Logistic growth model matches for numerical simulation case.

Fig. 3.6 shows results of the *EUR* values estimated dynamically at specific time intervals. In this case *EUR* was estimated every 60 days for 30 years to observe the rate of convergence of the *EUR* estimates to the "true" *EUR* value obtained from numerical simulation. As expected the PLE model approaches the 30-yr *EUR* estimate at a faster rate and results in a reliable reserve estimate. The Duong and logistic growth models stabilize at a higher *EUR* value overestimating reserves. The *EUR* estimation was allowed to continue until the end of the 30 years period. However, from Fig. 3.6, we note that after 2000 days the quality of match obtained using Duong model starts to decline when the transition and boundary effects become dominant features. If the analysis was stopped at that point, the 30 year reserve estimate would have stabilized around 19 BSCF as was estimated using Fig. 3.2 and indicated in Table 3.2. Logistic growth model *EUR* estimate approach the "true" *EUR* value at a faster rate. The model shows a good match during transient/transition flow regimes. However, when boundary effects dominate, the model lacks the characteristics to model the flow regime accurately. As a result, the model finally converges to a higher *EUR* value.

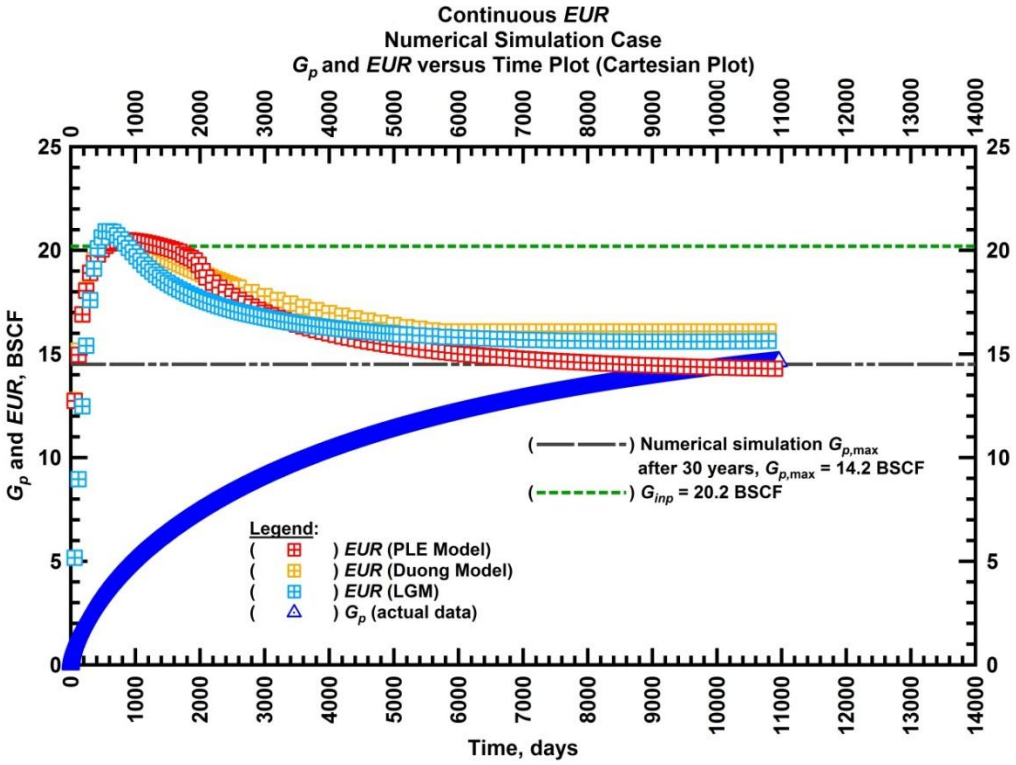

Figure 3.6 — (Cartesian Plot): *EUR* estimates from PLE, logistic growth, and Duong models matches and $G_{p,max}$ projected from numerical simulation case (horizontal well model with multiple transverse fractures).

3.4.2 Field Example: East Tx Tight Gas Well (SPE 84287)

Here we compare the time-rate models using production data obtained from a hydraulically fractured vertical well completed in a tight gas reservoir. The 6 year flow rate and cumulative production historical data is presented in **Fig. 3.7.** The figure shows the raw data together with the edited data which is used for analysis. A data diagnostic is a necessary step, in such cases where the production profile may be affected by liquid loading, unstable operating conditions or a change in well completion.

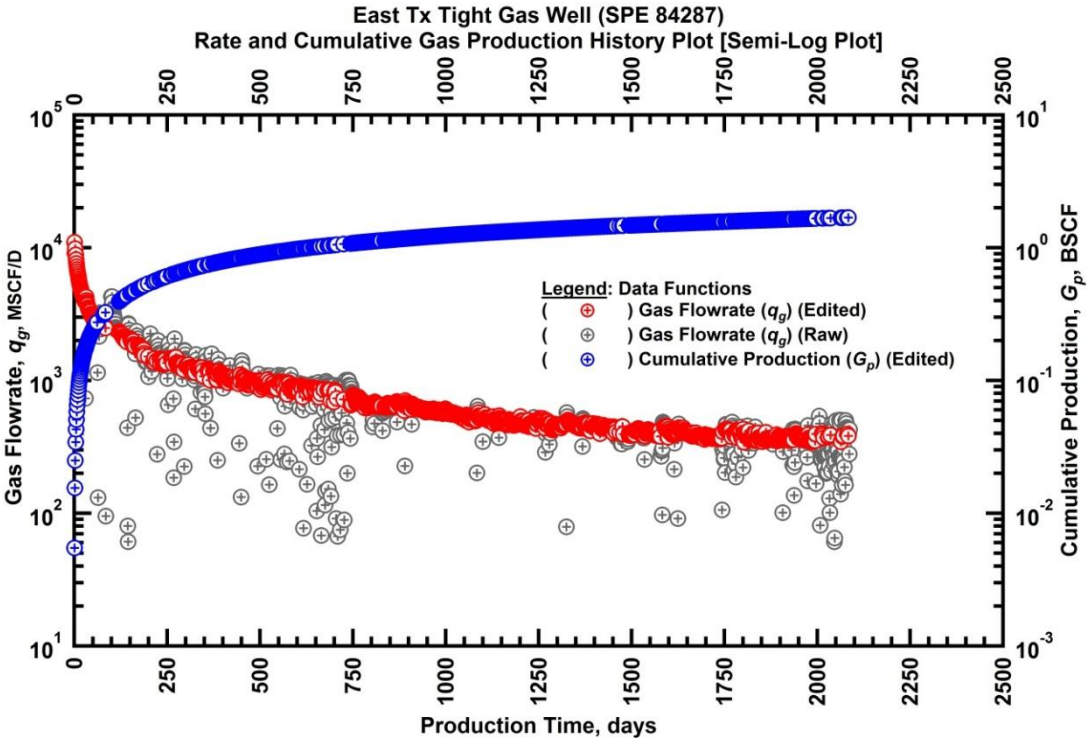

Figure 3.7 — (Semi-log Plot): Production history plot of East Tx tight gas well – flow rate (q_g) and cumulative production (G_p) versus production time.

Fig. 3.8 shows a "continuous *EUR*" analysis using the PLE model. The figure shows flow rate, *D*-, *b*-, parameters and β-derivative model matches at the successive time steps considered. In this case the diagnostic functions do not indicate boundary-dominated flow conditions. The *D*- parameter shows straight line decline behavior and does not show transition to a constant decline value at late times, which we would expect to see if boundary-dominated flow conditions were present. Similarly, the *b*-, and β-diagnostic functions do not show boundary characteristics at late times. Hence, the D_∞ parameter of the PLE model was not used during this analysis. The *b*-parameter trend shown on Fig. 3.8 illustrates apparent power-law behavior, and we note a slight upward inflection near the large-time endpoints. The

PLE model shows an excellent match across all observed flow regimes. The model matches seem to have stabilized after 800 days for each additional time step.

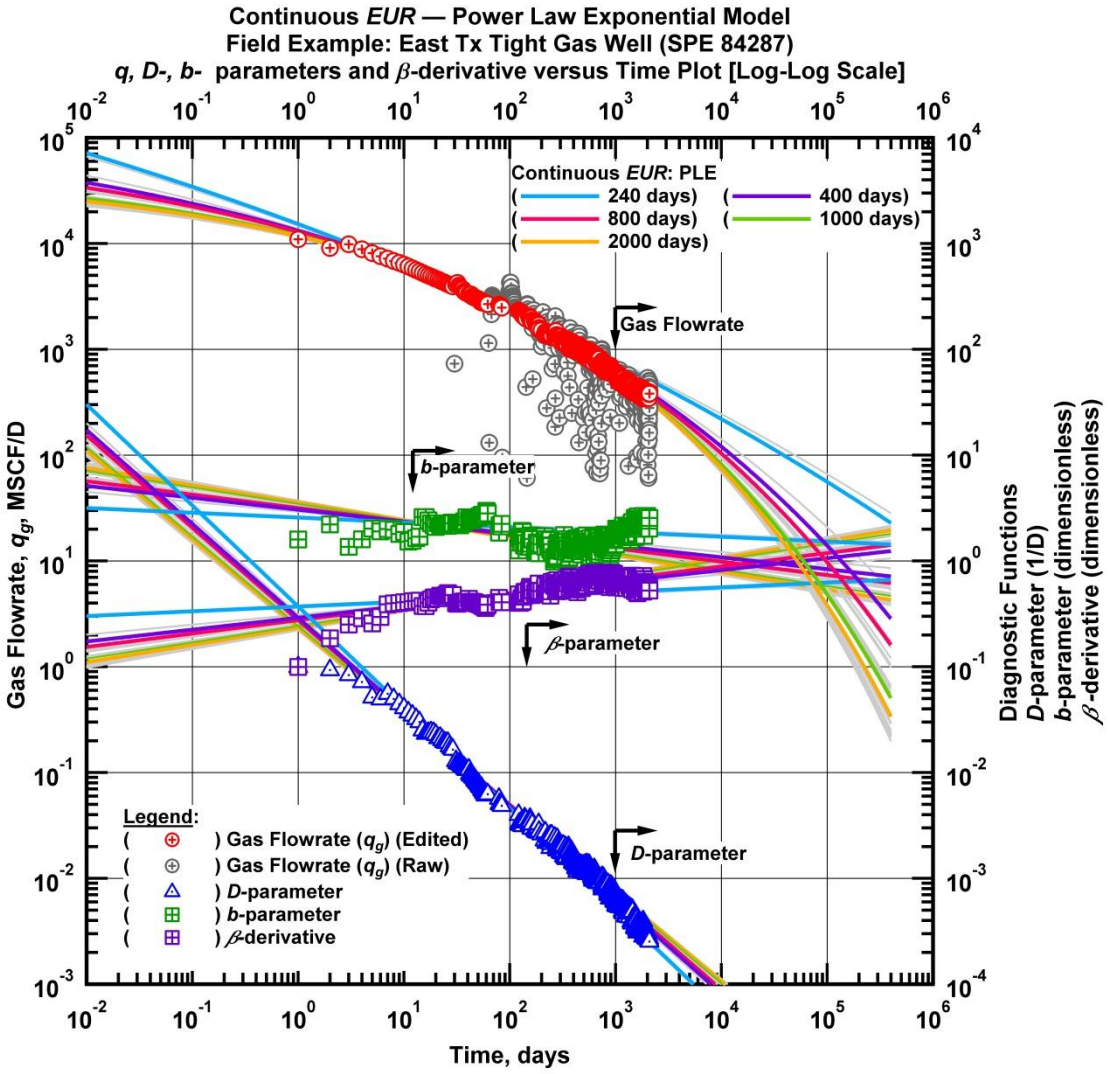

Figure 3.8 — (Log-log Plot): Continuous *EUR* analysis. Flow rate (q_g), *D*-, *b*-parameter and β-derivative versus production time. PLE model matches for East Tx tight gas well.

Fig. 3.9 shows the Duong model "continuous *EUR*" analysis. Similar to the PLE model, the Duong model results in a quality fit to the data. The model shows excellent match during the transient flow regime behavior that was observed. The model matches stabilize after about 1000 days for each additional time interval.

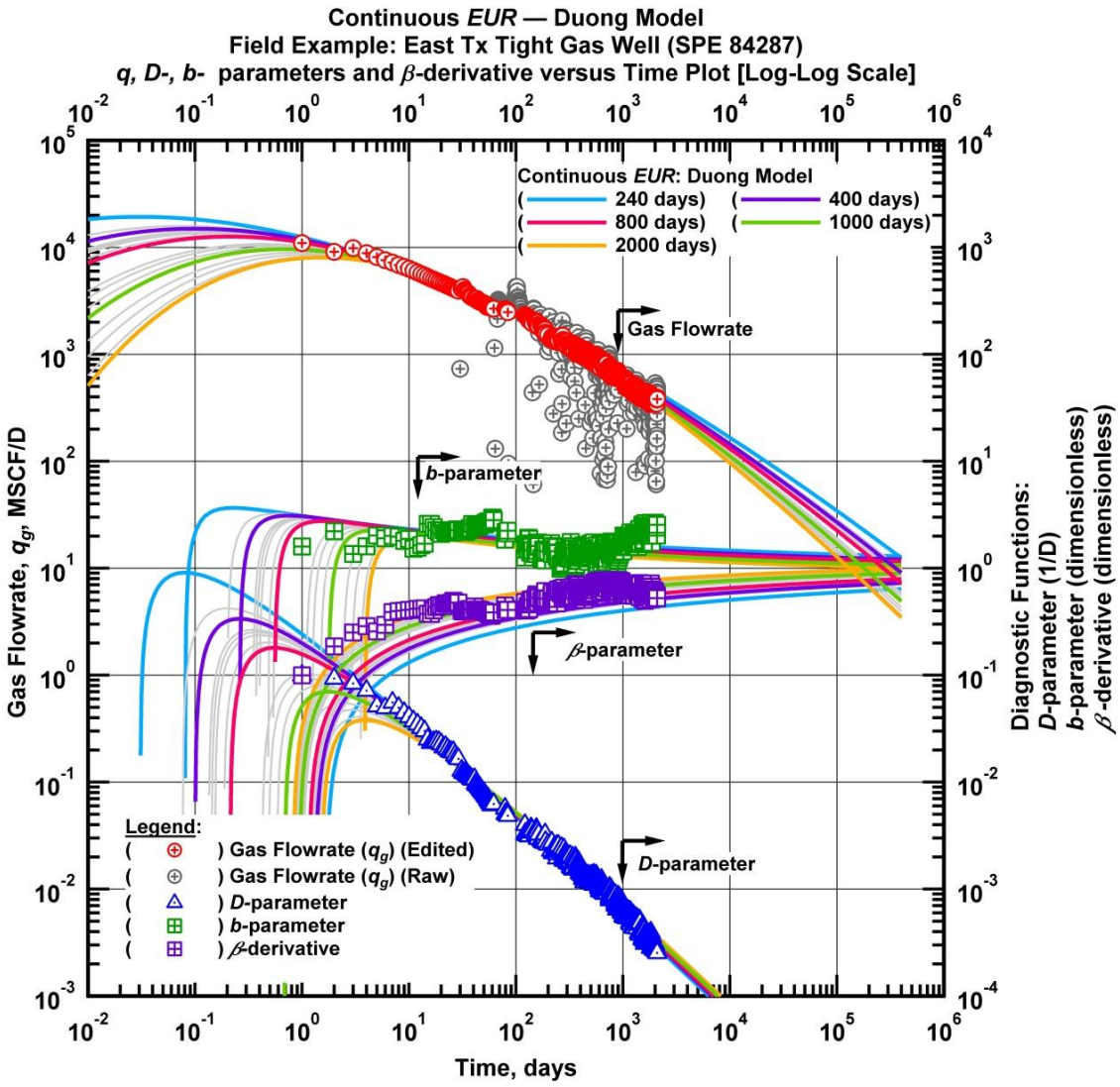

Figure 3.9 — (Log-log Plot): Continuous *EUR* analysis. Flow rate (q_g), *D*-, *b*-parameter and β-derivative versus production time. Duong model matches for East Tx tight gas well.

Fig. 3.10 shows results of "continuous *EUR*" analysis using logistic growth model. The model matches show quality match at successive time intervals to the flow regime observed. The model matches seem to have converged after about 800 days for the next successive time intervals.

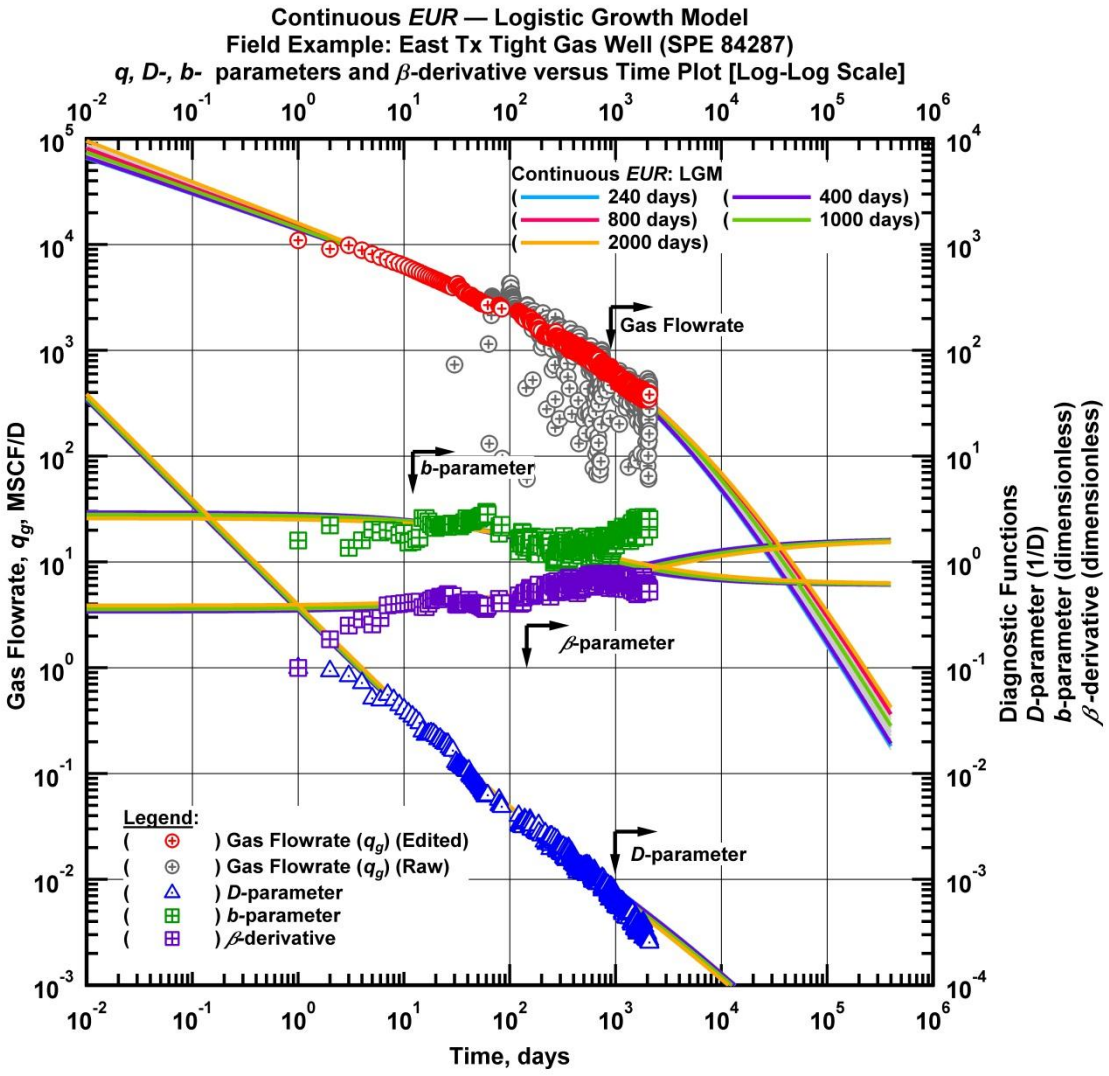

Figure 3.10 — (Log-log Plot): Continuous *EUR* analysis. Flow rate (q_g), *D*-, *b*-parameter and β-derivative versus production time. Logistic growth model matches for East Tx tight gas well.

Fig. 3.11 shows the *EUR* values calculated by the models at each successive time steps plotted against time. We can see that when boundary-dominated flow regime is not observed the 30 year *EUR* value converge at a *EUR* value of 3 BSCF. Specifically PLE converged at 2.97 BSCF while the Duong model converged at 3.14 BSCF and logistic growth model *EUR* estimates converged at 2.95 BSCF. The results show that in the absence of boundary-dominated flow regime all models converge to *EUR* value around 3 BSCF at the end of the 30 year time limit. The figure shows that PLE model converged after 750 days where as logistic growth model converged after about 1000 days and the Duong model converged after

about 1200 days. This shows that PLE model converges faster to a reliable *EUR* estimate when a limited set of data is available for analysis.

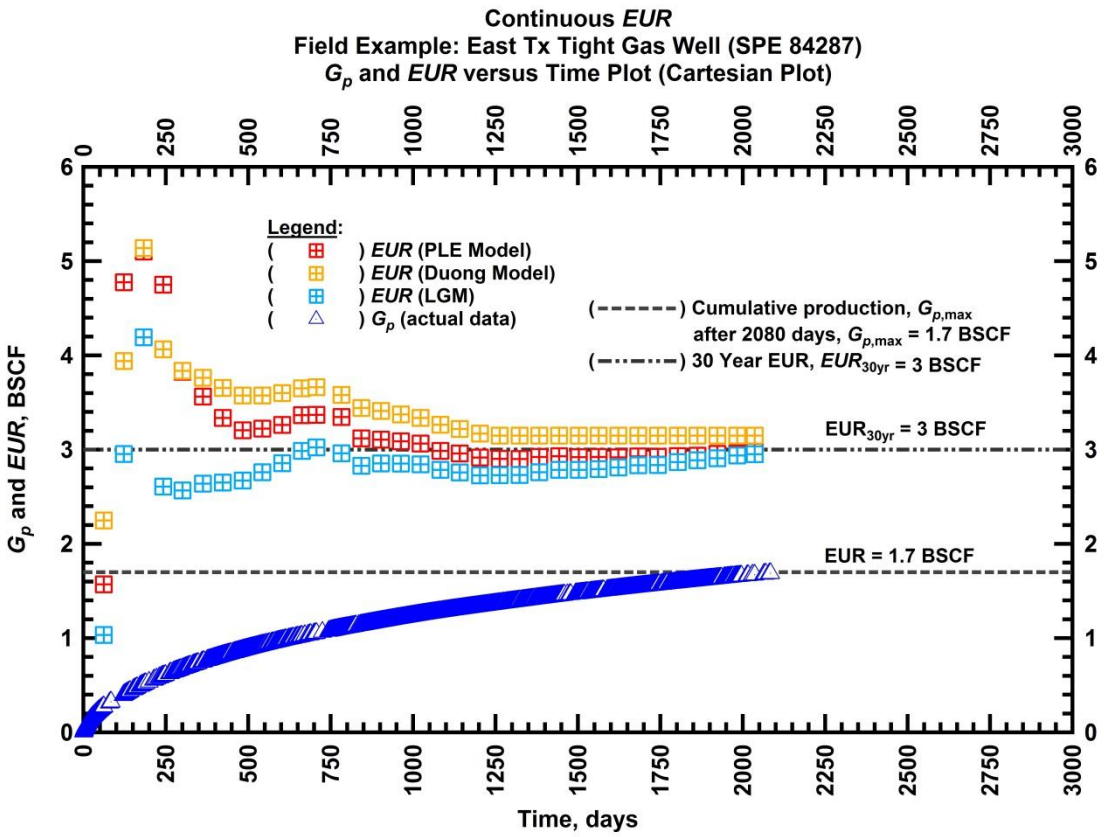

Figure 3.11 — (Cartesian Plot): *EUR* estimates from PLE, logistic growth, and Duong models matches and $G_{p,max}$ of East Tx tight gas well.

This analysis shows that, in the absence of boundary-dominated flow regime, all the models result in a quality match during transient flow regime and all models converge to a similar *EUR* value although at different rates. This shows that all time-rate relations can be used to model transient flow regimes.

3.4.3 Numerical Simulation Case: East Tx Tight Gas Well (SPE 84287)

In this section we consider production data generated from a numerical simulation of the field data case considered in the previous section. A vertical well model with finite conductivity vertical fractures is modeled. The numerical simulation data was generated by (Ilk et al. 2008a). The model input parameters are given in Table 1.1. Fig. 1.1 shows the historical flow rate and cumulative production data over a 6 year period.

In the previous section, we have seen that the field data did not exhibit the boundary-dominated flow regime. As a result, all of the models yielded a good match for the observed (transient) flow regime. **Fig. 3.12** shows the PLE model matches obtained from "continuous *EUR*" analysis of the simulated production data. In this case, the diagnostic functions show boundary-dominated flow regime. The *D*-, *b*-parameters and β-derivative show deviation from transient flow characteristics to transition/boundary-dominated flow regime after about 200 days of production. The *b*-parameter shows value greater than 0.5 during the early time periods because of dominant finite conductivity behaviors during this period.

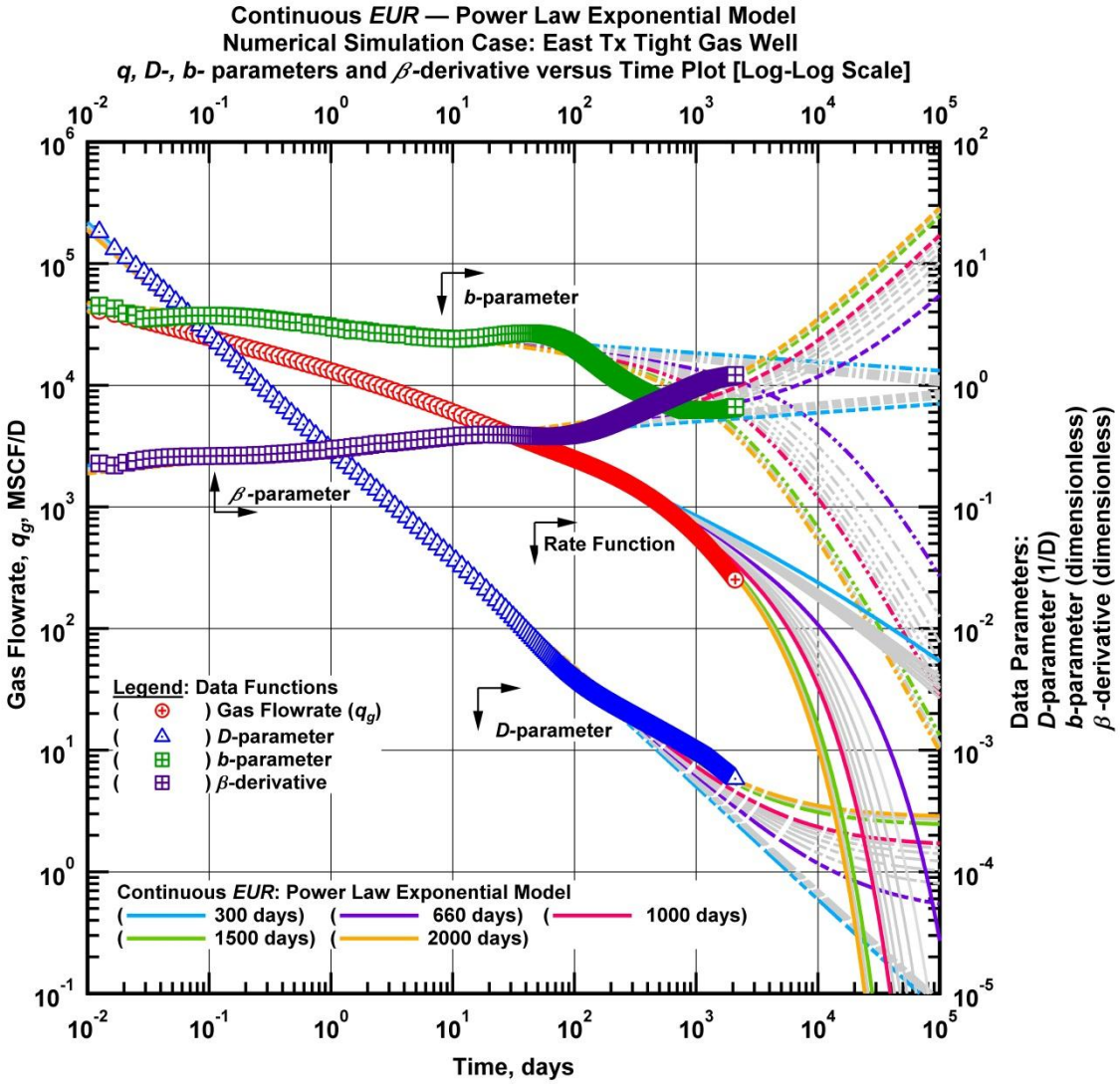

Figure 3.12 — (Log-log Plot): Continuous *EUR* analysis. Flow rate (q_g), *D*-, *b*-parameter and β-derivative versus production time. PLE model matches for numerical simulation case of East Tx tight gas well.

In this case the D_∞ parameter was used after about 300 days of production. As a result the model was able to match transient and boundary-dominated flow regimes successfully.

Fig. 3.13 shows the Duong model matches obtained from "continuous *EUR*" analysis. We can see that during early time period, the model matches the data very well. However, when boundary conditions dominate, the match quality is reduced. This shows that Duong model cannot match transition/boundary-dominated flow regimes very well and the model should not be forced to match this flow period.

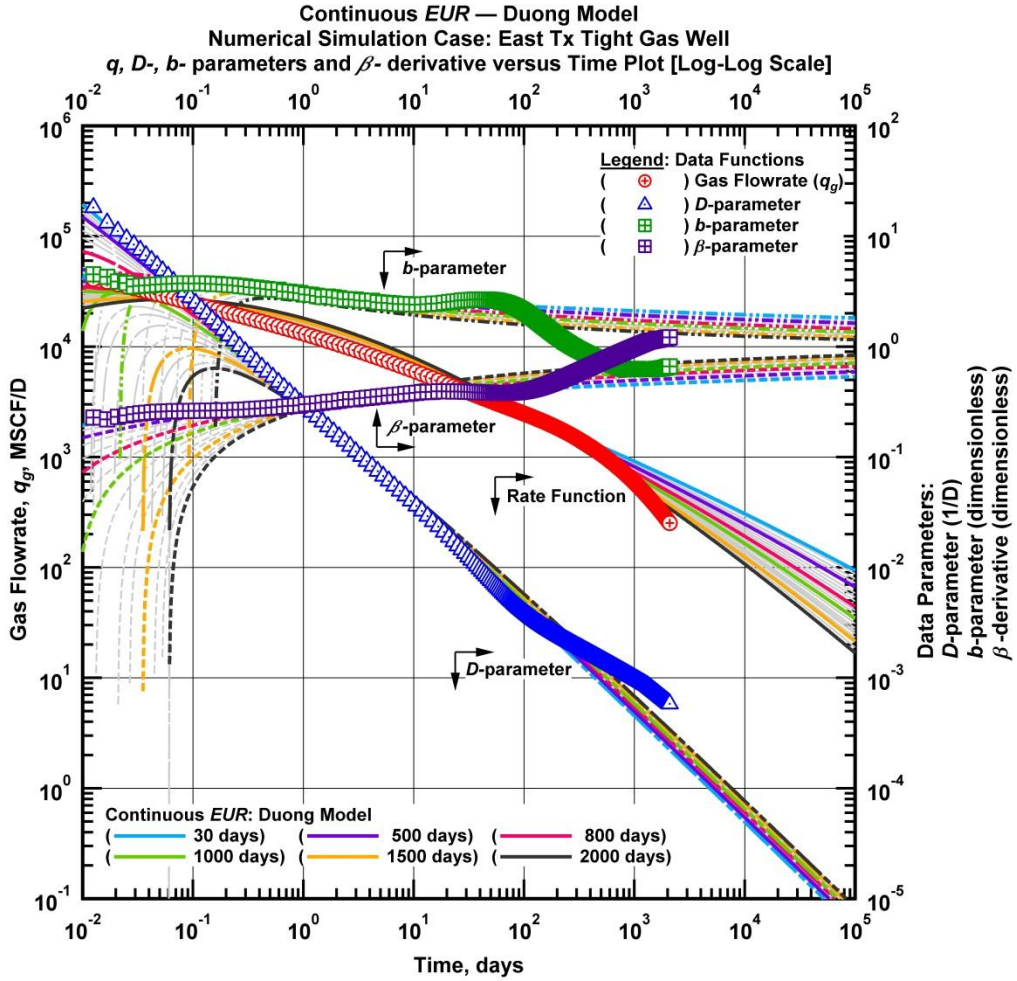

Figure 3.13 — (Log-log Plot): Continuous *EUR* analysis. Flow rate (q_g), *D*-, *b*-parameter and β-derivative versus production time. Duong model matches for numerical simulation case of East Tx tight gas well.

Fig. 3.14 shows logistic growth model matches obtained from "continuous *EUR*" analysis. The model was able to provide quality match to the data during the transient and transition flow regimes.

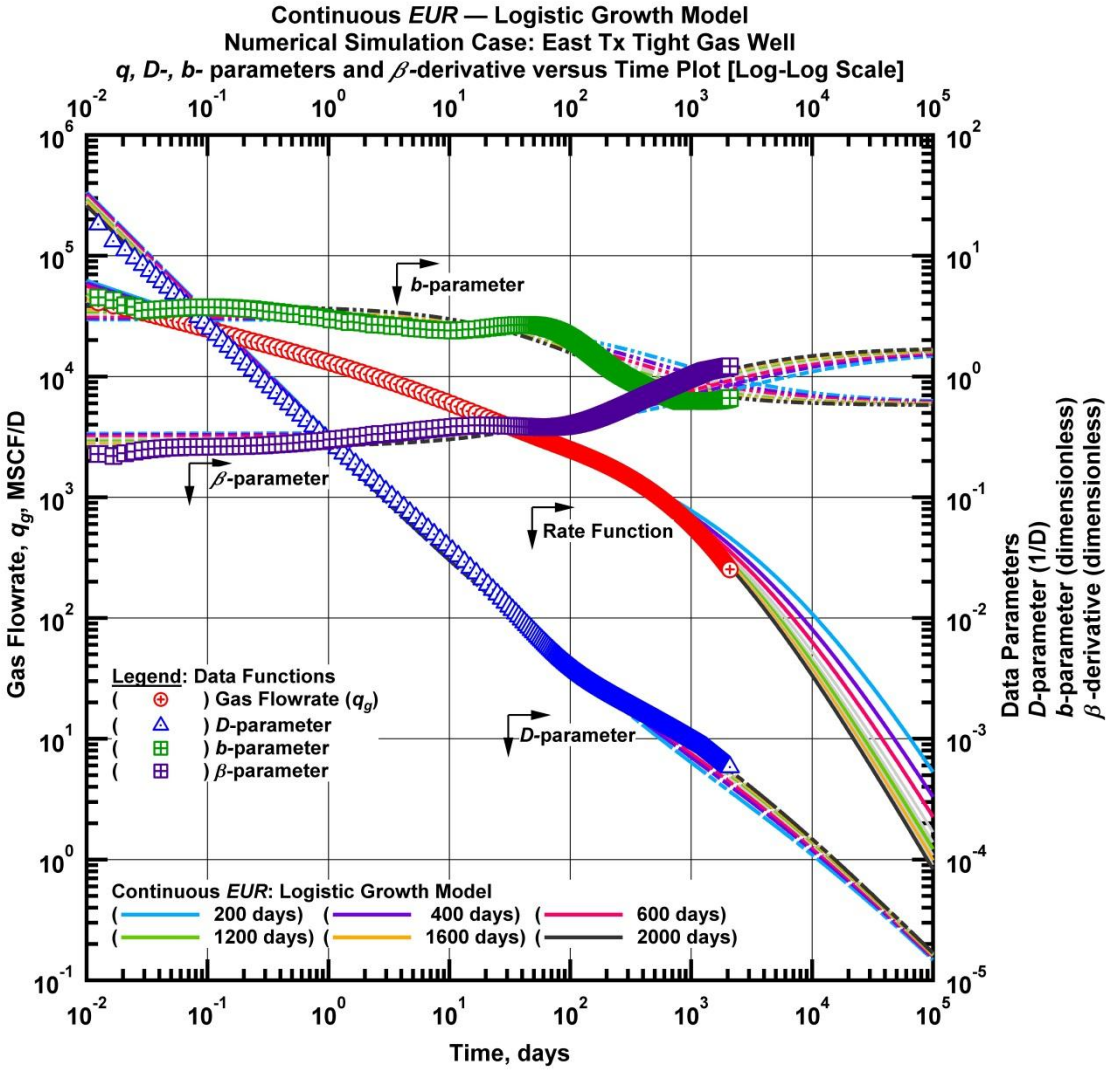

Figure 3.14 — (Log-log Plot): Continuous *EUR* analysis. Flow rate (q_g), *D*-, *b*-parameter and β-derivative versus production time. Logistic growth model matches for numerical simulation case of East Tx tight gas well.

Fig. 3.15 shows the *EUR* values calculated from the model matches at each successive time step plotted against the production time. The numerical simulation case was forecasted to a 30 year period to visualize the accuracy of the 30 year reserve estimate obtained from the models. The *EUR* values estimated for each model increase and then decrease significant at early times and stabilize soon after. As mentioned

earlier the D_∞ parameter of the PLE model was initiated after about 300 days when boundary effects were stating to dominate. The PLE model *EUR* estimates stabilize faster slightly underestimating reserves by 7 percent. The Duong model converges slowly in this case. The model matches of Duong model were forced until the *EUR* estimates converged. However, the model match results on Fig. 3.13 showed that that the quality of match was reduced for model matches obtained after about 300 days when boundary effects seem to have dominated the production data profile. If the "continuous *EUR*" analysis was stopped after the 300 days, the Duong model overestimates reserves by 135 percent. In this case the "continuous *EUR*" analysis was run until the model converged. Logistic growth model *EUR* estimates converged after about 1000 days with good fits to the data. The *EUR* values were overestimated by about 7%.

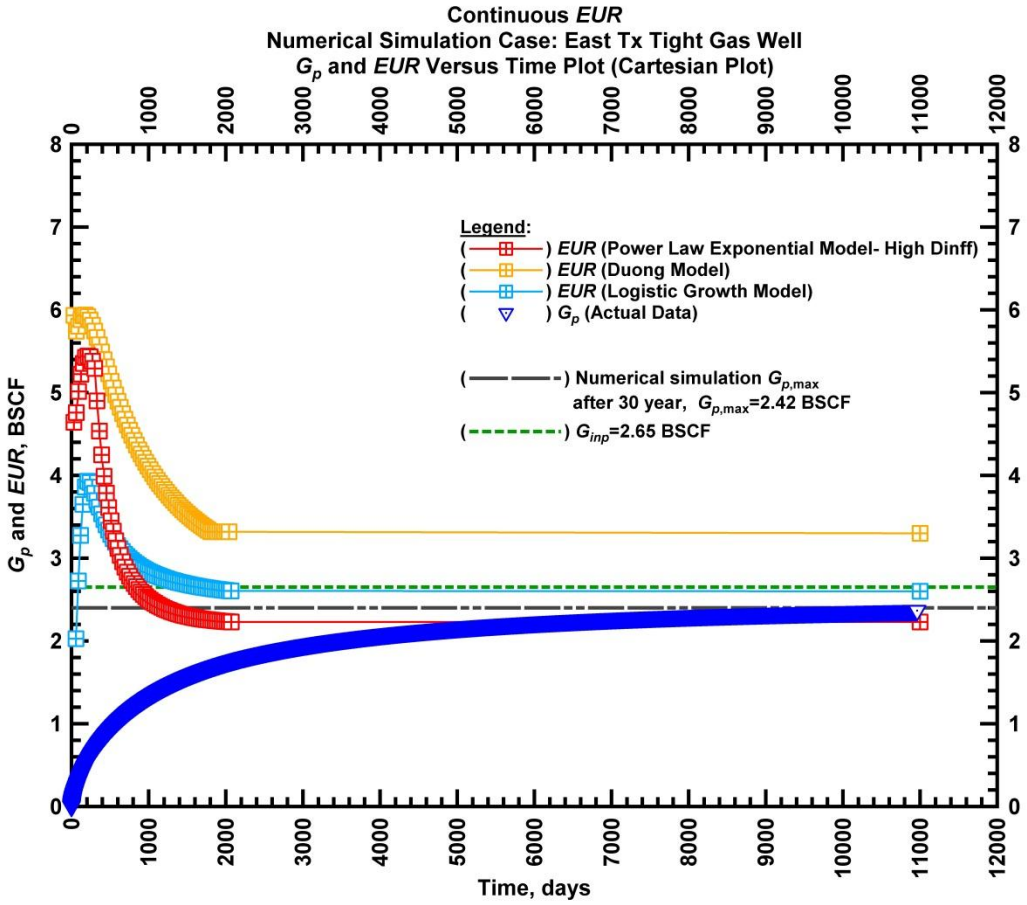

Figure 3.15 — (Cartesian Plot): *EUR* estimates from PLE, logistic growth, and Duong models matches and $G_{p,max}$ projected from numerical simulation case (East Texas tight gas well).

CHAPTER IV

MODIFIED TIME-RATE RELATIONS

In the previous chapter we demonstrated that the PLE model, logistic growth model, and Duong models yield good matches for the long transient flow regimes observed from horizontal multiply-fractured wells producing in unconventional reservoirs. We have shown that the PLE model behaves exceptionally well across all flow regimes observed from such reservoirs. However; the logistic growth model and the Duong model do not provide accurate matches to boundary-dominate flow behavior observed after long periods of production. As a result, production forecasting and reserve estimation using these models will result in significantly higher reserve estimates.

In this section we develop new time-rate relations based on the logistic growth model and the Duong models. We use diagnostic plots and development schemes to modify these models to take in to account the transition and boundary-dominated flow regimes.

4.1 Modified Duong Model – 1 (MDNG – 1)

This derivation of this modification of the Duong model is based on the exponential decline behavior that is observed when constant compressibility fluids are flowing at boundary-dominated flow conditions, where a constant flowing bottomhole pressure is maintained at the well in a closed reservoir system. The loss-ratio derivation of Arps' exponential time-rate relation is characterized by a constant decline parameter ($1/D$). Eq. 4.1 shows the D-parameter derivation for the Duong model. The loss-ratio derivation of Duong model shows time dependence at all times. We can re-write the loss-ratio derivation by including a constant decline parameter, D_{DNG}, at late times. This technique parallels the methods used in the derivation of the power law exponential model (Ilk et al. 2008a). The new Duong model loss-ratio relation is given by:

$$D(t) = mt^{-1} - at^{-m} + D_{DNG} \quad \text{.....(4.1)}$$

From the loss-ratio derivation we can derive, the time-rate relation of modified Duong model (MDNG-1). The derivation is shown in **Appendix A**. The time rate relation of MDNG-1 is given by:

$$q(t) = q_{t_1}\left(\frac{t_1}{t}\right)^m \exp\left[\frac{a}{1-m}\left(t^{1-m} - t_1^{1-m}\right) - D_{DNG}(t - t_1)\right] \quad \text{.....(4.2)}$$

In this derivation q_{t1} is the rate estimated at t_1. The b-parameter and β-derivative of MDNG-1 are given by:

$$b(t) = \frac{mt^m(t^m - at)}{(at - t^m(m + D_{DNG}t))^2} \quad \text{.....(4.3)}$$

$$\beta(t) = t[D_{DNG} + \frac{m}{t} - at^{-m}] \quad \text{.....(4.4)}$$

It should be noted that MDNG-1 does not allow for the direct development of a cumulative production relation. Hence, numerical methods are used to estimate cumulative production.

4.2 Modified Duong Model – 2 (MDNG – 2)

In this case we consider characteristics of production data obtained from unconventional reservoirs when plotted on a q/G_p versus *time* plot. **Fig 4.1** shows q/G_p versus *time* plot of production data generated from three numerical simulation cases with different permeability values. The input parameters are given in Table. 3.1.

Fig. 4.1 shows a straight line with a negative slope during the early time linear flow period. However the straight-line behavior deviates towards late time periods characterizing the boundary conditions that prevail during that time.

The early time straight-line behavior and the declining characteristics during late time can be characterized by power law behavior for the early time linear flow and with an exponential decline relation for the observed boundary characteristics. A new q/G_p relation can be formulated by integrating the early time power-law characteristics and late time exponential decline characteristics. The new q/G_p ratio relation is given by:

$$\frac{q}{G_p} = at^{-m}\exp[-D_{DNG}t] \quad \text{.....(4.5)}$$

The new time-rate relation can be derived from Eq. 4.5. The derivation is shown in **Appendix B.** Eq. 4.6 shows the new time rate relation.

$$q_g(t) = q_{t_1}\left(\frac{t_1}{t^m}\right)^m \exp\left[D_{DNG}(t_1 - t) + aD_{DNG}{}^{m-1}\left(\Gamma[1-m, D_{DNG}t_1] - \Gamma[1-m, D_{DNG}t]\right)\right] \quad \text{.....(4.6)}$$

In this derivation q_{t1} is the rate estimated at t_1. The associated *D*-, *b*-, and β-parameters are given as follows:

$$D(t) = D_{DNG} + \frac{m}{t} - a\exp[-D_{DNG}t]t^{-m} \quad \text{.....(4.7)}$$

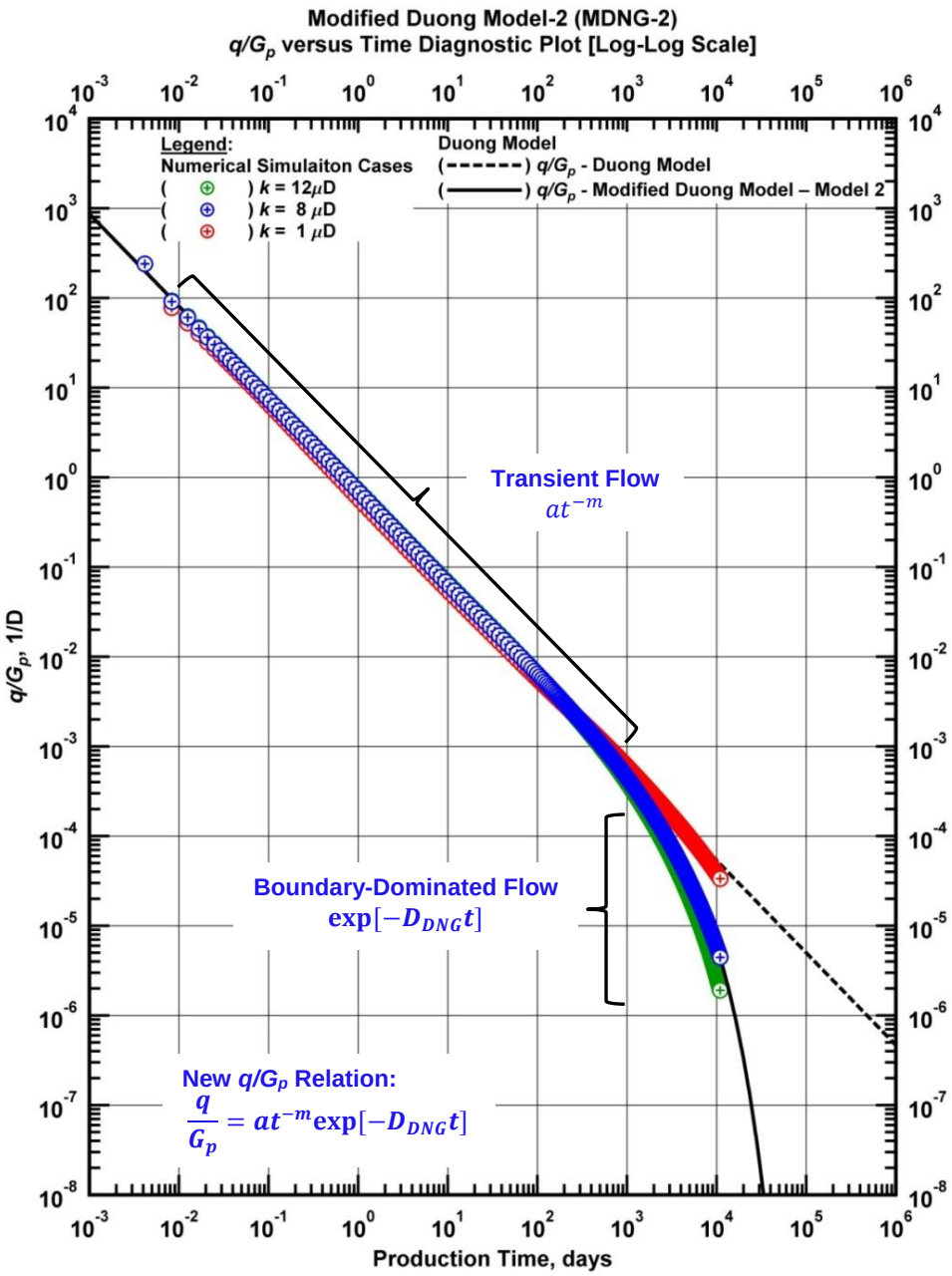

Figure 4.1 — (Log-log Plot): q/G_p versus production time. Duong model and Modified Duong Model – 2 (MDNG – 2) diagnostic plot match for numerical simulation cases.

$$b(t) = \frac{\exp[D_{DNG}t]t^m[\exp[D_{DNG}t]mt^m - at(m + D_{DNG}t)]}{[at - \exp[D_{DNG}t]t^m(m + D_{DNG}t)]^2} \quad \text{..... (4.8)}$$

$$\beta(t) = D_{DNG}t + m - a\exp[-D_{DNG}t]t^{-m+1} \quad \text{..... (4.9)}$$

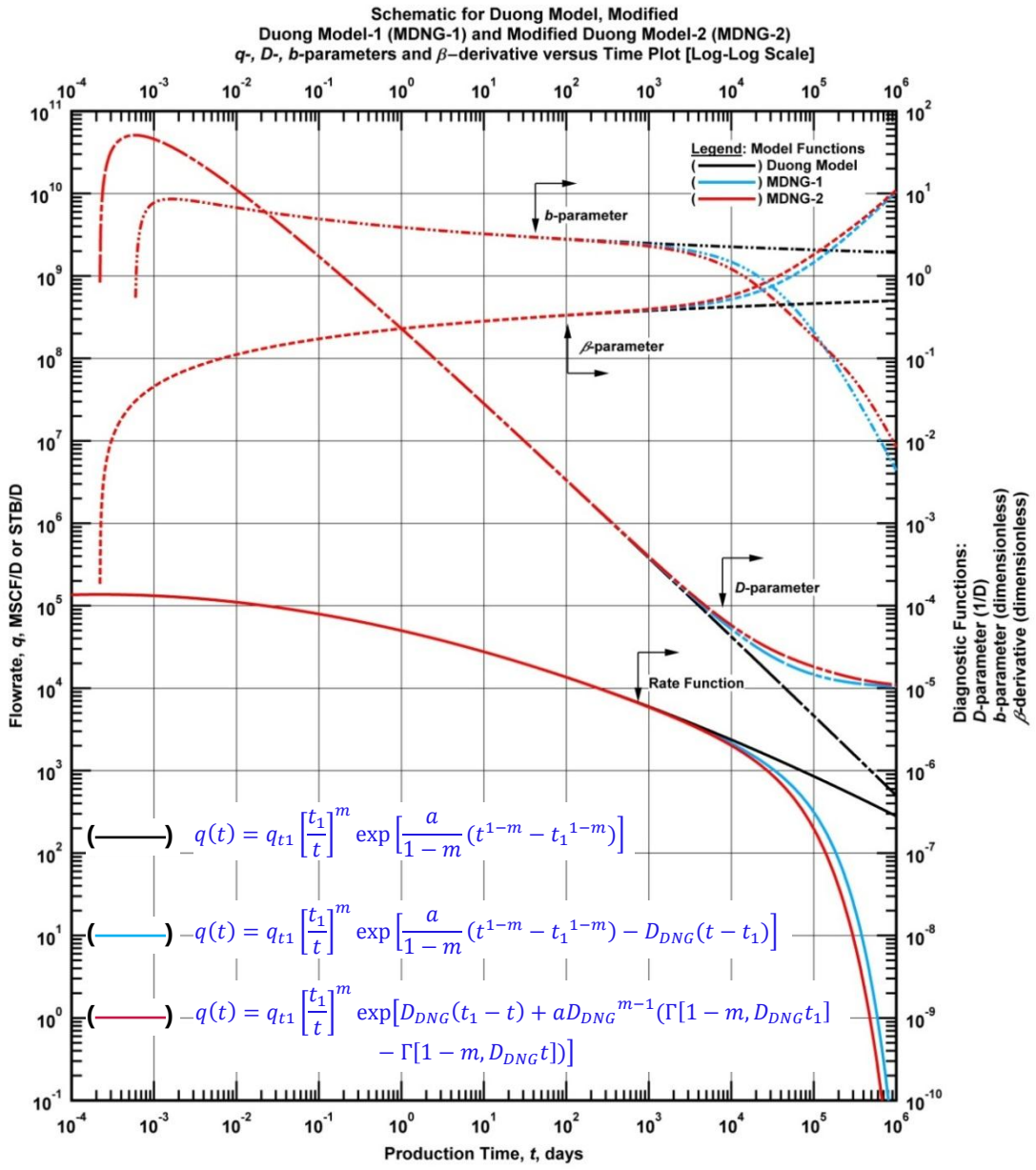

Figure 4.2 — (Log-log Plot): Flow rate (q_g), *D*-, *b*-parameter and β-derivative versus production time. Schematic of Duong model, MDNG – 1, and MDNG – 2 time rate models.

The cumulative production relation can be explicitly derived. It is given by:

$$G_p(t) = \frac{q_{t_1}}{a}{t_1}^m \exp\left[D_{DNG}t_1 + a{D_{DNG}}^{m-1}\left(\Gamma[1-m, D_{DNG}t_1] - \Gamma[1-m, D_{DNG}t]\right) - \exp\left[D_{DNG}t_1\right]\right] \quad \text{..... (4.10)}$$

Fig. 4.2 shows a schematic of the new time rate relations (MDNG-1, MDNG-2) as well as the original Duong model showing the time-rate, *D*-, *b*- and β-derivative behaviors. We can see that the new models do accurately characterize the boundary-dominated flow regime.

4.3 Modified Logistic Growth Model – 1 (MLGM – 1)

Similar to the derivation method used for MDNG-1, we apply a constant decline parameter to the loss-ratio derivation of logistic growth model to characterize the exponential decline behavior observed during boundary conditions. The inverse "loss-ratio" derivation (*D*-parameter) of logistic growth model is given by Eq. 4.11. The modified *D*-parameter is given by:

$$D(t) = \frac{\hat{a} - \hat{a}\hat{n} + (1+\hat{n})t^{\hat{n}}}{t(\hat{a} + t^{\hat{n}})} + D_{LGM} \quad \text{..... (4.11)}$$

The time-rate relations can be derived from the new *D*-parameter formulation (Eq. 4.11). The derivation is shown in **Appendix C**. The time-rate relation and *b*- parameter are given by:

$$q_g(t) = \frac{\hat{a}K\hat{n}t^{(\hat{n}-1)}}{(\hat{a} + t^{\hat{n}})^2} \exp[-D_{LGM}t] \quad \text{..... (4.12)}$$

$$b(t) = \frac{-\hat{a}^2(\hat{n}-1) - 2\hat{a}(\hat{n}^2-1)t^n + (\hat{n}+1)t^{2\hat{n}}}{(\hat{a}(1-\hat{n}+D_{LGM}t) + t^{\hat{n}}(1+\hat{n}+D_{LGM}t))^2} \quad \text{..... (4.13)}$$

Fig. 4.4 shows schematics of the new time-rate relation (MLGM-1).

4.4 Modified Logistic Growth Model (MLGM – 2)

This derivation is based on the characteristics of the ratio of gas in place to cumulative production data obtained from unconventional reservoirs. (Clark et al. 2011) have shown that the logistic growth model can be written as:

$$\frac{K}{Q_g(t)} - 1 = \hat{a}t^{-\hat{n}} \quad \text{..... (4.14)}$$

In Eq. 4.14, *K* is the initial gas in place determined through volumetric calculations. **Fig. 4.3** shows plot of *K/Q*(t) – 1 plotted against time for a data generated from a numerical simulation. Eq. 4.14 suggests that the plot should display a straight line behavior with negative slope. However, investigation of long-term production data from unconventional reservoirs shows straight line behavior followed by a fast decline and finally converging at a constant value. This is observed on Fig. 4.3. Based on this diagnostic plot we can suggest a new relation for *K/Q*(*t*) – 1 to represent the linear flow regime with a power-law relation, the

boundary-dominated flow regime with an exponential decline relation and finally converges at a constant value. The new $K/Q(t) - 1$ formulation is given by:

$$\frac{K}{Q_g(t)} - 1 = \hat{a}t^{-\hat{n}} \exp[-D_{LGM}t] + R \quad \text{..... (4.15)}$$

In Eq. 4.15, the parameter "D_{LGM}" characterizes boundary-dominated flow regime. The parameter R describes the percentage of the initial gas-in-place that cannot be produced under the existing completion conditions and production constraints.

The time-rate relation can be derived from Eq. 4.15. The derivation is shown in **Appendix D**. The time-rate relation is given by:

$$q_g(t) = \frac{\hat{a}\exp[D_{LGM}t]Kt^{\hat{n}-1}(\hat{n} + D_{LGM}t)}{\left(\hat{a} + (1+R)\exp[D_{LGM}t]t^{\hat{n}}\right)^2} \quad \text{..... (4.16)}$$

And the cumulative production relation is given by:

$$Q_g(t) = \frac{Kt^{\hat{n}}\exp[D_{LGM}t]}{\hat{a} + (1+R)\exp[D_{LGM}t]t^{\hat{n}}} \quad \text{..... (4.17)}$$

The D- and b-parameters are given by:

$$D(t) = \frac{\hat{n} + (\hat{n} + D_{LGM}t)^2 - 2\psi}{t(\hat{n} + D_{LGM}t)} \quad \text{..... (4.18)}$$

$$b(t) = \frac{2\psi^2 - \psi(2(\hat{n} + (\hat{n} + D_{LGM}t)^2)) + \hat{n}(\hat{n} + (\hat{n} + D_{LGM}t)^2 + 2D_{LGM}t)}{(\hat{n} + (\hat{n} + D_{LGM}t)^2 - 2\psi)^2} \quad \text{..... (4.19)}$$

Where ψ is given by:

$$\psi(t) = \frac{\hat{a} + (\hat{n} + D_{LGM})^2}{\hat{a} + \exp[D_{LGM}t](1+R)t^{\hat{n}}} \quad \text{..... (4.20)}$$

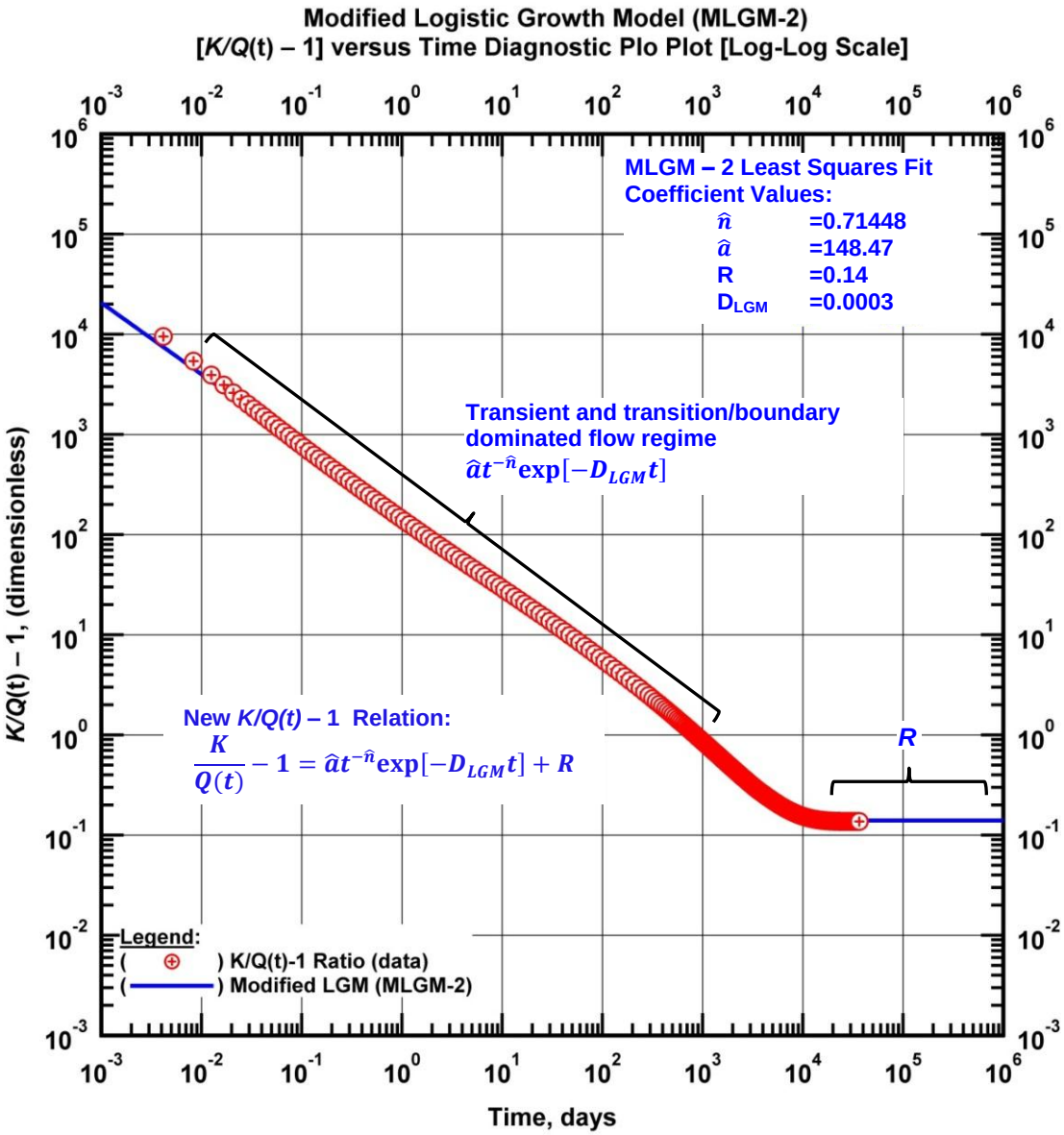

Figure 4.3 — (Log-log Plot): $K/G_p - 1$ versus production time. Modified Logistic Growth Model (MLGM – 2) match for numerical simulation case.

Fig. 4.4 shows schematic of the modified and original logistic growth model.

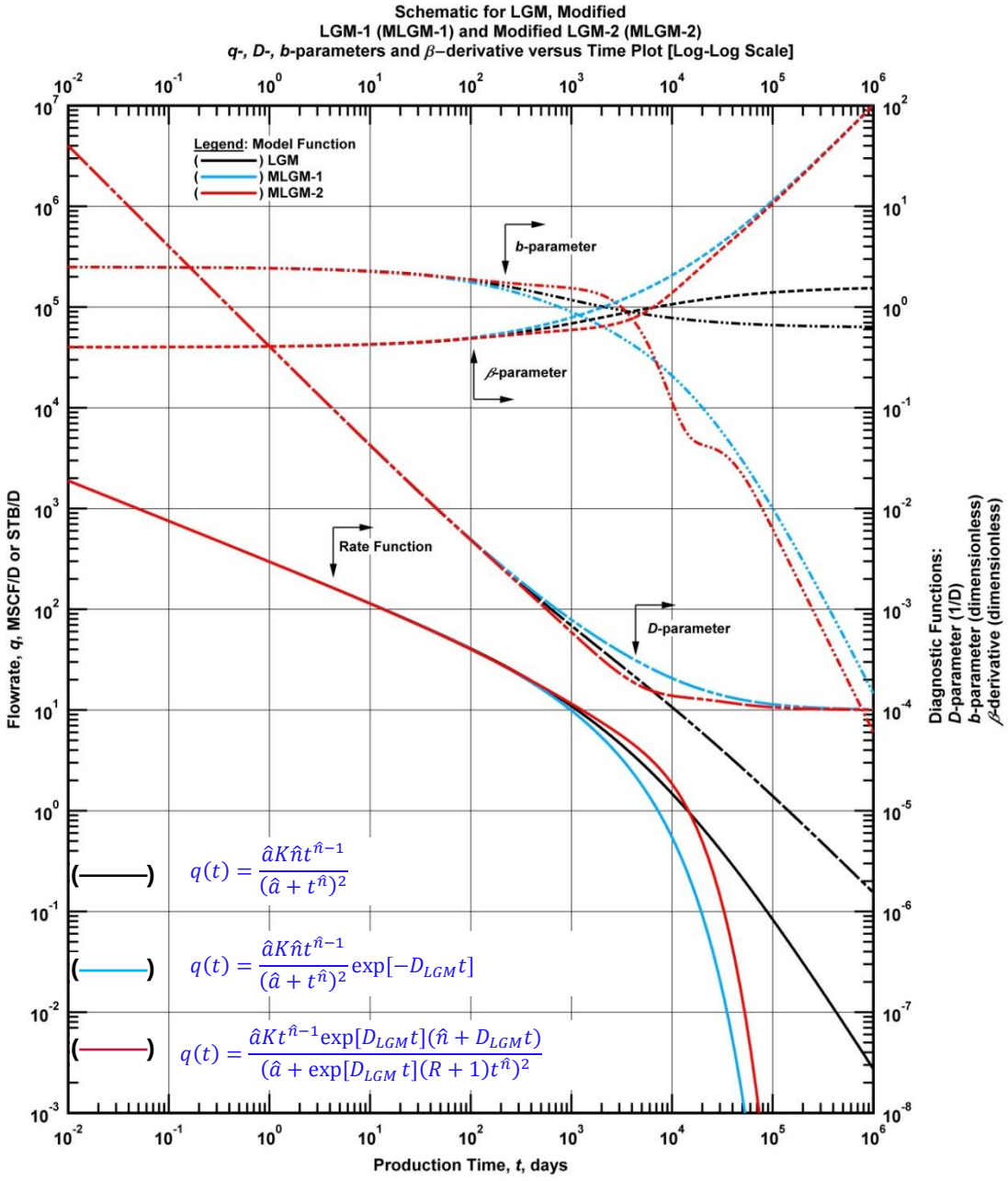

Figure 4.4 — (Log-log Plot): Flow rate (q_g), *D*-, *b*-parameter and β-derivative versus production time. Schematic of logistic growth model, MLGM – 1, and MLGM – 2.

The diagnostic functions shown in **Fig. 4.4** verify that the modified logistic growth model relations do correctly characterize the transition and boundary-dominated flow regimes.

We next present application of the new time-rate models using production data obtained from wells completed in tight/shale gas reservoirs.

4.5 Field Example 1 – Mexico Tight Gas Well

In this case we consider a hydraulically fractured vertical well completed in a tight gas reservoir. The reservoir has permeability less than 0.001 md (Blasingame et al. 2007). This well is the only one producing in the field. **Fig. 4.5** shows the historical production data over a 40 year period. A data diagnostics was conducted to remove irregular data points. Then the diagnostic functions were evaluated using the Bourdet derivative algorithm with the time-rate data.

In this case, all of the diagnostic functions indicate typical linear flow and boundary-dominated flow regimes. The *b*-parameter has a constant value of 2 during the early time period lasting for about 10 years. Similarly the β-derivative has a value of 0.5 lasting for the same time period. During late time period, the diagnostic functions deviate from the linear flow regime trend. The β-derivative shows a unit slope behavior at late times indicating boundary-dominated flow regime. Similarly the *D*-and *b*- parameters deviate during the boundary-dominated flow regime.

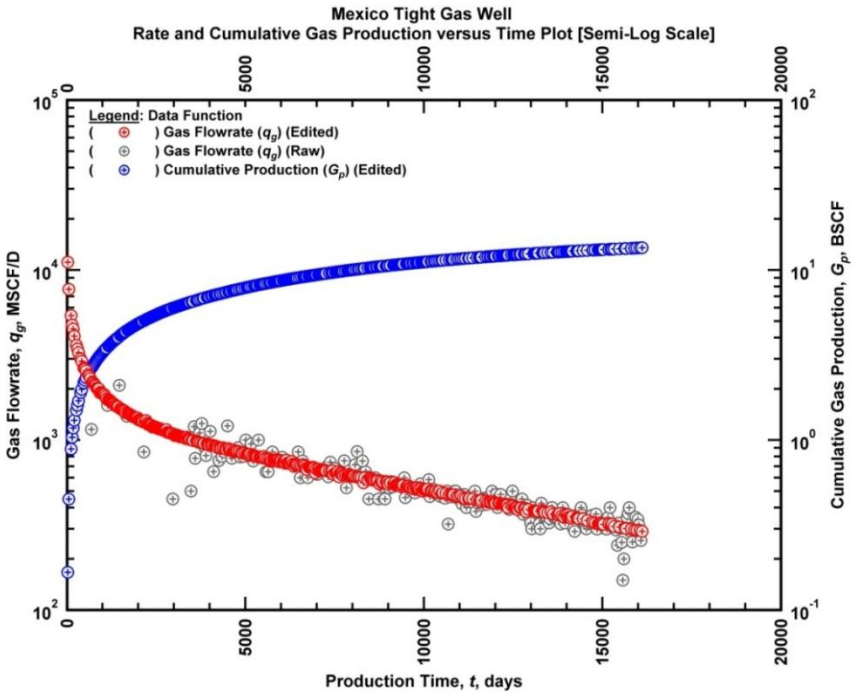

Figure 4.5 — (Semi-log Plot): Production history plot for field data case – flow rate (q_g) and cumulative production (G_p) versus time (Mexico tight gas well).

The objective when using the modified parameters is to obtain a quality match across all flow regimes. First we consider MDNG-1 and MLGM-1 since these both rely on the *D*-parameter diagnostic plot for their derivation. Since the data shows boundary-dominated flow regime, first the linear flow regime is matched by setting the constant decline parameters (D_{DNG} and D_{LGM}) to zero. First we match the linear flow regime. Then, the constant decline parameters are adjusted to match the boundary-dominated flow regime. **Table 4.1** shows the model match parameters for MDNG-1 and MLGM-1.

Table 4.1 — MDNG – 1 and MLGM – 1 time-rate relations model parameters (Mexico tight gas well).

Modified Duong Model (MDNG – 1)

q_{t1}=0.0042 day (MSCFD)	a	m	D_{Dng} (D^{-1})
32,460	0.59	0.996	0.0000398

Modified Logistic Growth Model (MLGM – 1)

K (MSCF)	$\hat{a}$	$\hat{n}$	D_{LGM} (D^{-1})
106,733,955.8	1289.7	0.55	0.0000002

Next we match the data using MDNG – 2 model. In this analysis the model parameters (a, m, and D_{DNG}) are determined on a plot of *q/Gp* versus *time*. This diagnostic plot is shown in **Fig. 4.6.**

Model parameter q_{t1} is then estimated by fixing the remaining parameters and matching the data manually or through regression to obtain a fit to the time-rate data. In this case q_{t1} is estimated at t_1=1 Days. This approach is probably the simplest way to obtain the model parameters. It is also possible to estimate the model parameters using the time-rate relation of MDNG – 2 (Eq. 4.6) if advanced computational tools are available. The model parameters are summarized in **Table 4.2.**

Table 4.2 — MDNG – 2 time-rate relation model parameters (Mexico tight gas well).

Modified Duong Model (MDNG – 2)

q_{t1}=0.0042 day (MSCFD)	a	m	D_{Dng} (D^{-1})
32,460.8	0.59	0.996	0.000032

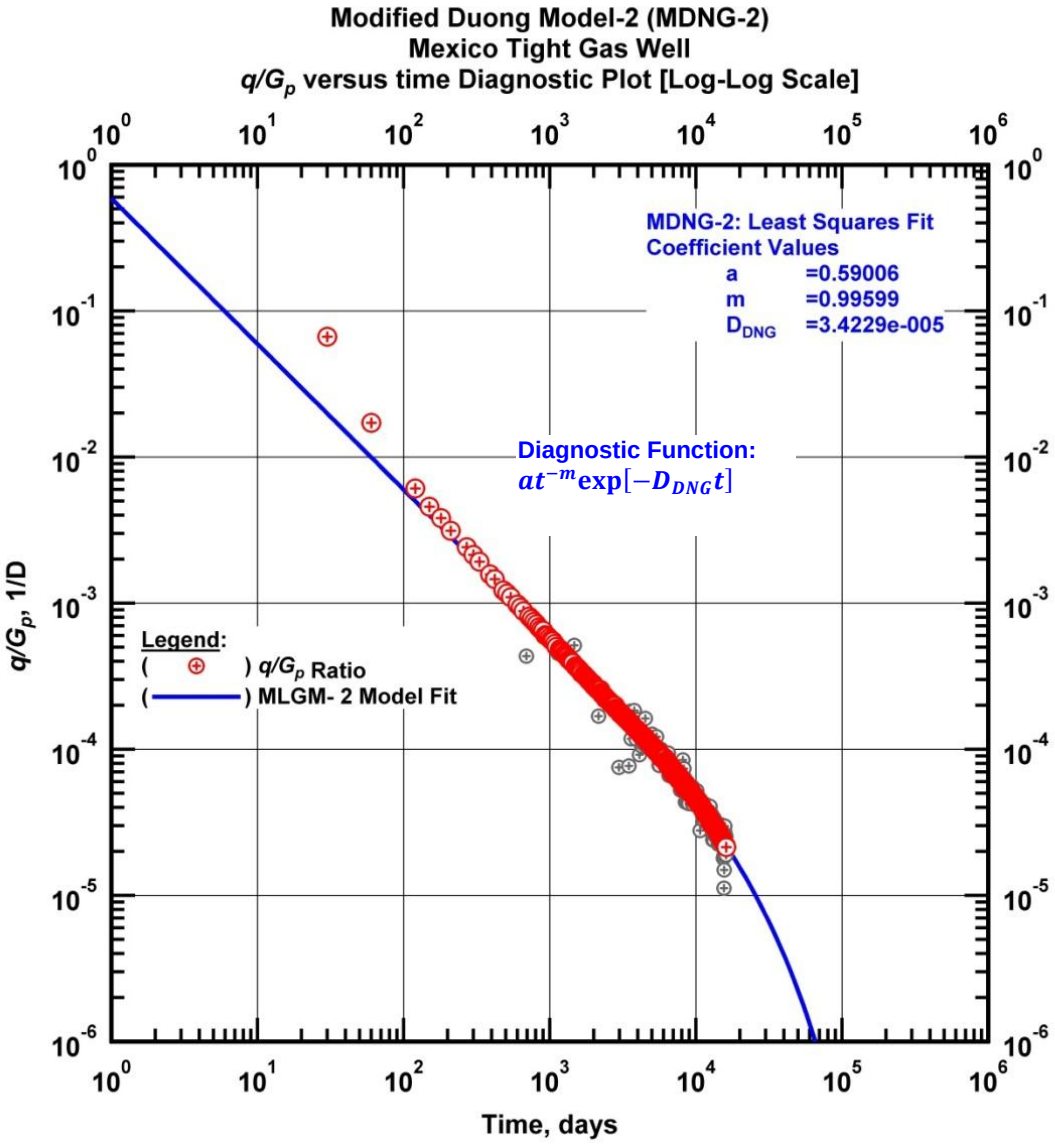

Figure 4.6 — (Log-log Plot): q/G_p versus production time. Modified Duong Model – 2 (MDNG – 2) diagnostic plot matches for Mexico tight gas well.

Next we match the data using MLGM – 2 model. In this case, the model parameters are estimated on plot of *K/Q* – 1 versus *time* plot. In this case, prior estimate of *K* (initial gas in place) was available from volumetric calculations. Hence, all the unknown parameters were estimated from the *K/Q* – 1 versus *time* diagnostic plot.

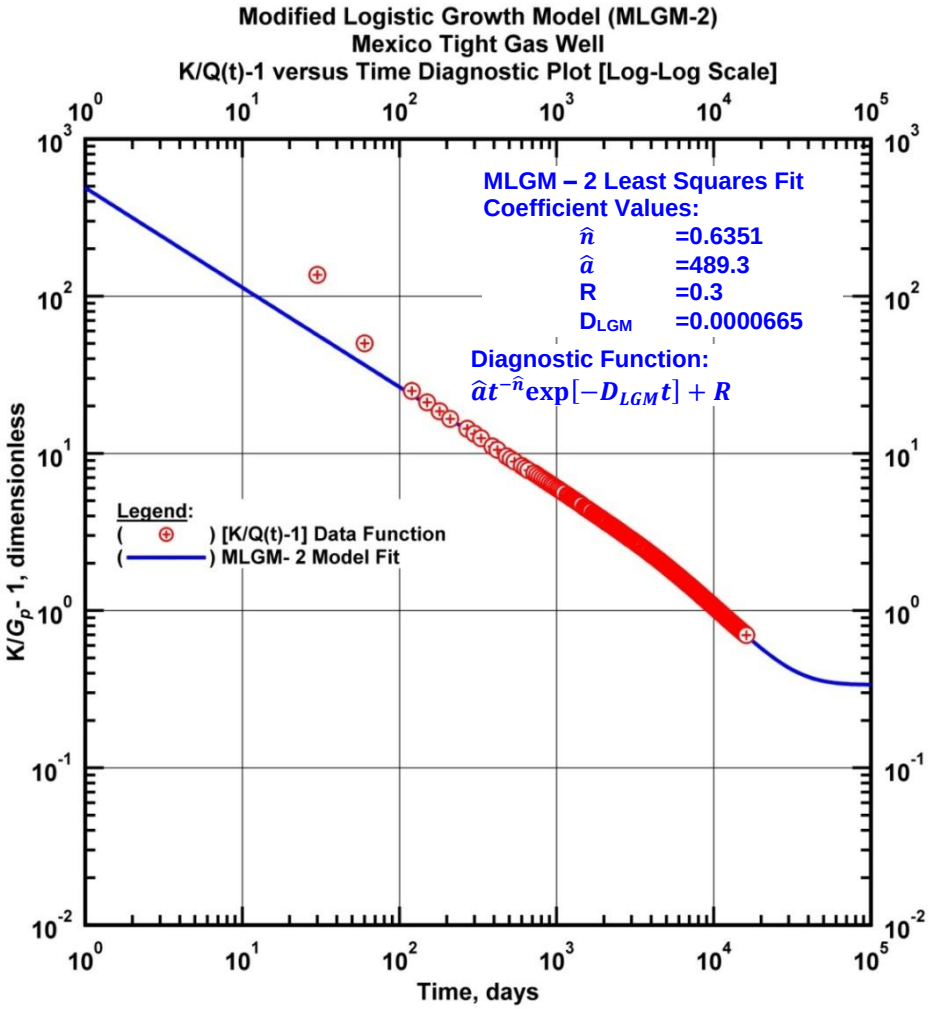

Figure 4.7 — (Log-log Plot): $K/G_p - 1$ versus production time. Modified Logistic Growth Model – 2 (MLGM – 2) diagnostic plot match for Mexico tight gas well.

Fig. 4.7 shows the diagnostic plot necessary to evaluate the model parameters. The model parameters are summarized in **Table 4.3.**

Fig 4.8 shows the resulting model match from all the time-rate relations. The modified relations have provided a quality match to the flow rate, *D*-,*b*-, parameters and to the β-derivative during the transient, transition and boundary dominated flow regimes. Duong and logistic growth model resulted in a poor match to the boundary-dominated flow regime.

Table 4.3 — MLGM – 2 time-rate relation model parameters (Mexico tight gas well).

Modified Duong Model (MLGM – 2)			
K			D_{LGM}
MSCF	$\hat{a}$	$\hat{n}$	(D^{-1})
22,959,527	489.3	0.635	0.0000665

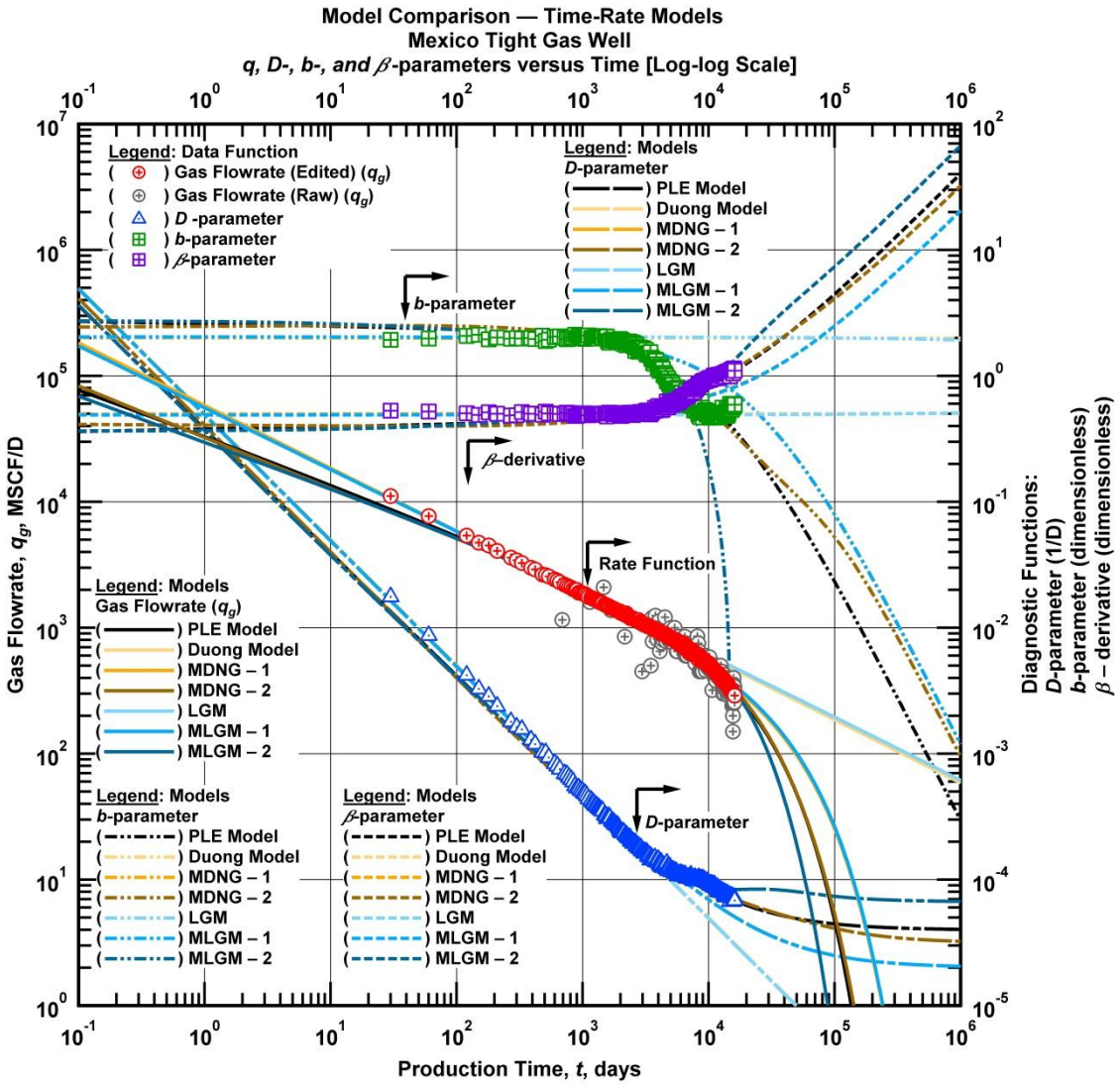

Figure 4.8 — (Log-log Plot): Flow rate (q_g), *D*-, *b*-parameter and β-derivative versus production time. PLE, logistic growth, Duong model, MLGM – 1, MLGM – 2, MDNG – 1, and MDNG – 2 time rate model matches for Mexico tight gas well.

Fig. 4.9 shows model match on the historical rate and cumulative production data. The modified relations successfully matched the early time data as well as late time boundary-dominated flow regimes.

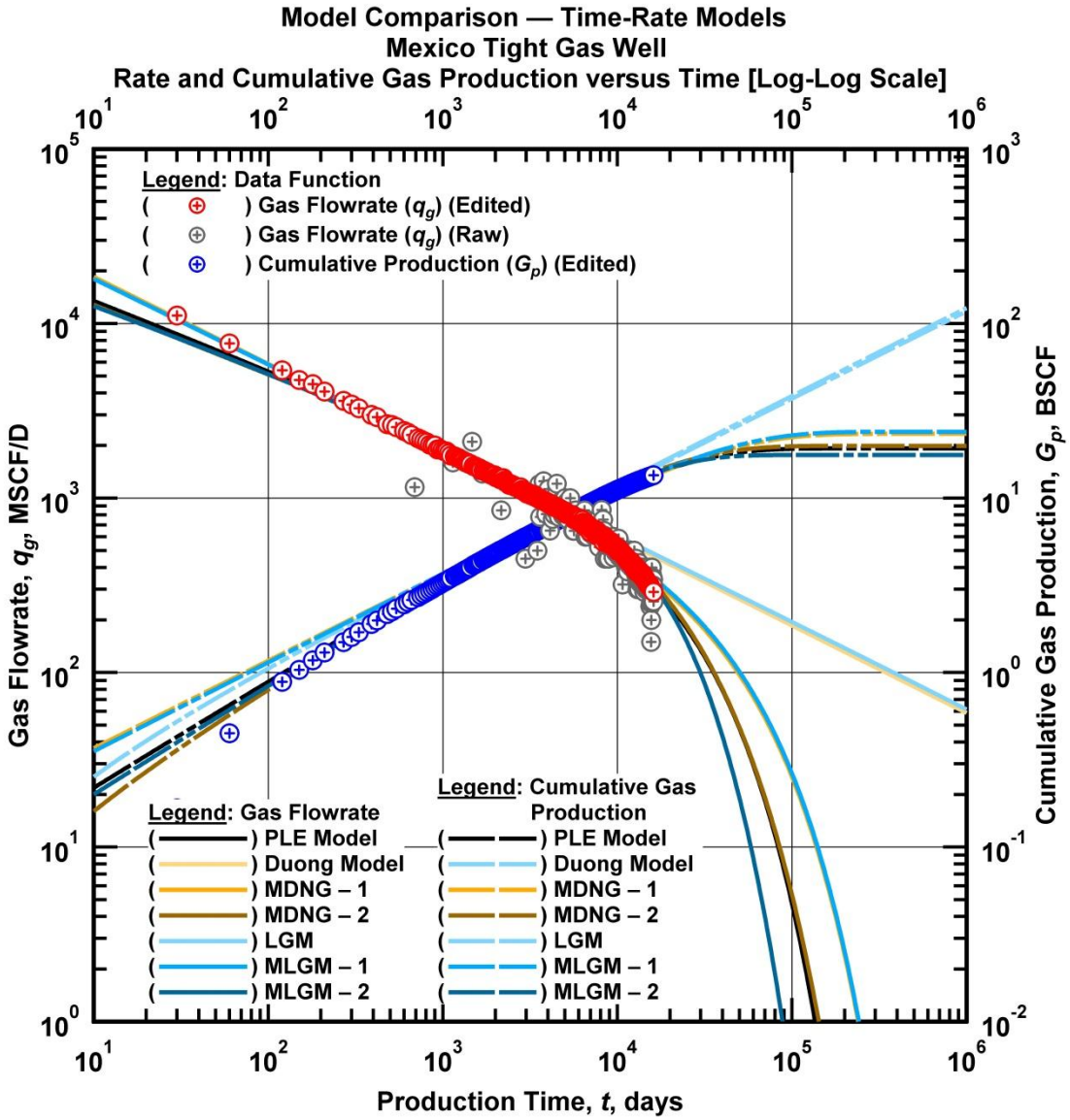

Figure 4.9 — (Log-log Plot): Rate and cumulative production versus time plot. PLE, logistic growth, Duong , MLGM – 1, MLGM – 2, MDNG – 1, and MDNG – 2 time-rate models matches for Mexico tight gas well.

Table 4.4 shows the cumulative production calculated at the end of the historical production using each of the models. The Duong and logistic growth models have significantly overestimated the cumulative production. The PLE and the modified relations have provided a reliable value of the cumulative production (and hence, *EUR*).

Table 4.4 — Comparison of calculated cumulative production values for Mexico tight gas well ($G_{p,max}$ = 13.52 BSCF).

Time-rate models	$G_{p,max}$
Duong model	14.84 BSCF
Logistic growth model	15.22 BSCF
Power-law exponential model (PLE)	13.70 BSCF
Modified Duong Model – 1 (MDNG – 1)	13.50 BSCF
Modified Duong Model – 2 (MDNG – 2)	13.80 BSCF
Modified Logistic Growth Model – 1 (MLGM – 1)	13.72 BSCF
Modified Logistic Growth Model – 2 (MLGM – 2)	13.83 BSCF

4.6 Field Example 2 – Barnett Shale Gas Well

This case is a vertical well with a single hydraulically fracture (of infinite conductivity) in a shale gas reservoir. Approximately 10 years of production history is available for analysis. A data quality control process is conducted to remove erroneous data points. The diagnostic functions were evaluated using the Bourdet derivative algorithm using the time-rate data. The historical production data is shown in **Fig. 4.10.**

The diagnostic functions indicate transient linear flow and boundary-dominated flow regimes. Although, the diagnostic function derivations are affected by the erratic time-rate data, the *D*-parameter **(Fig. 4.13)** shows a straight-line trend during the early time periods and then deviates towards the late time periods indicating boundary-dominated flow regime. Similarly, the β-derivative deviates with a unit slope line during the late time periods.

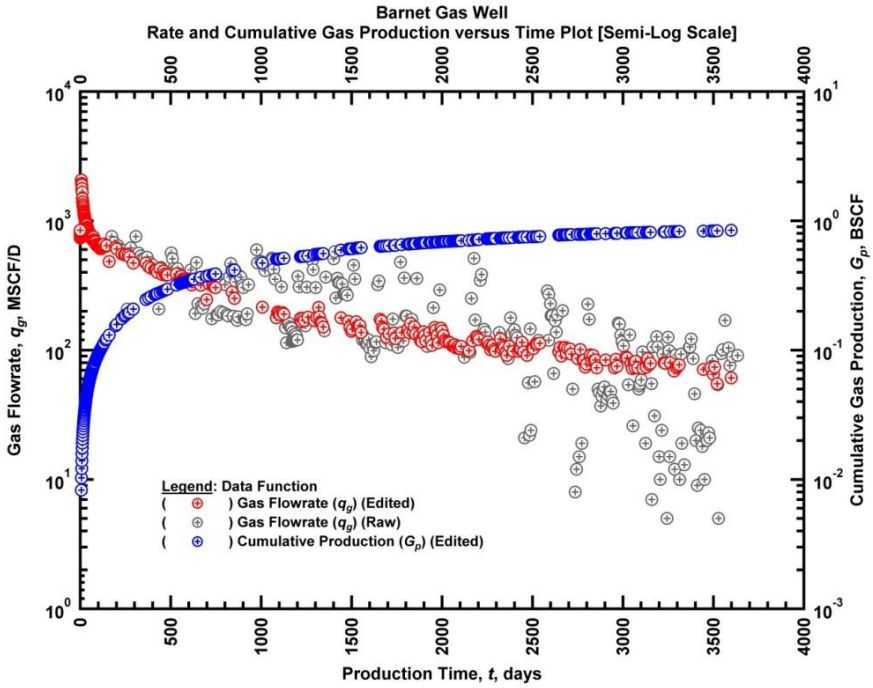

Figure 4.10 — (Semi-log Plot): Production history plot for numerical simulation case – flow rate (q_g) and cumulative production (G_p) versus time (Barnett shale gas well).

The objective when using the modified parameters is to obtain a quality match across all flow regimes. First we consider MDNG-1 and MLGM-1 since they both rely on the *D*-parameter diagnostic plot for their derivation. Since the data shows boundary-dominated flow regime, first the linear flow regime is matched by setting the constant decline parameters (D_{DNG} and D_{LGM}) to zero. Once a quality match is obtained in the linear flow regime, the constant decline parameters are adjusted to match the boundary-dominated flow regime. **Table 4.5** shows the model match parameters for MDNG-1 and MLGM-1.

Table 4.5 — MDNG – 1 and MLGM – 1 time-rate relations model parameters (Barnett shale gas well).

Modified Duong Model (MDNG – 1)

$q_{t1=0.001\ day}$ (MSCFD)	a	m	D_{Dng} (D^{-1})
70100	0.67	1.00005	0.000345

Modified Logistic Growth Model (MLGM – 1)

K (MSCF)	$\hat{a}$	$\hat{n}$	D_{LGM} (D^{-1})
13,776,210	3210.4	0.7	0.00025

Next we match the data using the MDNG-2 model. In this analysis the model parameters are determined on a plot of q/G_p versus *time*. This diagnostic plot is shown in **Fig. 4.11.**

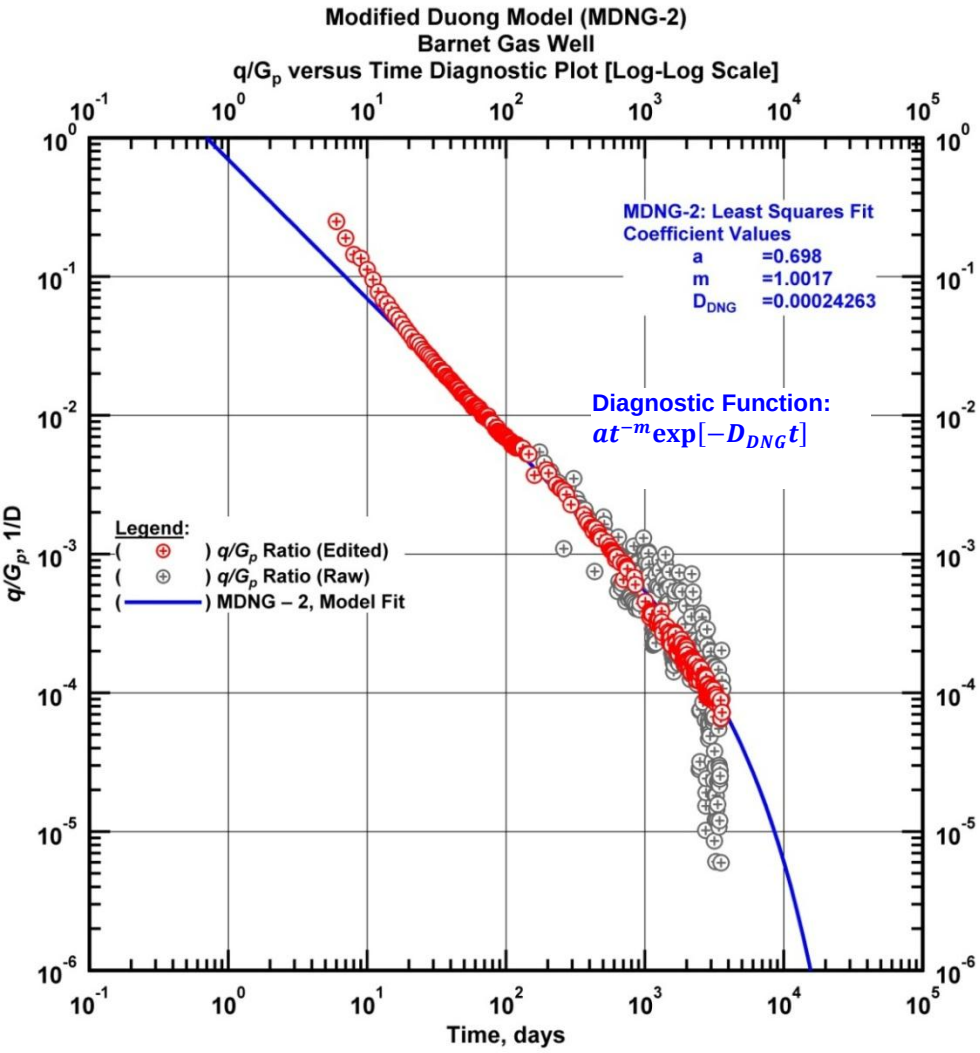

Figure 4.11 — (Log-log Plot): q/G_p versus production time. Modified Duong Model – 2 (MDNG – 2) diagnostic plot matches for Barnett shale gas well.

The model parameter q_{t1} is then estimated by fixing the remaining parameters and matching the data manually or through regression to obtain a fit to the time-rate data. In this case q_{t1} is estimated at t_1=1 days. This approach is the simplest way to obtain the model parameters. It is also possible to estimate the model parameters using the time-rate relation (Eq. 4.6) if advanced computation tools are available. The model parameters are summarized in **Table 4.6**

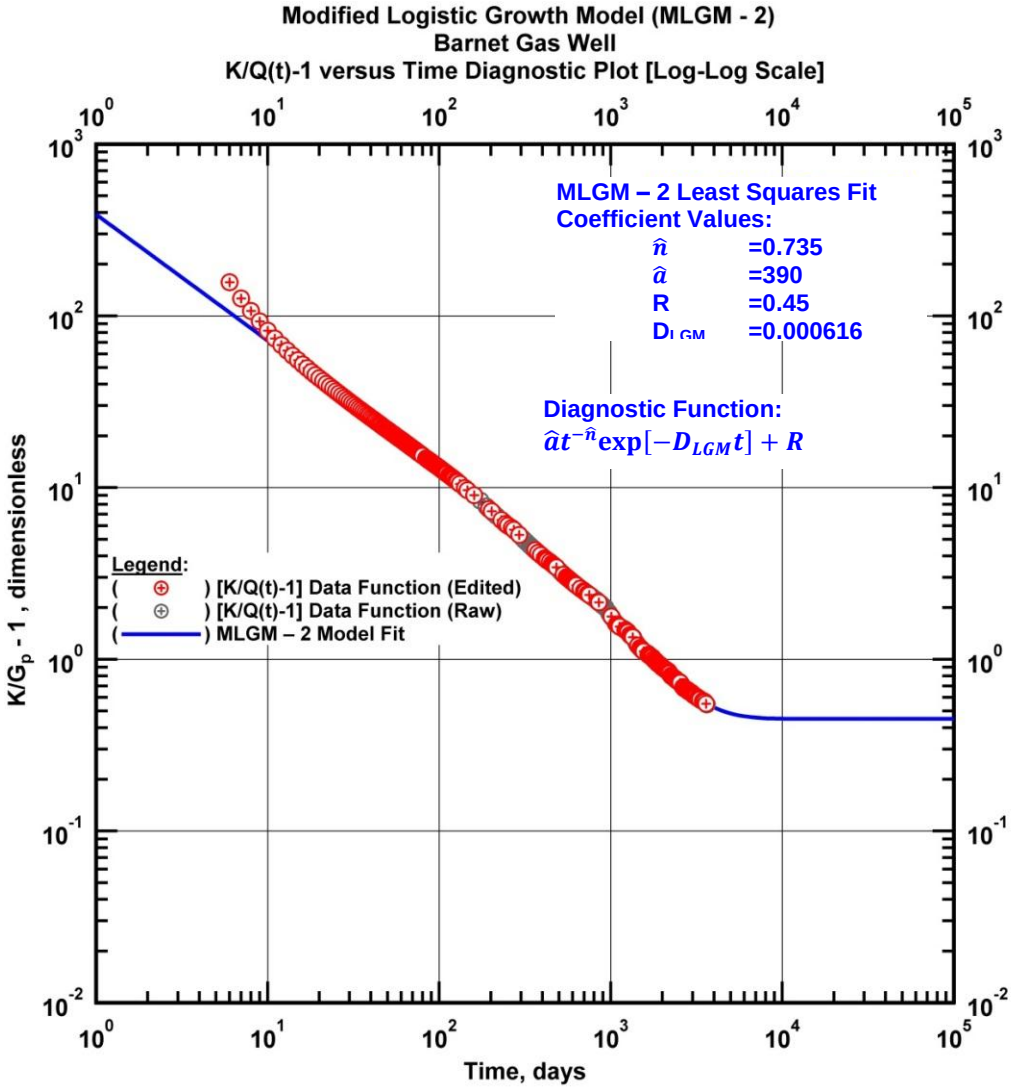

Figure 4.12 — (Log-log Plot): $K/G_p - 1$ versus production time. Modified Logistic Growth Model – 2 (MLGM – 2) diagnostic plot match for Barnett shale gas well.

Table 4.6 — MDNG – 2 time-rate relation model parameters (Barnett shale gas well).

Modified Duong Model (MDNG – 2)			
$q_{t1=0.0001\ day}$ (MSCFD)	a	m	D_{Dng} (D^{-1})
50,000	0.7	1.0017	0.000243

Next we match the data using MLGM-2 model. In this case, the model parameters are estimated on plot of K/Q-1 versus *time* plot. **Fig. 4.12** shows the diagnostic plot necessary to evaluate the model parameters. In this analysis K is the initial gas in place which was available from volumetric estimates. Hence, all the

unknown parameters were estimated from the *K/Q*-1 versus *time* diagnostic plot. The model parameters for MLGM-2 are summarized in **Table 4.7**. The resulting model matches are shown in **Fig. 4.13.**

Table 4.7 — MLGM – 2 time-rate relation model parameters (Barnett shale gas well).

Modified Logistic Growth Model (MLGM-2)

K *MSCF*	$\hat{a}$	$\hat{n}$	R	D_{LGM}
1,310,000	390	0.735	0.45	0.000616

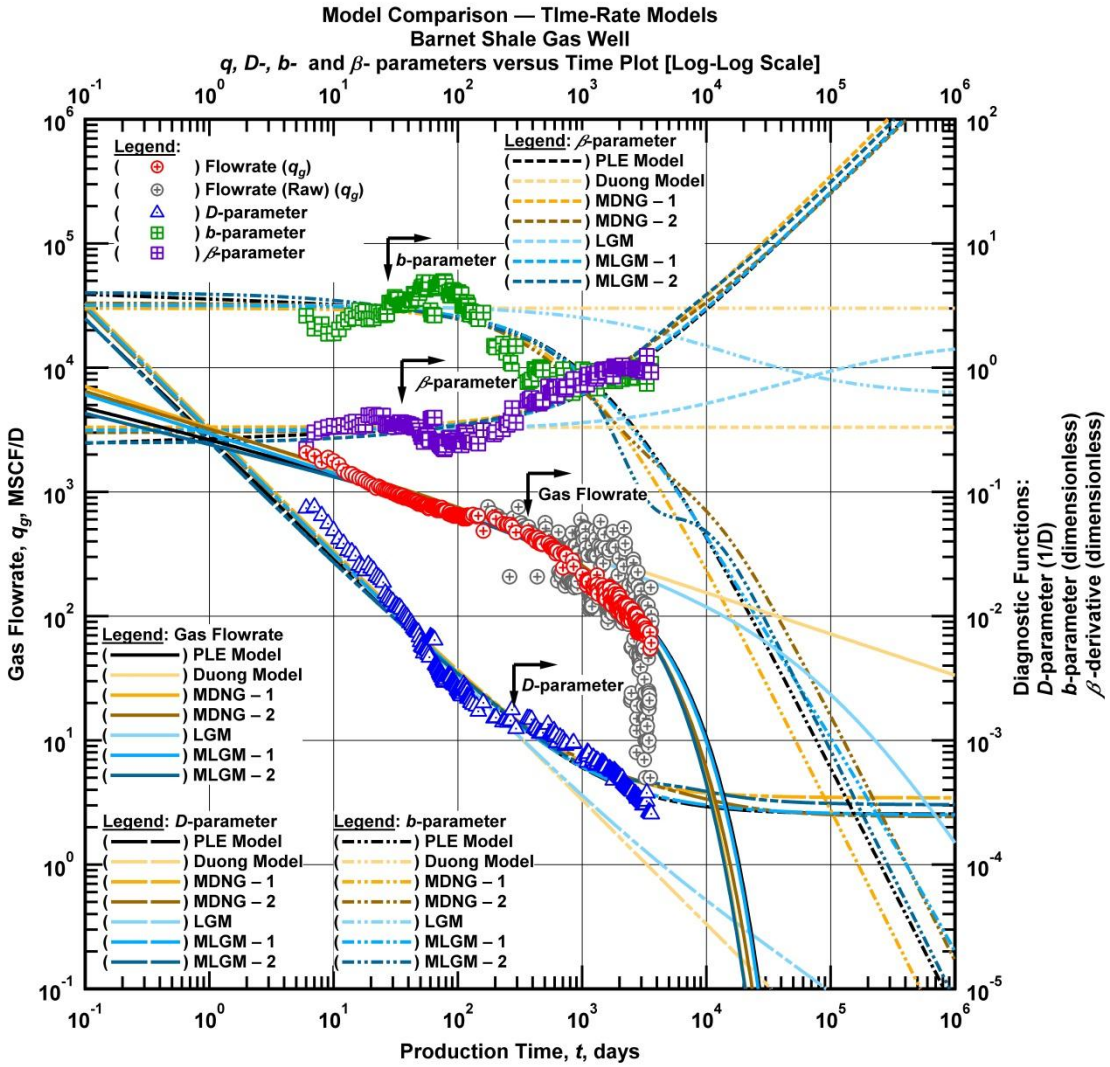

Figure 4.13 — (Log-log Plot): Flow rate (q_g), *D*-, *b*-parameter and β-derivative versus production time. PLE, logistic growth, Duong, MLGM – 1, MLGM – 2, MDNG – 1, and MDNG – 2 time rate model matches for Barnett shale gas well.

Fig. 4.14 shows model match on the historical rate and cumulative production data. The modified relations were able to match both the early time data and late time boundary-dominated flow regime successfully.

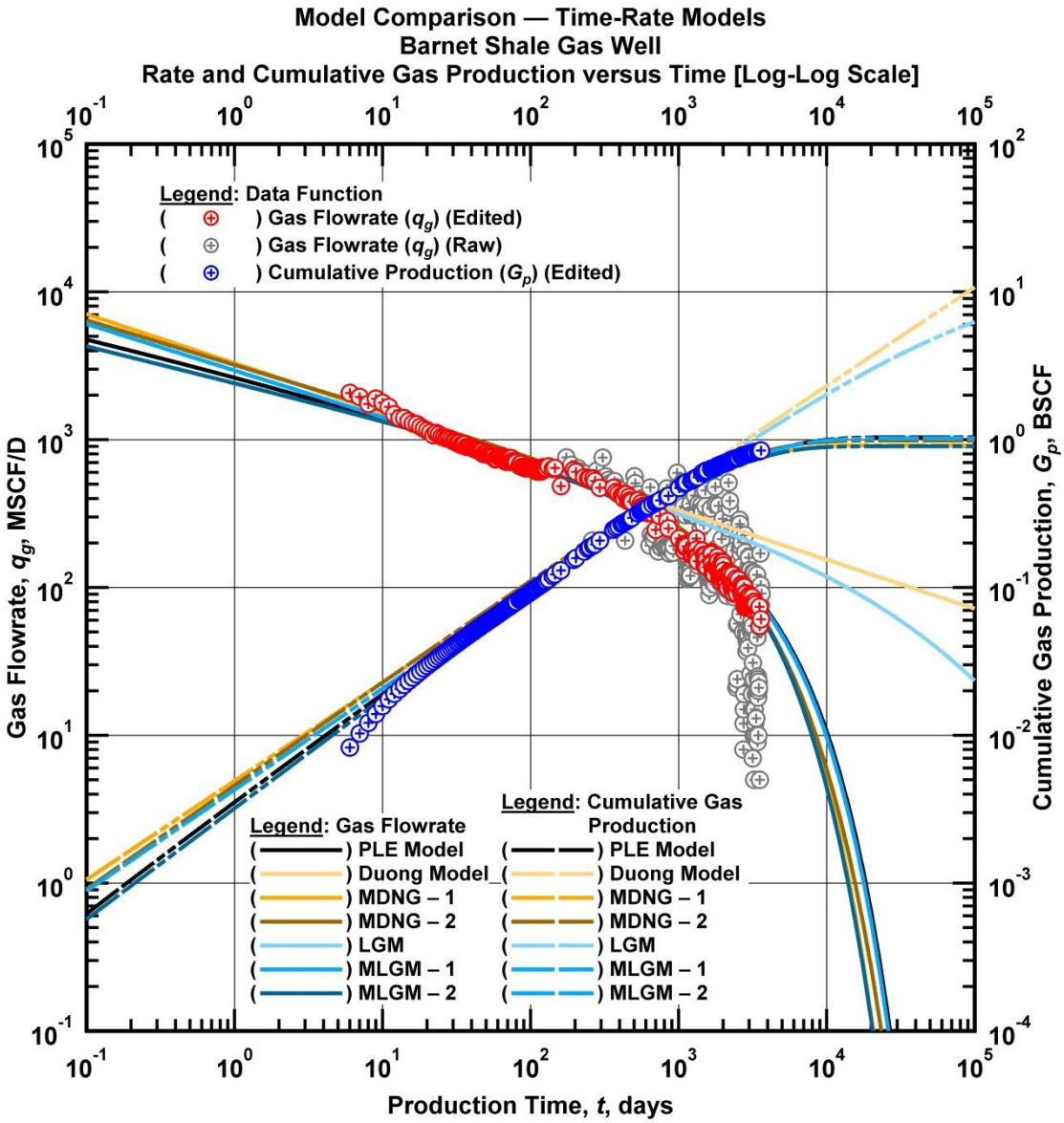

Figure 4.14 — (Log-log Plot): Rate and cumulative production versus time plot. PLE, logistic growth, Duong model, MLGM – 1, MLGM – 2, MDNG – 1, and MDNG – 2 time-rate model matches for Barnett shale gas well.

Fig. 4.13 shows that Duong and logistic growth models have failed to match the boundary-dominated flow regime. The modified time-rate relations have provided a quality match to the transient and boundary dominated flow regime. **Table 4.8** shows the cumulative production calculated using the models at the end of the historical production period. The Duong and logistic growth models have overestimated the cumulative production. The PLE and the modified relations have provided a reliable value of the cumulative production.

Table 4.8 — Comparison of calculated cumulative production values for Barnett shale gas well (Gp,max = 0.84 BSCF).

Time-rate models	$G_{p,max}$
Duong model	1.20 BSCF
Logistic growth model	1.10 BSCF
Power-law exponential model (PLE)	0.79 BSCF
Modified Duong Model – 1 (MDNG – 1)	0.78 BSCF
Modified Duong Model – 2 (MDNG – 2)	0.82 BSCF
Modified logistic growth Model – 1 (MLGM – 1)	0.80 BSCF
Modified logistic growth Model – 2 (MLGM – 2)	0.78 BSCF

CHAPTER V

INTEGRATION OF PRODUCTION DATA ANALYSIS AND TIME-RATE ANALYSIS VIA PARAMETRIC CORRELATION – THEORETICAL CONSIDERATION

In this section we demonstrate a methodology to integrate model-based production analysis techniques with rate-time analysis techniques using parametric correlations. We consider the time-rate model considered thus far (the PLE, logistic growth, and Duong models). Here we provide a theoretical consideration to the methodology using data generated from a numerical simulation model of a horizontal well with multiple transverse fractures in low permeability reservoir. The methodology demonstrated here is based on fracture conductivity and 30 year *EUR* values, although similar methodology can be followed using permeability and fracture half-length.

This methodology assumes that completion parameters and production constrains are kept fairly constant for all cases considered. Production factors like bottomhole pressure, number of fractures and well-length are kept constant in order to narrow the unknown parameter to the fundamental reservoir properties like permeability (k) and fracture conductivity (F_c).

5.1 Methodology

A horizontal well model in a low permeability reservoir with multiple transverse fractures is modeled **(Fig. 5.1).** Several simulation runs were made keeping all parameters constant except for the fracture conductivity. The model input parameters are given in **Table 5.1**.

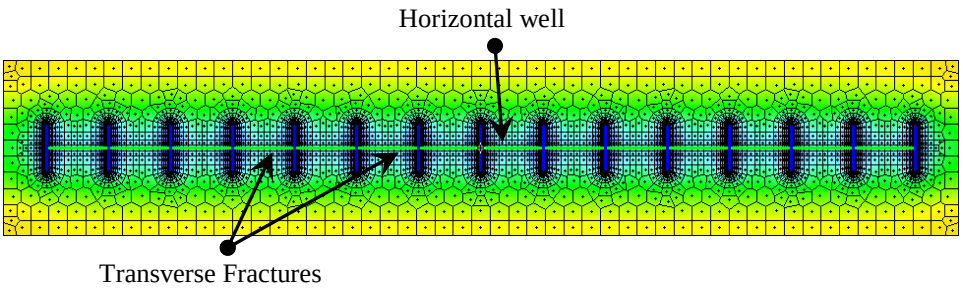

Figure 5.1 — Diagram of the numerical simulation model showing horizontal well and multiple transverse fractures.

Table 5.1 — Reservoir and fluid properties for numerical simulation case (horizontal well with multiple transverse fractures).

Reservoir Properties		
Net pay thickness, h	=	160 ft
Formation permeability, k	=	0.5 µD
Fracture conductivity	=	0.005 – 0.7 md-ft
Wellbore Radius, r_w	=	0.1 ft
Formation compressibility, c_f	=	3 x 10^{-6} psi^{-1}
Porosity, ϕ	=	0.05 (fraction)
Initial reservoir pressure, p_i	=	5000 psi
Gas saturation, s_g	=	1.0 fraction
Skin factor, s	=	-5 (dimensionless)
Reservoir temperature, T_r	=	212 °F
Fluid properties:		
Gas specific gravity, γ_g	=	0.7 (air = 1)
Hydraulically fractured well model parameters:		
Fracture half-length, x_f	=	164.0 ft
Number of fractures	=	15
Horizontal well length	=	6561.7 ft
Production parameters:		
Flowing pressure, p_{wf}	=	500 psia
Production time, t	=	10,958 days (30 years)

We have generated 15 simulation cases with different fracture conductivity values, ranging between 0.005 – 0.7 md-ft, and keeping all other model parameters constant.

We performed rate decline analysis of the production data generated from the numerical simulation runs using the models we have considered in the previous chapter. We have used the Bourdet algorithm (Bourdet et al. 1989) to calculate the *D*-, *b*- and β-derivatives to help in matching the production data. A log-log plot and a semi-log plot of rate q, *D*-, *b*-parameters and β-derivative plotted against production time is provided to show the model matches.

Once we match each of the production data, the next step is to study the relationship between the parameters of the rate decline models and the reservoir parameters considered here, in this case fracture conductivity (*Fc*) and 30 year *EUR* (EUR_{30yr}). We have performed a cross-plot analysis of the individual rate decline model parameters and the reservoir parameters to identify a correlating parametric function. We intend to right each reservoir parameter in terms of the rate decline model parameters. For example:

$$F_c = f(p) \quad \text{..... (5.1)}$$

And

$$EUR_{30yr} = f(p) \quad \text{.....(5.2)}$$

Here, p is a parameter of one of the models under consideration.

First, we identify the type of correlating function; then we combine each of the individual correlating functions to find an integrating parametric correlation for estimation of the reservoir parameters directly from rate decline model parameters. The integrating parametric correlation can be written as:

$$F_c = f(p, q, r...) \quad \text{.....(5.3)}$$

And

$$EUR_{30yr} = f(p, q, r...) \quad \text{.....(5.4)}$$

p, q, and r indicate (sample) parameters for the rate decline model parameters being considered.

Finally we demonstrate that it is possible to estimate reservoir properties from rate decline model parameters when production constraints and completion parameters are kept constant.

5.2 PLE Model – Parametric Correlations

We develop integrating parametric correlations using parameters of the PLE model parameters. The flowrate q, D-, b-parameters, and β-derivatives plots are given below (**Figs. 5.2, 5.3,** and **5.4**). The diagnostic functions indicates boundary-dominated flow regime. In this analysis, we focus on the behavior of the linear flow regime when fracture conductivity values are changing.

Earlier we have seen that the b-parameter has a value of 2 in the linear flow regime, when the fracture conductivity is large. Here we have considered fairly low fracture conductivity values and as a result the b-parameters range between 3 for the highest conductivity case (0.7 md-ft) to 10 for the lowest conductivity case (0.005 md-ft) **(Fig. 5.2).** Similarly the β-derivative ranges between 0.07 for the lowest fracture conductivity case (0.005 md-ft) to 0.3 for the highest fracture conductivity case (0.7 md-ft). As mentioned earlier we not use the D_∞ parameter in the development of the parametric correlation.

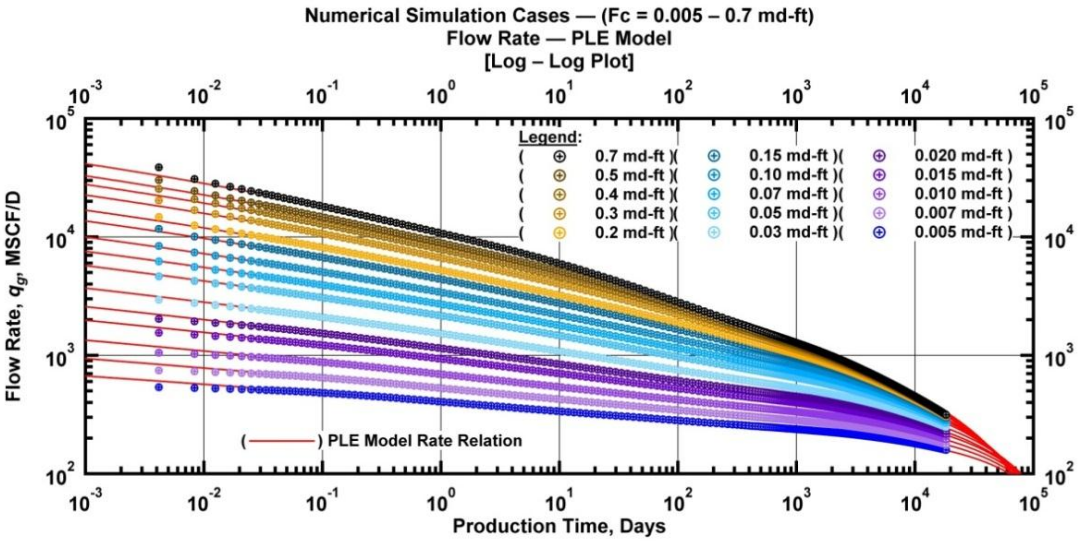

Figure 5.2 — (Log-log Plot): Flow rate (q_g) versus production time. PLE model matches of 15 numerical simulation cases.

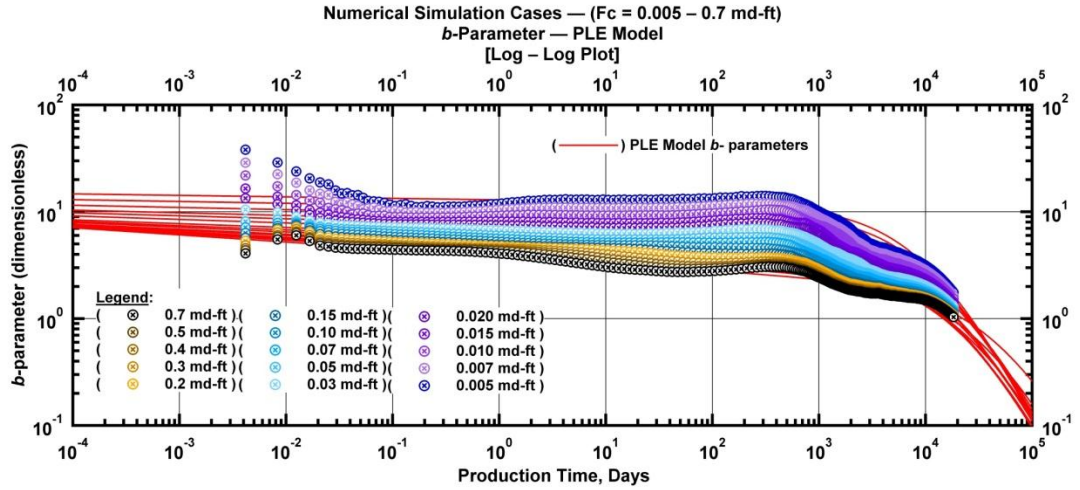

Figure 5.3 — (Log-log Plot): *b*-parameter versus production time. PLE model matches of 15 numerical simulation cases.

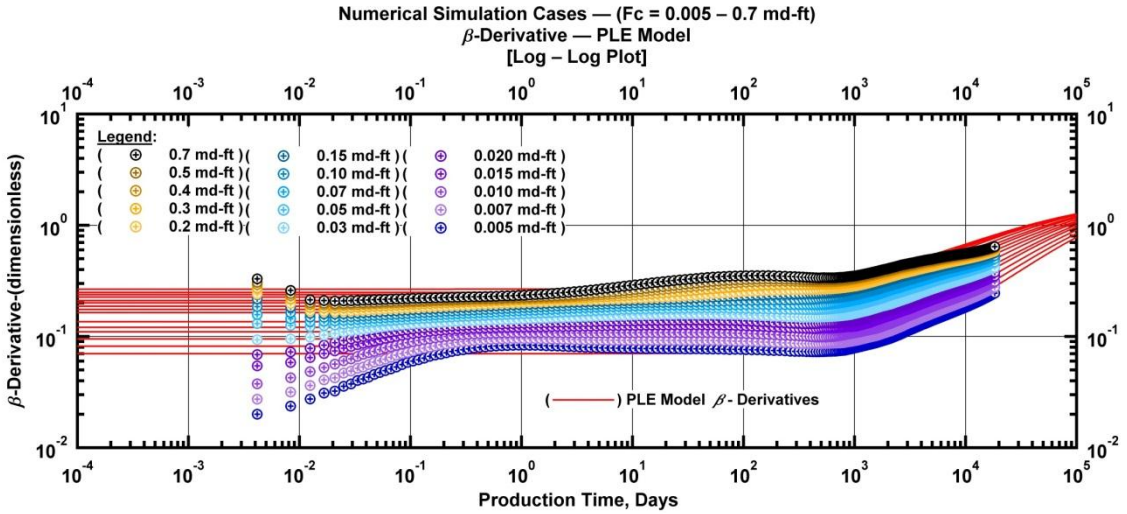

Figure 5.4 — (Log-log Plot): β-parameter versus production time. PLE model matches of 15 numerical simulation cases.

Table 5.2 shows the matching model parameters.

Table 5.2 — Power Law Exponential model (PLE) parameters. Model matches to 15 numerical simulation cases.

Num. Sim. Cases		*PLE Model Parameters*				
F_c (md-ft)	$G_{p,\ max\ (30\ yr)}$ (BSCF)	D_∞ (D^{-1})	n (d.less)	$\hat{D}_i$ (D^{-1})	$\hat{q}_{gi}$ (MSCFD)	EUR_{PLE} (BSCF)
0.005	2.24	3.2E-06	0.014	5.47	95,974.3	2.24
0.007	2.59	3.6E-06	0.017	5.25	100,328.9	2.58
0.010	2.98	2.5E-06	0.020	5.03	105,777.6	2.97
0.015	3.46	3.0E-07	0.025	4.78	111,222.0	3.46
0.020	3.82	3.0E-07	0.028	4.61	115,385.6	3.82
0.030	4.36	0.0E+00	0.033	4.37	120,961.6	4.34
0.050	5.09	4.0E-06	0.035	4.49	193,018.7	5.09
0.070	5.60	4.0E-06	0.040	4.31	199,789.8	5.58
0.100	6.15	4.5E-06	0.044	4.11	207,364.2	6.15
0.150	6.76	1.1E-05	0.047	4.10	264,901.5	6.78
0.200	7.16	1.7E-05	0.050	4.00	286,229.0	7.16
0.300	7.67	2.2E-05	0.054	3.90	330,134.6	7.68
0.400	7.98	2.2E-05	0.058	3.80	353,264.0	7.97
0.500	8.18	1.3E-05	0.062	3.70	363,276.7	8.18
0.700	8.43	5.1E-06	0.067	3.65	413,795.1	8.44

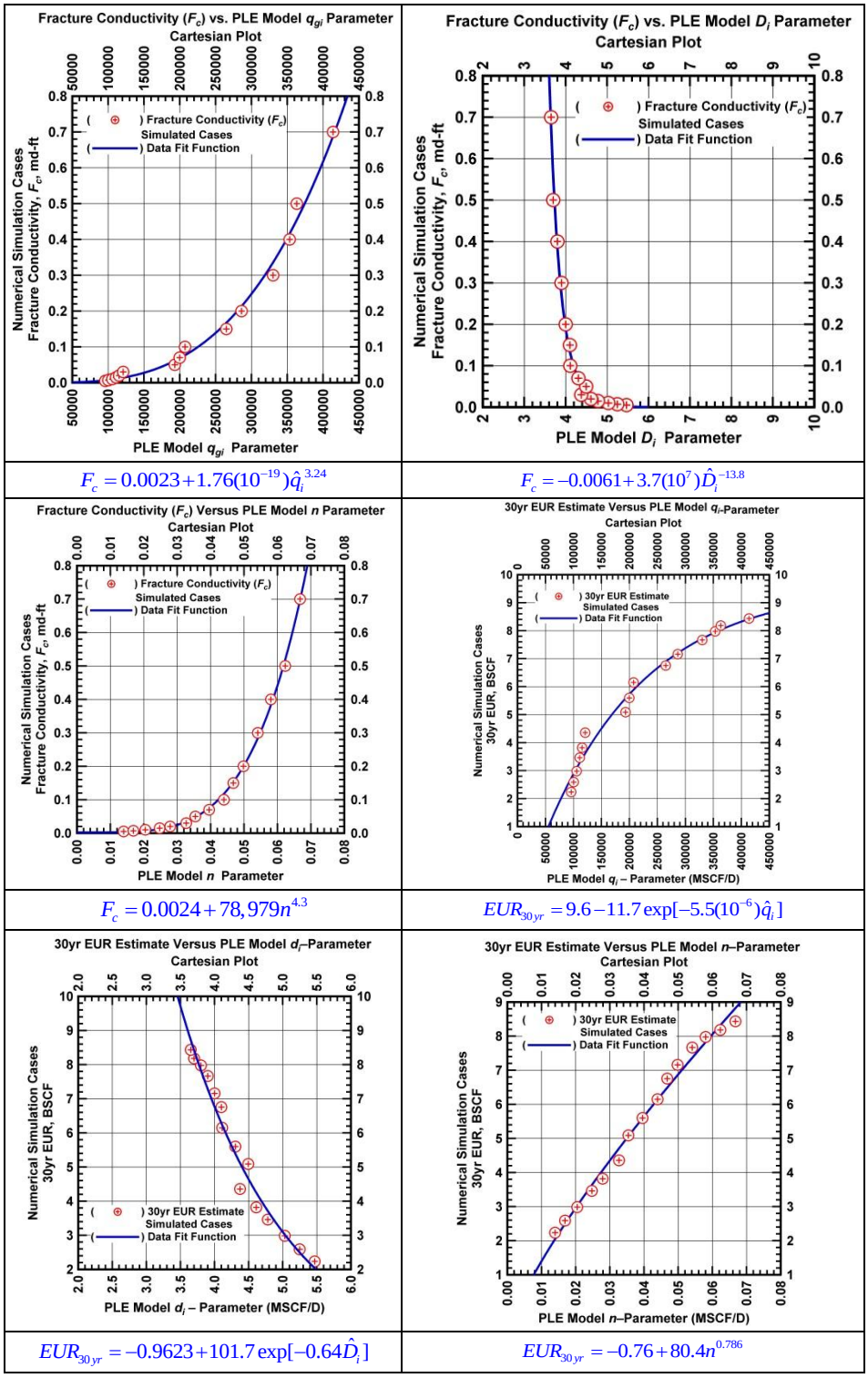

Figure 5.5 — Cross-plots showing relationship between PLE model parameters and numerical simulation case fracture conductivity (F_c) and 30 year *EUR* estimates.

We next study the relationship between the PLE model parameter and the reservoir parameters (F_c and EUR_{30yr}) by plotting the reservoir parameters against each of the model parameters. We then fit a simple parametric function to the data to establish a suitable correlating function. **Fig. 5.5** shows the cross-plots along with the correlating function.

Finally, we propose parametric correlations based on the correlating functions we identified earlier (Fig. 5.5), to relate the reservoir parameters with PLE model parameters. From **Fig. 5.5** we notice that fracture conductivity (F_c) is related to PLE model parameters n, D_i and q_i with a power-law function. Eq. 5.5 shows the proposed correlating function.

$$F_c = a_{01} n^{a_{02}} \hat{D}_i^{a_{03}} \hat{q}_{gi}^{a_{04}} \quad \text{.....(5.5)}$$

Here, a_{01}, a_{02}, a_{03} and a_{04} are *coefficients* to be determined through least square regression. Similarly we can propose the following correlating function to estimate the 30 year *EUR* (EUR_{30yr}).

$$EUR_{30yr} = a_{01} n^{a_{02}} \exp[a_{03}\hat{D}_i] \exp[a_{04}\hat{q}_{gi}] \quad \text{.....(5.6)}$$

Fig. 5.6 shows the resulting model fit. We can see that proposed correlating function provides a reliable estimate of the reservoir properties. This shows that if we obtain a production data from another well within the same reservoir system, we can match the production data using PLE model and use the correlations shown in Fig 5.6 to estimate the reservoir properties (F_c and $EUR_{30\ yr}$) using the PLE model parameters.

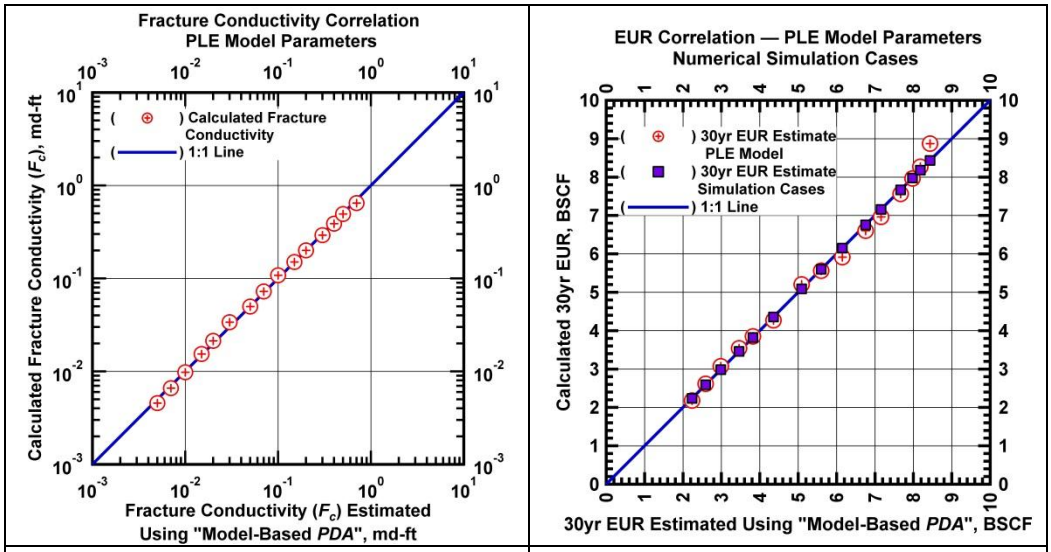

$F_C = 1E-07 n^{1.7} D_i^{4E-08} q_i^{1.6}$ | $EUR_{30yr} = 70.3 n^{1.4} \exp[0.46 d_i] \exp[2E-07 q_i]$

Figure 5.6 — Comparison of fracture conductivity and 30 year *EUR* values calculated using parametric correlations developed using PLE model parameters versus numerical simulation models.

5.3 Duong Model – Parametric Correlations

Here, we consider Duong model parameters to develop parametric correlations to integrate reservoir properties with the rate decline model parameters. We have considered the same numerical simulation data set that was used in the previous section. Duong model is used to match only the linear flow-regime. No attempt was made to match the boundary-dominated flow regime. In Chapter 4 we have demonstrated the limitations of Duong model at modeling boundary dominated flow-regimes. The model matches here overestimate the 30 year *EUR* values. The resulting model matches are shown in **Figs. 5.7, 5.8** and **5.9** on a log-log plot of flow rate, *b*- parameter and $\wp$-derivative plots respectively.

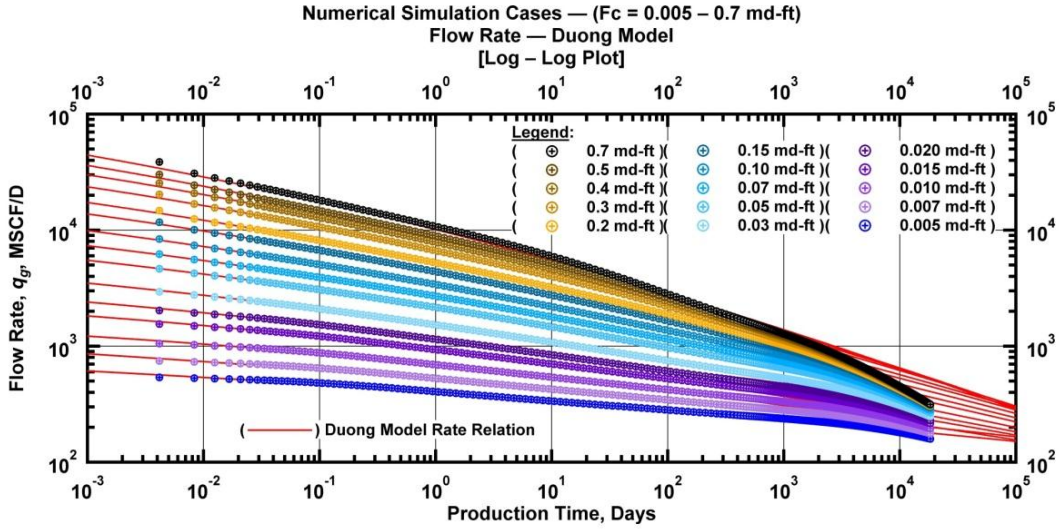

Figure 5.7 — (Log-log Plot): Flow rate (q_g) versus production time. Duong model matches of 15 numerical simulation cases.

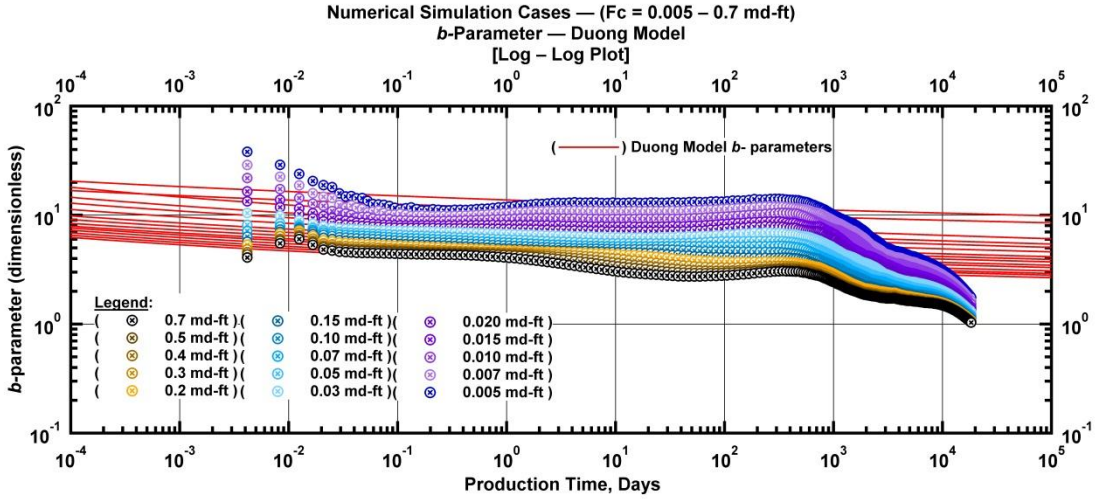

Figure 5.8 — (Log-log Plot): *b*-parameter versus production time. Duong model matches of 15 numerical simulation cases.

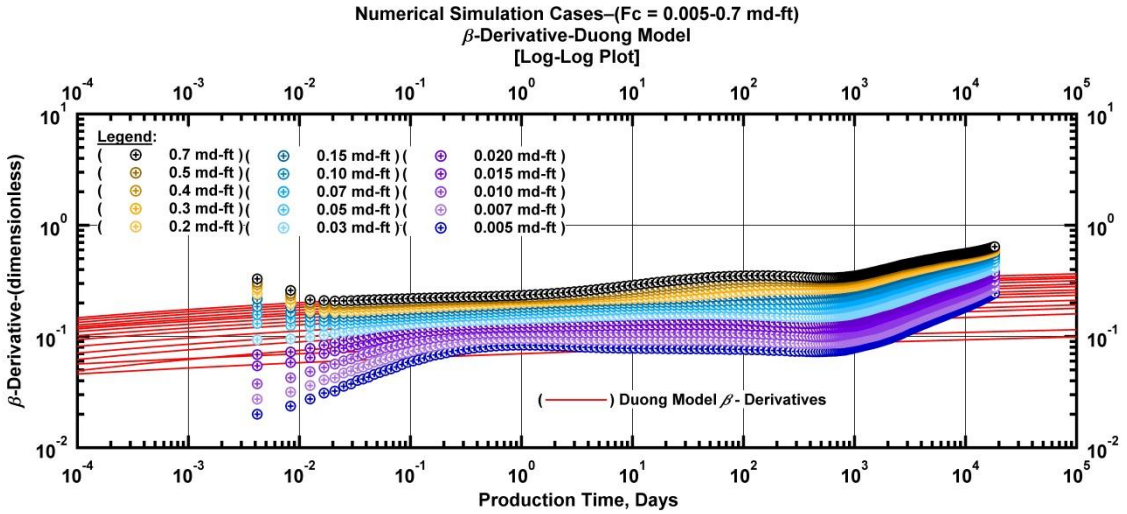

Figure 5.9 — (Log-log Plot): β-parameter versus production time. Duong model matches of 15 numerical simulation cases.

The resulting model parameters are given in **Table 5.3.**

Table 5.3 — Duong model parameters. Model matches to 15 numerical simulation cases.

Num. Sim. Cases		*Duong Model Parameters*			
F_c (md-ft)	$G_{p,\ max\ (30\ yr)}$ (BSCF)	a (D^{-1})	m (d.less)	q_1 (MSCFD)	$EUR_{DNG,30yr}$ (BSCF)
0.005	2.24	0.932	1.0050	565.0	2.0895
0.007	2.59	0.921	1.0054	781.8	2.4447
0.010	2.98	0.906	1.0059	1,109.6	2.7957
0.015	3.46	0.890	1.0064	1,624.1	3.2749
0.020	3.82	0.880	1.0067	2,110.6	3.6545
0.030	4.36	0.866	1.0073	3,018.7	4.2444
0.050	5.09	0.849	1.0081	4,656.5	5.1233
0.070	5.60	0.838	1.0085	6,142.4	5.8076
0.100	6.15	0.828	1.0089	8,187.1	6.6362
0.150	6.76	0.816	1.0098	11,235.4	7.5835
0.200	7.16	0.807	1.0105	13,975.5	8.2810
0.300	7.67	0.795	1.0117	18,867.7	9.2248
0.400	7.98	0.783	1.0125	23,659.3	9.7001
0.500	8.18	0.774	1.0130	28,132.1	10.0494
0.700	8.43	0.768	1.0140	34,108.8	10.9947

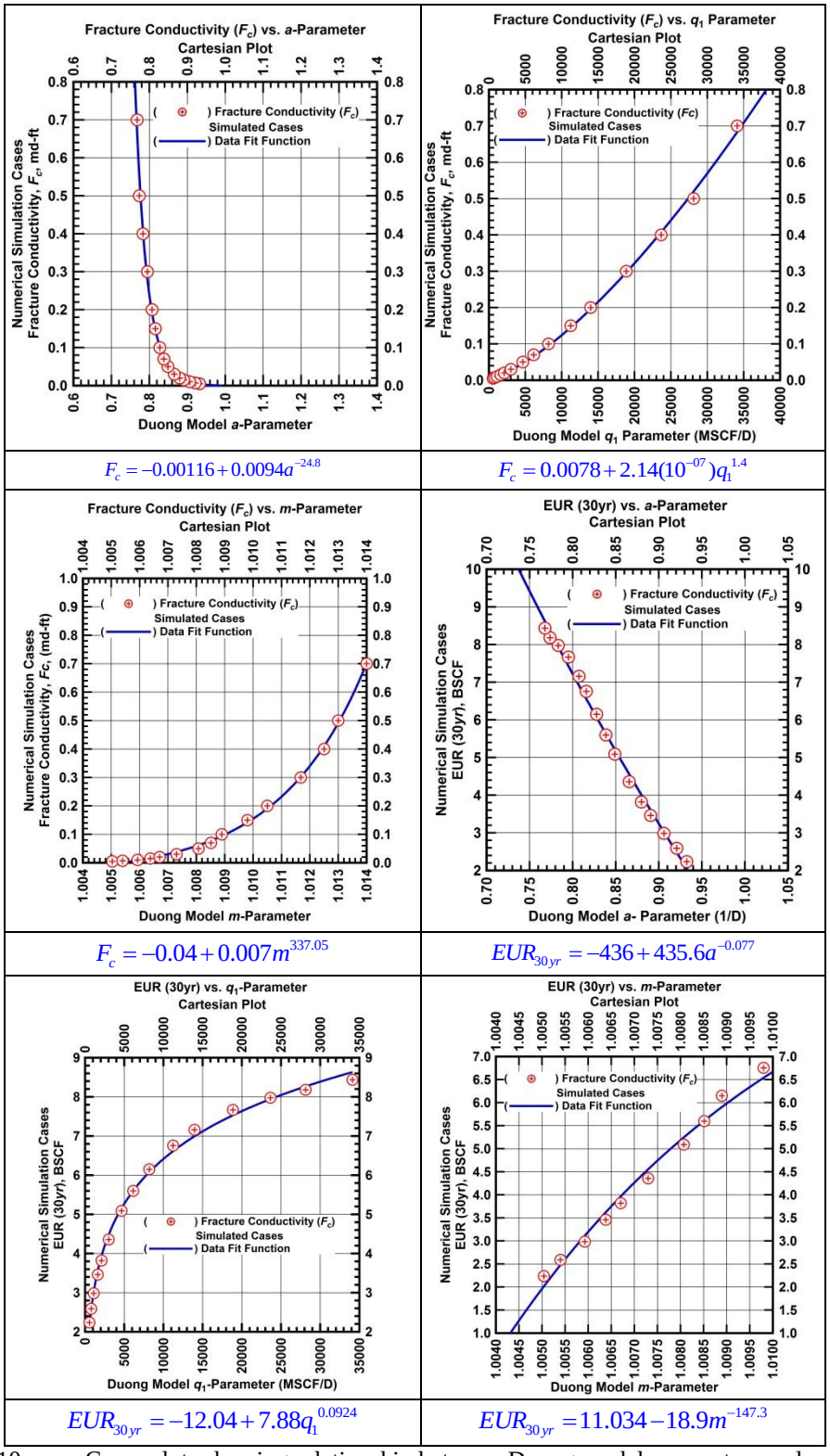

Figure 5.10 — Cross-plots showing relationship between Duong model parameters and numerical simulation cases fracture conductivity (F_c) and 30 year *EUR* values.

Next we identify the relationship between the model parameters and the reservoir properties by plotting the reservoir properties against Duong model parameters. The cross-plot analysis is shown in **Fig. 5.10.** After considering several parametric correlations, the best fitting correlating function is matched to the data. The corresponding correlating function is shown in the figure (Fig. 5.10).

Finally, we propose parametric correlations based on the correlating functions we identified earlier (Fig. 5.10), to relate the reservoir parameters with Duong model parameters. From Fig. 5.10 we notice that fracture conductivity (F_c) is related to Duong model parameters *m* and *a* with a power-law function. Eq. 5.7 shows the proposed correlating function.

$$F_c = a_{01} m^{a_{02}} a^{a_{03}} \quad \text{.....(5.7)}$$

Here, a_{01}, a_{02}, a_{03} and a_{04} are *coefficients* to be determined through least square regression. Similarly we can propose the following correlating function to estimate the 30 year *EUR* (EUR_{30yr}).

$$EUR_{30yr} = a_{01} a^{a_{02}} q_1^{a_{03}} \quad \text{.....(5.8)}$$

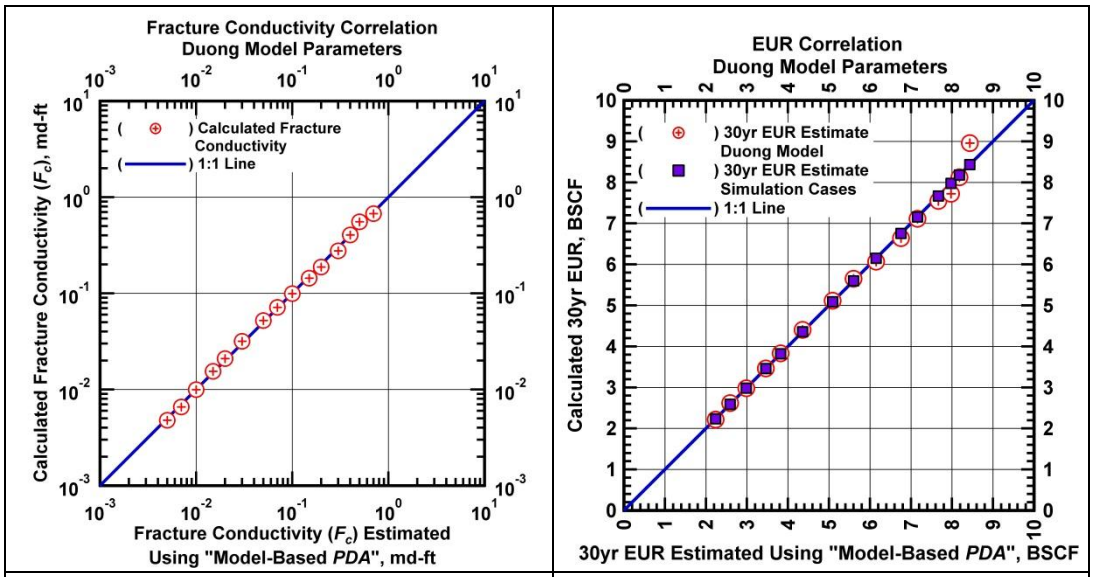

$F_C = 36.9 m^{-8.8} a^{0.85}$ | $EUR_{30yr} = 0.0074 a^{14.76} q_1^{1.06}$

Figure 5.11 — Comparison of fracture conductivity and 30 year *EUR* values calculated using parametric correlations developed using Duong model parameters versus numerical simulation models.

Fig. 5.11 shows the resulting model fit. We can see that proposed correlating function provides a reliable estimate of the reservoir properties. This shows that if we obtain a production data from another well within the same reservoir system, we can match the production data using Duong model and use the correlations shown in Fig. 5.11 to estimate the reservoir properties (Fc and $EUR_{30\,yr}$) using the matching Duong model parameters.

5.4 Logistic Growth Model – Parametric Correlations

Here, a parametric correlation is developed using logistic growth model parameters. The flow rate, b-parameter and β-derivatives are shown in **Figs. 5.12, 5.13,** and **5.14.** As mentioned previously, the K parameter of the logistic growth model describes the initial gas in place. In this case, since we have the initial gas in place value available from the numerical model, we have kept the K parameter constant for all model matches.

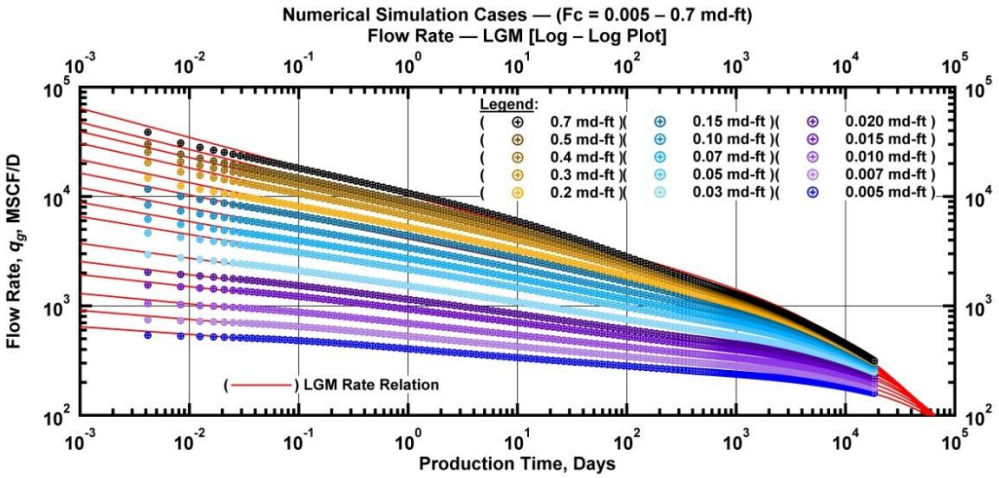

Figure 5.12 — (Log-log Plot): Flow rate (q_g) versus production time. Duong model matches of 15 numerical simulation cases.

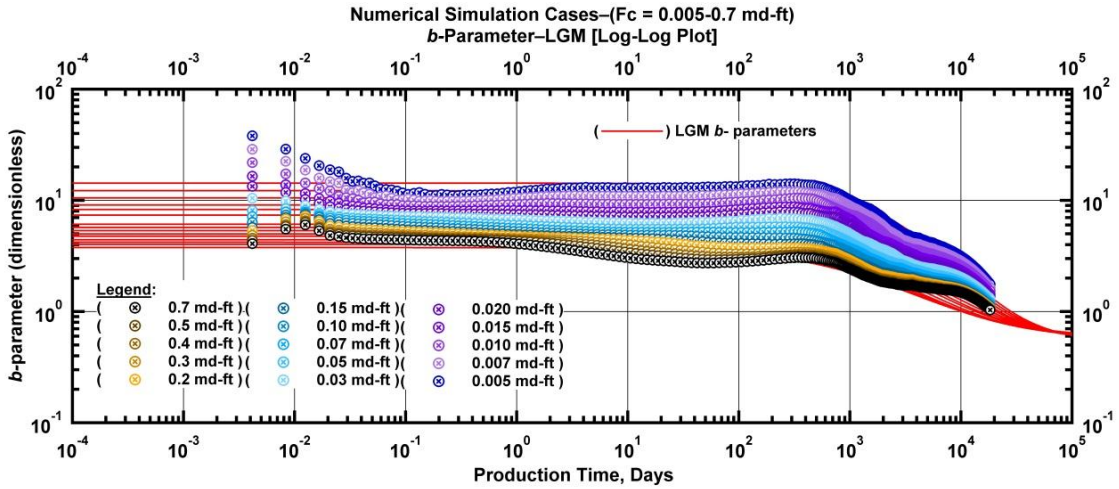

Figure 5.13 — (Log-log Plot): *b*-parameter versus production time. Duong model matches of 15 numerical simulation cases.

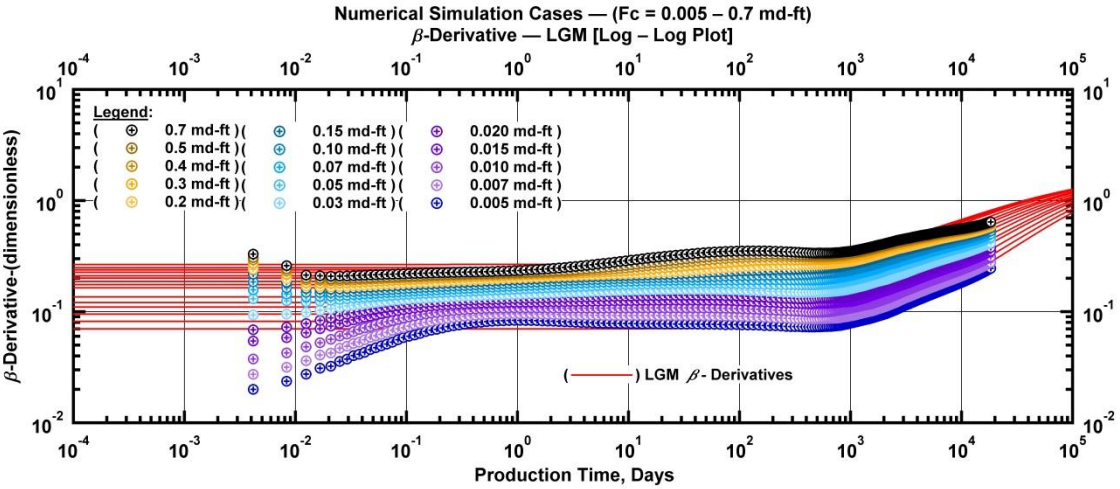

Figure 5.14 — (Log-log Plot): β-parameter versus production time. Duong model matches of 15 numerical simulation cases.

The resulting model parameters are given in **Table 5.4.**

Table 5.4 — Logistic growth model matches to 15 numerical simulation cases.

Num. Sim. Cases		*Logistic Growth Model*			
F_c (md-ft)	$G_{p,\,max\,(30\,yr)}$ (BSCF)	K (MSCF)	$\hat{n}$ (d.less)	$\hat{a}$	$EUR_{LGM,30yr}$ (BSCF)
0.005	2.24	31,022,140.8	0.9300	72,573.7	2.26
0.007	2.59	31,022,140.8	0.9181	55,201.1	2.63
0.010	2.98	31,022,140.8	0.9051	41,659.4	3.04
0.015	3.46	31,022,140.8	0.8900	30,563.2	3.54
0.020	3.82	31,022,140.8	0.8794	24,668.6	3.92
0.030	4.36	31,022,140.8	0.8644	18,360.1	4.48
0.050	5.09	31,022,140.8	0.8360	12,273.3	5.04
0.070	5.60	31,022,140.8	0.8248	9,712.7	5.62
0.100	6.15	31,022,140.8	0.8131	7,618.8	6.26
0.150	6.76	31,022,140.8	0.7997	5,817.7	7.01
0.200	7.16	31,022,140.8	0.7896	4,824.5	7.54
0.300	7.67	31,022,140.8	0.7742	3,728.7	8.21
0.400	7.98	31,022,140.8	0.7618	3,119.6	8.59
0.500	8.18	31,022,140.8	0.7514	2,724.9	8.83
0.700	8.43	31,022,140.8	0.7341	2,234.1	9.07

Next we identify the relationship between the model parameters and the reservoir properties by plotting the reservoir properties with logistic growth model parameters. The cross-plot analysis is shown in **Fig. 5.15.** After considering several parametric correlations, the best fitting correlating function is matched to the data. The corresponding correlating function is shown with the figures (Fig. 5.15).

Finally, we propose parametric correlations based on the correlating functions we identified earlier (Fig 5.15), to relate the reservoir parameters with logistic growth model parameters. From Fig. 5.15 we notice that fracture conductivity (F_c) is related to logistic growth model parameters –*n* and *a* with a power-law function. Eq. 5.9 shows the proposed correlating function.

$$F_c = a_{01}\hat{n}^{a_{02}}\hat{a}^{a_{03}} \quad \text{.....(5.9)}$$

Here, a_{01}, a_{02}, and a_{03} are *coefficients* to be determined through least square regression. Similarly we can propose the following correlating function to estimate the 30 year *EUR* (EUR_{30yr}).

$$EUR_{30\,yr} = a_{01}\hat{n}^{a_{02}}\hat{a}^{a_{03}} \quad \text{.....(5.10)}$$

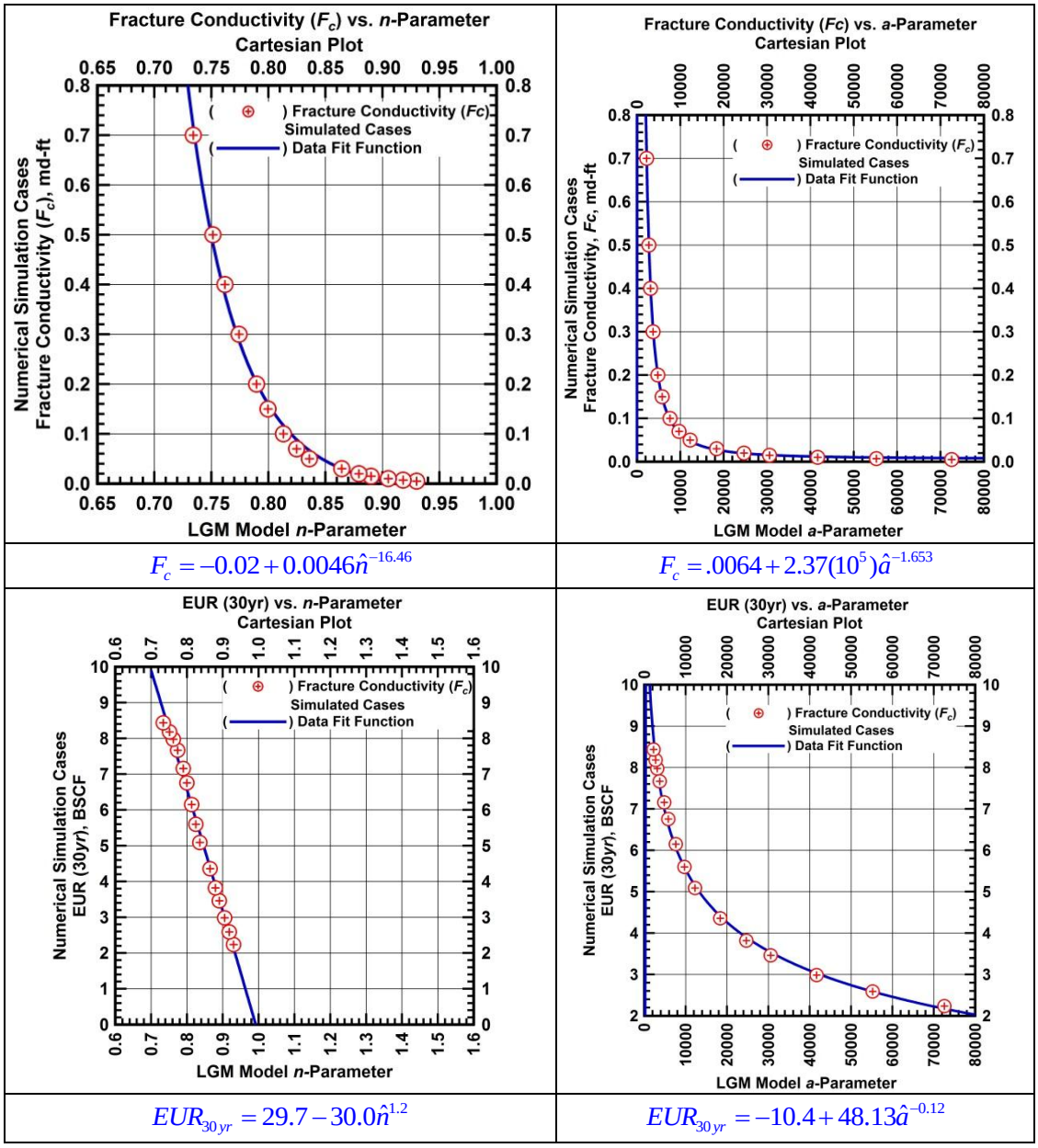

Figure 5.15 — Cross-plots showing relationship between logistic growth model parameters and numerical simulation cases fracture conductivity (F_c) and 30 year *EUR* values.

Fig 5.16 shows the resulting model fit. We can see that proposed correlating function provides a reliable estimate of the reservoir properties. This shows that if we obtain a production data from another well within the same reservoir system, we can match the production data using Duong model and use the correlations shown in Fig 5.16 to estimate the reservoir properties (*Fc* and $EUR_{30\ yr}$) using the matching Duong model parameters.

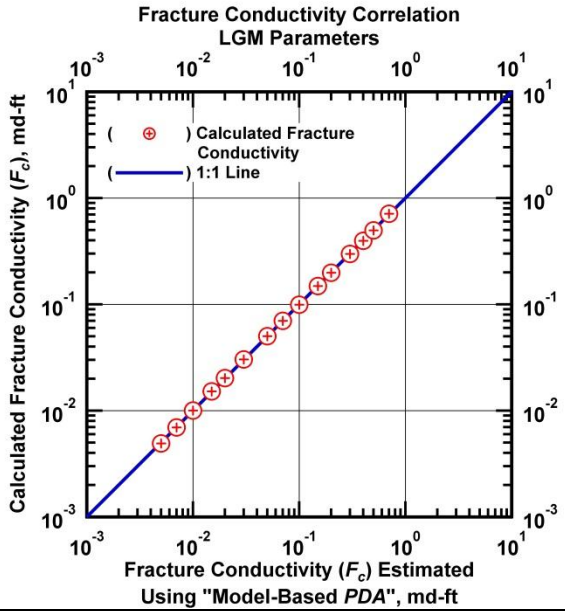

$$F_C = 36.9\hat{n}^{-8.8}\hat{a}^{0.85}$$

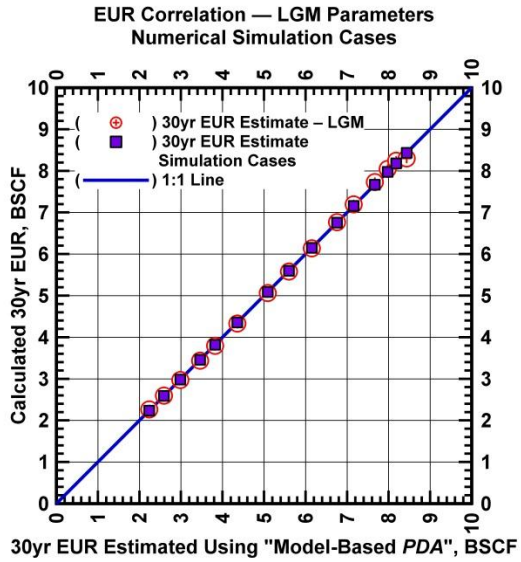

$$EUR_{30\,yr} = 27473\hat{n}^{6.1}\hat{a}^{-0.8}$$

Figure 5.16 — Comparison of fracture conductivity and 30 year *EUR* values calculated using parametric correlations developed using logistic growth model parameters versus numerical simulation models.

CHAPTER VI

SUMMARY, CONCLUSIONS, AND RECOMMENDATIONS FOR FUTURE WORK

6.1 Summary

In this work we performed a complete performance analysis study using modern rate decline models (PLE, logistic growth, and Duong), where the root of this study is based on diagnostic data and model functions. We considered the quality of match and accuracy of reserve estimates using production data obtained from unconventional reservoirs. We showed that our proposed time-rate relations are capable of modeling the dominant transient and transition flow regimes observed from production data analysis of hydraulically fractured wells in low/ultra-low permeability reservoirs.

We demonstrated that the PLE model is capable of modeling boundary-dominated flow regimes whereas the logistic growth and the Duong models lack the character to model boundary-dominated flow behavior. The "continuous *EUR*" approach was used to study performance of the time-rate models in estimating ultimate recovery as a function of time. Finally, we proposed new time rate-relations to improve the reserve estimates and production forecasts for the logistic growth and the Duong models. The proposed time-rate relations do capture boundary-dominated flow behavior, thereby constraining reserve estimates.

We also developed a methodology to formulate a parametric correlation to integrate reservoir properties with rate decline model parameters by analyzing time-rate data generated from a reservoir simulation of a multi-fractured horizontal well in low/ultra-low permeability reservoir. The developed correlation allows estimation of reservoir properties using parameters of the time-rate models (obviously one must have benchmark results to establish such correlations). In particular, we focused on the correlation of fracture conductivity (F_C) and *EUR* using the results of time-rate analyses.

6.2 Conclusions

- We showed that the PLE, Duong and logistic growth models all successfully model transient flow regimes. However, the Duong and the logistic growth models lack the fundamental character to model boundary-dominated flow behavior.

- Our new proposed time-rate relations derived from diagnostic functions provide a quality match to the production data across all flow regimes.

- Diagnostic functions should always be used to establish representative time-rate analyses.

- The parametric correlations of results from model-based production data analyses and time-rate (decline) curve analyses do appear to be unique and distinct.

6.3 Recommendations for Future Work

- Identification of other diagnostic function which may allow accurate model parameter estimation and assist in the derivation of additional time-rate models.

NOMENCLATURE

a	=	Duong model intercept, 1/D
b	=	"Loss-ratio" derivative, dimensionless
$\hat{a}$	=	LGM time-rate equation model parameter, Days
a_{01}	=	Model parameter for empirical correlation, md-D^2/MSCF
a_{02}	=	Model parameter for empirical correlation, dimensionless
a_{03}	=	Model parameter for empirical correlation, dimensionless
a_{04}	=	Model parameter for empirical correlation, dimensionless
a_{05}	=	Model parameter for empirical correlation, BSCF
a_{06}	=	Model parameter for empirical correlation, Days
a_{07}	=	Model parameter for empirical correlation, dimensionless
$\hat{b}$	=	LGM time-rate equation model parameter, D
D	=	"Loss-ratio", 1/D
D_{∞}	=	Power-law exponential decline relation at infinite time, 1/D
D_{DNG}	=	Modified Duong model decline parameter, 1/D
$\hat{D}_i$	=	Power-law exponential decline relation, 1/D
D_{LGM}	=	Modified Duong model decline parameter, 1/D
EUR	=	Estimated ultimate recovery, MSCF
$EUR_{30\text{-Yr}}$	=	Estimated ultimate recovery after 30 years, MSCF
F_C	=	Fracture conductivity, md-ft
k	=	Model permeability, md
K	=	Logistic growth model parameter (Carrying capacity), MSCF
m	=	Duong model Slope
n	=	Power-law exponential relation time exponent, dimensionless
$\hat{n}$	=	LGM time-rate relation model parameter
p	=	Sample model variable
q_1	=	Rate at day 1, MSCF/D
q_{t1}	=	Rate at day t=t_1, MSCF/D
$\hat{q}_{gi}$	=	Power-law exponential relation rate intercept, MSCF/D
r	=	Sample model variable
s	=	Sample model variable
t	=	Production time, days

REFERENCES

Arps, J.J. 1945. Analysis of Decline Curves. *Trans.* AIME 160: 228-247.

Blasingame, T.A., Amini, S., and Rushing, J. 2007. Evaluation of the Elliptical Flow Period for Hydraulically-Fractured Wells in Tight Gas Sands -- Theoretical Aspects and Practical Considerations. Paper presented at the SPE Hydraulic Fracturing Technology Conference, College Station, Texas, U.S.A. Society of Petroleum Engineers 106308-MS.

Blumberg, A.A. 1968. Logistic Growth Rate Functions. *Journal of Theoretical Biology* 21 (1): 42-44.

Bourdet, D., Ayoub, J.A., and Pirard, Y.M. 1989. Use of Pressure Derivative in Well Test Interpretation. *SPE Formation Evaluation* 4 (2): 293-302. 12777-PA

Camacho, R. and Raghavan, R. 1989. Boundary-Dominated Flow in Solution Gas-Drive Reservoirs. Paper presented at the Low Permeability Reservoirs Symposium, Denver, Colorado. Society of Petroleum Engineers SPE 77689-PA.

Carter, R.D. 1985. Type Curves for Finite Radial and Linear Gas-Flow Systems: Constant-Terminal-Pressure Case. *Society of Petroleum Engineers Journal* 25 (5): 719-728.

Clark, A.J. 2011. Decline Curve Analysis in Unconventional Resource Plays Using Logistic Growth Models. M.S Thesis, The University of Texas, Austin, Texas.

Clark, A.J., Lake, L.W., and Patzek, T.W. 2011. Production Forecasting with Logistic Growth Models. Paper presented at the SPE Annual Technical Conference and Exhibition, Denver, Colorado, USA. Society of Petroleum Engineers SPE 144790-MS.

Currie, S.M., Ilk, D., and Blasingame, T.A. 2010. Continuous Estimation of Ultimate Recovery. Paper presented at the SPE Unconventional Gas Conference, Pittsburgh, Pennsylvania, USA. Society of Petroleum Engineers. SPE-132352.

Cutler, W.W. 1924. Estimation of Underground Oil Reserves by Oil-Well Production Curves. *Bull.* USBM 228 (1).

Duong, A.N. 2011. Rate-Decline Analysis for Fracture-Dominated Shale Reservoirs. *SPE Reservoir Evaluation & Engineering* 14 (3): 377-387. SPE-137748-PA.

Fetkovich, M.J. 1980. Decline Curve Analysis Using Type Curves. *JPT*. 32 (6): 1065-1077. SPE-4629-PA.

Freeman, C.M., Moridis, G.J., Ilk, D. et al. 2009. A Numerical Study of Performance for Tight Gas and Shale Gas Reservoir Systems. Paper presented at the SPE Annual Technical Conference and Exhibition, New Orleans, Louisiana. SPE 124961.

Ilk, D., Currie, S.M., Symmons, D. et al. 2010. Hybrid Rate-Decline Models for the Analysis of Production Performance in Unconventional Reservoirs. Paper presented at the SPE Annual Technical Conference and Exhibition, Florence, Italy. SPE 135616.

Ilk, D., Rushing, J.A., and Blasingame, T.A. 2011. Integration of Production Analysis and Rate-Time Analysis Via Parametric Correlations -- Theoretical Considerations and Practical Applications. Paper presented at the SPE Hydraulic Fracturing Technology Conference, The Woodlands, Texas, USA. SPE 140556.

Ilk, D., Rushing, J.A., Perego, A.D. et al. 2008a. Exponential Vs. Hyperbolic Decline in Tight Gas Sands — Understanding the Origin and Implications for Reserve Estimates Using Arps' Decline Curves. Paper presented at the SPE Annual Technical Conference and Exhibition, Denver, Colorado, USA. SPE 116731-MS.

Johnson, R.H. and Bollens, A.L. 1927. The Loss Ratio Method of Extrapolating Oil Well Decline Curves. *Trans.* AIME 77:771.

Lewis, J.O. and Beal, C.H. 1918. Some New Methods for Estimating the Future Production of Oil Wells. *Trans.* AIME 59: 492-525.

Maley, S. 1985. The Use of Conventional Decline Curve Analysis in Tight Gas Well Applications. Paper presented at the SPE/DOE Low Permeability Gas Reservoirs Symposium, Denver, Colorado. SPE 13898-MS.

Martinez, A.S., González, R.S., and Terçariol, C.A.S. 2008. Continuous Growth Models in Terms of Generalized Logarithm and Exponential Functions. *Physica A: Statistical Mechanics and its Applications* 387 (23): 5679-5687.

Robertson, S. 1988. Generalized Hyperbolic Equation. Paper SPE 18731 available from SPE, Richardson, Texas.

Texas. Rushing, J.A., Perego, A.D., Sullivan, R. et al. 2007. Estimating Reserves in Tight Gas Sands at Hp/Ht Reservoir Conditions: Use and Misuse of an Arps Decline Curve Methodology. Paper presented at the SPE Annual Technical Conference and Exhibition, Anaheim, California, U.S.A. SPE 109625.

Tsoularis, A. and Wallace, J. 2002. Analysis of Logistic Growth Models. *Mathematical Biosciences* 179 (1): 21-55.

Valko, P.P. 2009. Assigning Value to Stimulation in the Barnett Shale: A Simultaneous Analysis of 7000 Plus Production Histories and Well Completion Records. Paper presented at the SPE Hydraulic Fracturing Technology Conference, The Woodlands, Texas. Society of Petroleum Engineers SPE-119369-MS.

Van Kruysdijk, C.P.J.W. and Dullaert, G.M. 1989. A Boundary Element Solution to the Transient Pressure Response of Multiply Fractured Horizontal Wells. Paper presented at the 2nd European Conference on the Mathematics of Oil Recovery, Cambridge, England.

APPENDIX A

MODIFIED DUONG MODEL — 1 (MDNG – 1)

Long term behavior of *D*-parameter derivation of production data from unconventional reservoirs shows a deviation from the straight power law decline behavior during boundary dominated flow regimes. It has been observed that long term decline behaviors can be approximated by exponential decline behavior which is described by a constant decline parameter during boundary-dominated flow regimes. This is similar to the logic behind the derivation of the power law exponential model. The *D*-parameter of Duong model does not show a constant decline characteristic during boundary conditions.

The *D*-parameter of the Duong model is given by:

$$D(t) = mt^{-1} - at^{-m} \quad \text{(A-1)}$$

A constant decline parameter, $D_{DNG,}$ is added to A-1to model boundary conditions. The modified *D*-parameter is given by:

$$D(t) = mt^{-1} - at^{-m} + D_{DNG} \quad \text{(A-2)}$$

The new time rete relation can be derived from the new *D*-parameter relation. From the loss-ratio relation we know that:

$$\frac{1}{D} = -\frac{q_g}{dq_g / dt} \quad \text{(A-3)}$$

Substituting A-2 in A-3 we get:

$$\frac{dq(t)}{dt} \Big/ q(t) = at^{-m} - \frac{m}{t} - D_{DNG} \quad \text{(A-4)}$$

Integrating both sides of A-4 from t_1 to t we get:

$$\int_{t_1}^{t} \frac{\frac{dq(t)}{dt}}{q(t)} dt = \int_{t_1}^{t} (at^{-m} - \frac{m}{t} - D_{DNG}) dt \quad \text{(A-5)}$$

After integration and simplifying we get:

$$\ln\left[\frac{q(t)}{q_{t_1}}\right]=\left(\frac{t_1}{t}\right)^m \exp\left[\frac{a}{1-m}\left(t^{1-m}-t_1^{1-m}\right)-D_{DNG}(t-t_1)\right] \quad \text{(A-6)}$$

Taking the exponential on both sides and solving for $q(t)$ we get:

$$q(t)=q_{t_1}\left(\frac{t_1}{t}\right)^m \exp\left[\frac{a}{1-m}\left(t^{1-m}-t_1^{1-m}\right)-D_{DNG}(t-t_1)\right] \quad \text{(A-7)}$$

In this derivation q_{t1} is the rate to be estimated at t_1.

And the b-parameter of the modified Duong model is given by:

$$b(t)=\frac{mt^m(-at+t^m)}{(at-t^m(m+D_{DNG}t))^2} \quad \text{(A-8)}$$

Direct integration of the time-rate relations (A-7) to obtain the corresponding cumulative production relation is not possible. As a result, cumulative production needs to be calculated using numerical methods.

In this work we have demonstrated that the modified Duong model (MDNG-1) is capable of modeling the transient, transition and boundary-dominated flow regimes.

APPENDIX B

MODIFIED DUONG MODEL — 2 (MDNG – 2)

Duong model (Duong 2011) was derived based on characteristics observed when production data from unconventional resources is plotted on a log-log plot of q/G_p versus time. Duong model consider only the straight line observed on this plot. However extended flow periods show boundary characteristics that deviate from the straight line behavior. The new Duong model uses the same diagnostic plot, but the q/G_p relation is modified to accommodate boundary characteristics as well. The modified relation is given by:

$$\frac{q}{G_p} = at^{-m}\exp[-d_{dng}t] \quad \text{..... (B-1)}$$

Where the boundary characteristics is given by the constant decline parameter, d_{dng}.

Based on the new q/G_p relation, we can calculate the associated rate and cumulative relations. The derivation follows similar steps shown by (Duong 2011).

Re-writing A-1 we get:

$$G_p = \frac{q}{\varepsilon(t)} \quad \text{..... (B-2)}$$

Where $\varepsilon(t) = at^{-m}\exp[-d_{dng}t]$

Taking derivative with respect to time, we get:

$$\frac{d}{dt}G_p = \frac{d}{dt}\left[\frac{q}{\varepsilon(t)}\right] \quad \text{..... (B-3)}$$

Noting that $\frac{d}{dt}G_p(t) = q(t)$ and taking the derivative we get:

$$\frac{dq(t)}{dt}\frac{1}{\varepsilon(t)} - q(t)\frac{d\varepsilon(t)}{dt}\frac{1}{\varepsilon^2(t)} = q(t) \quad \text{..... (B-4)}$$

or

$$\frac{dq(t)}{q(t)} = \frac{d\varepsilon(t)}{\varepsilon(t)} + \varepsilon(t)d(t) \quad \text{(B-5)}$$

Integrating both sides of A-5 from $t = t_1$ to t, we get:

$$\ln\left[\frac{q}{q_{t_q}}\right] = \ln\left[\frac{\varepsilon(t)}{\varepsilon(t_1)}\right] + \int_{t_1}^{t} \varepsilon(t)dt \quad \text{(B-6)}$$

After taking the exponential on both sides:

$$\frac{q}{q_{t_q}} = \frac{\varepsilon(t)}{\varepsilon(t_1)} \exp\left[\int_{t_1}^{t} \varepsilon(t)dt\right] \quad \text{(B-7)}$$

Here, q_{t1} is the rate at $t=t_1$.

In the modified form $\varepsilon(t)$ is given by:

$$\varepsilon(t) = at^{-m} \exp[-d_{dng}t] \quad \text{(B-8)}$$

After taking the integral and simplifying the time-rate relation is given by:

$$q_g(t) = \frac{q_{t_1}}{t^m} t_1^{\,m} \exp\left[D_{DNG}(t_1 - t) + aD_{DNG}^{\,m-1}\left(\Gamma[1-m, D_{DNG}t_1] - \Gamma[1-m, D_{DNG}t]\right)\right] \quad \text{(B-9)}$$

A numerical solution of Eq. B.7 and analytical solution of Eq. B-9 are computed to check the consistency of the analytical solution. **Fig. B.1** shows results of the numerical and analytical solution of the rate relation. Fig. B.1 shows that the analytical solution indicated by Eq. B.9 provides accurate solution.

And the modified Duong cumulative relation is given by:

$$G_p(t) = \frac{q_{t_1}}{a} t_1^{\,m} \exp\left[D_{DNG}t_1 + aD_{DNG}^{\,m-1}\left(\Gamma[1-m, D_{DNG}t_1] - \Gamma[1-m, D_{DNG}t]\right) - \exp[D_{DNG}t_1]\right] \quad \text{(B-10)}$$

The corresponding *D*- and *b*- parameters are given by:

$$D(t) = D_{DNG} + \frac{m}{t} - a\exp[-D_{DNG}t]t^{-m} \quad \text{(B-11)}$$

$$b(t) = \frac{\exp[D_{DNG}t]t^m[\exp[D_{DNG}t]mt^m - at(m + D_{DNG}t)]}{[at - \exp[D_{DNG}t]t^m(m + D_{DNG}t)]^2} \quad \text{..... (B-12)}$$

And the β - parameter is given by:

$$\beta(t) = D_{DNG}t + m - a\exp[-D_{DNG}t]t^{-m+1} \quad \text{..... (B-13)}$$

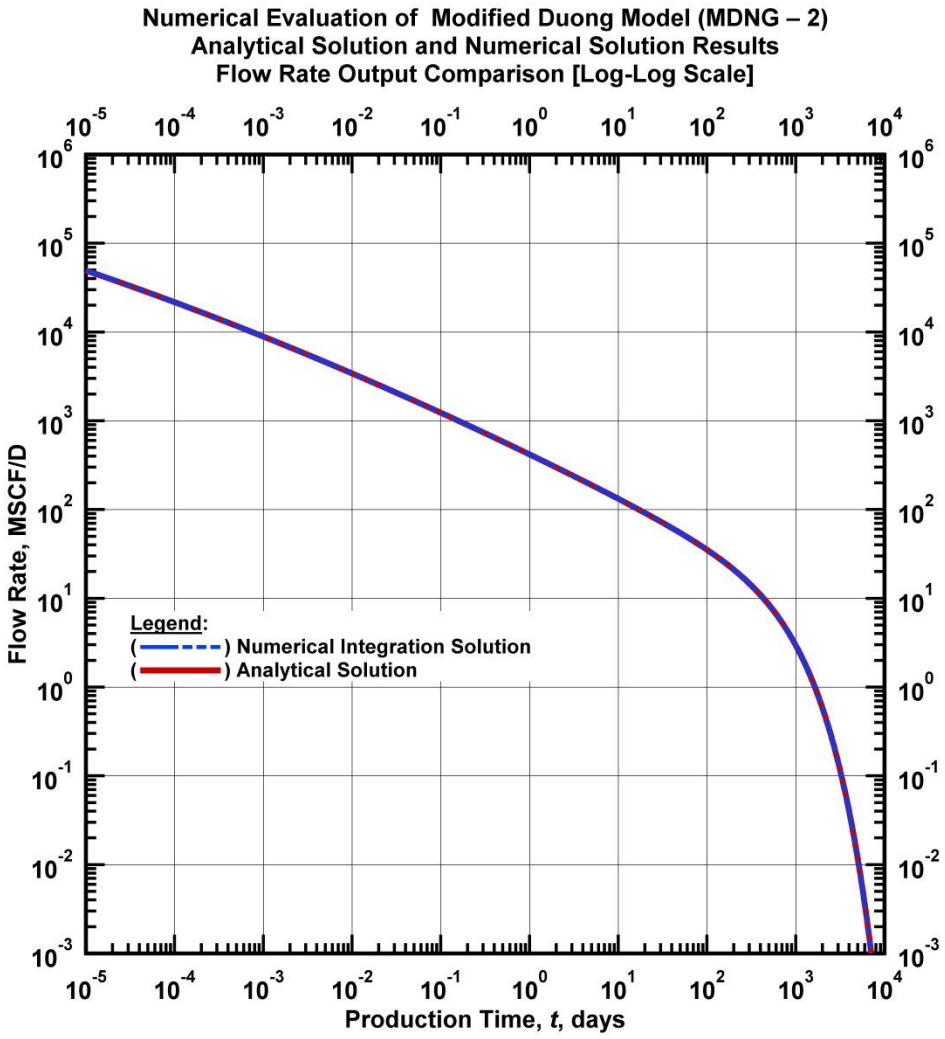

Figure B.1 – (Log-Log Plot): Analytical solution and numerical solution of modified Duong model (MDNG – 2) time-rate relation.

APPENDIX C

MODIFIED LOGISTIC GROWTH MODEL — 3 (MLGM – 1)

The exponential decline behavior that is observed during boundary dominated flow regimes of gas wells from unconventional reservoirs is not fully modeled in logistic growth model. The exponential decline trend observed during boundary dominated flow regimes from production data of gas wells in unconventional reservoirs can be modeled more accurately by applying a constant decline parameter to the *D*-parameter derivation of the logistic growth model. This approach is similar to the method used to derive the power-law exponential (PLE) model The *D*- parameter of the logistic growth model is given by:

$$D(t) = \frac{\hat{a} - \hat{a}\hat{n} + (1+\hat{n})t^{\hat{n}}}{t(\hat{a} + t^{\hat{n}})} \quad \text{..... (C-1)}$$

Applying the constant decline parameter, D_{LGM} we get:

$$D(t) = \frac{\hat{a} - \hat{a}\hat{n} + (1+\hat{n})t^{\hat{n}}}{t(\hat{a} + t^{\hat{n}})} + D_{LGM} \quad \text{..... (C-2)}$$

The time-rate relation can be derived from the modified *D*-parameter relation. The time-rate relation is given by:

$$q_g(t) = \frac{\hat{a}K\hat{n}t^{(\hat{n}-1)}}{(\hat{a} + t^{\hat{n}})^2}\exp[-D_{LGM}t] \quad \text{..... (C-3)}$$

And the *b*-parameter of the modified logistic growth model (MLGM – 1) is given by:

$$b(t) = \frac{-\hat{a}^2(\hat{n}-1) - 2\hat{a}(\hat{n}^2-1)t^{\hat{n}} + (\hat{n}+1)t^{2\hat{n}}}{(\hat{a}(1-\hat{n}+D_{LGM}t) + t^{\hat{n}}(1+\hat{n}+D_{LGM}t))^2} \quad \text{..... (C-4)}$$

It is not possible to integrate the rate relation to obtain the rate form. Numerical methods are necessary to determine cumulative production.

The modified logistic growth model (MLGM-1) can model transient, transition and boundary dominated flow regimes. When using this model care should be taken not to use the decline parameter (D_{LGM}) during transition regions. The logistic growth model has hyperbolic characteristics which can model transition regions very well. The exponential decline parameter should be used only when boundary-dominated flow regimes are observed.

APPENDIX D

MODIFIED LOGISTIC GROWTH MODEL – 4 (MLGM – 2)

The logistic growth model describes the maximum cumulative production that can be obtained if production was to continue to a very long period of time. The carrying capacity (*K*) parameter of the model can hence, describe the initial gas in place (Clark et al. 2011). The cumulative form of the logistic growth model is given by:

$$Q_g(t) = \frac{Kt^{\hat{n}}}{\hat{a} + t^{\hat{n}}} \quad \text{..... (D-1)}$$

The cumulative relation (D-1) can be re-formulated to describe the ratio of the gas in place remaining in the reservoir at a given time. This relation is given as follows:

$$\frac{K}{Q_g(t)} - 1 = \hat{a}t^{-\hat{n}} \quad \text{..... (D-2)}$$

The relation shown in D-2 indicates that the percentage decline of the gas in place to cumulative production ratio (*K/Q*(t)) can be described by a power-law relation when the data is plotted on a lo-log plot. However, long term characteristics of production data from unconventional gas resources indicate that during boundary conditions the plot behavior deviates from the straight line characteristics. This behavior can be described by an exponential relation. Furthermore, it is observed that because of production constraints and completion methods employed, it is not possible to withdraw the gas in place completely. If we describe percentage of the remaining gas in place at infinite time by *R*, relation D-2 can be re-formulated by taking in to account the boundary regime exponential decline behavior and the constant remaining reserve at infinite time as follows:

$$\frac{K}{Q_g(t)} - 1 = \hat{a}t^{-\hat{n}} \exp[-D_{LGM}t] + R \quad \text{..... (D-3)}$$

Relation D-3 can be re-formulated to describe the cumulative production relation as follows:

$$Q_g(t) = \frac{Kt^{\hat{n}} \exp[D_{LGM}t]}{\hat{a} + (1+R)\exp[D_{LGM}t]t^{\hat{n}}} \quad \text{..... (D-4)}$$

The time-rate relation is obtained by taking the derivative of the cumulative production relation with respect to time. The time-rate relation is given by:

$$q_g(t) = \frac{\hat{a}\exp[D_{LGM}t]Kt^{\hat{n}-1}(\hat{n}+D_{LGM}t)}{\left(\hat{a}+(1+R)\exp[D_{LGM}t]t^{\hat{n}}\right)^2} \quad \text{(D-4)}$$

The *D*- and *b*-parameters of MLGM-2 are given by Eqs. D-5 and D-6 respectively.

If ψ is defined by:

$$\psi(t) = \frac{\hat{a}+(\hat{n}+D_{LGM})^2}{\hat{a}+\exp[D_{LGM}t](1+R)t^{\hat{n}}}$$

Then

$$D(t) = \frac{\hat{n}+(\hat{n}+D_{LGM}t)^2-2\psi}{t(\hat{n}+D_{LGM}t)} \quad \text{(D-5)}$$

$$b(t) = \frac{2\psi^2-\psi(2(\hat{n}+(\hat{n}+D_{LGM}t)^2))+\hat{n}(\hat{n}+(\hat{n}+D_{LGM}t)^2+2D_{LGM}t)}{(\hat{n}+(\hat{n}+D_{LGM}t)^2-2\psi)^2} \quad \text{(D-6)}$$

This approach assumes that there is a prior estimate of the initial gas in place (*K*). If initial estimate is not available, the straight line fit for Eq. D-3 on a log-log, can be used to obtain the *K* parameter for production data matching purposes.

APPENDIX E

SEMI-LOG PLOTS – PARAMETRIC CORRELATION STUDY

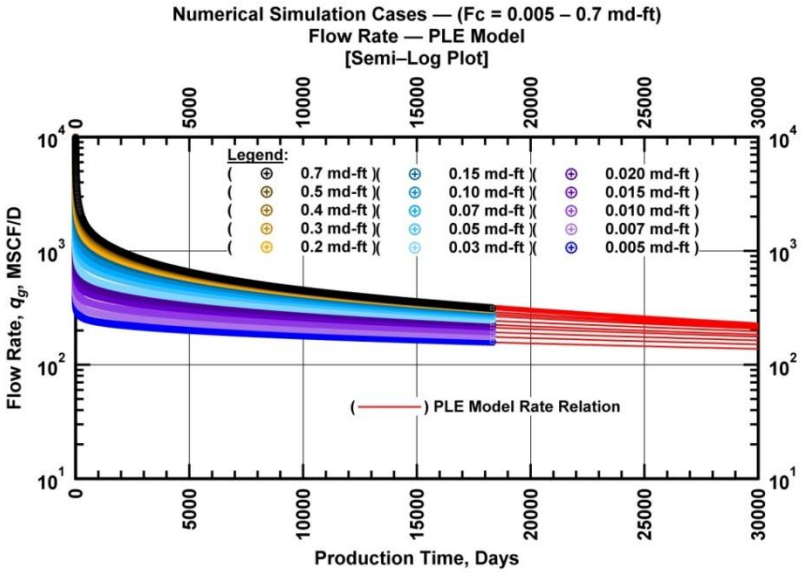

Figure E.1 — (Semi-log Plot): Flow rate (q_g) versus production time. PLE model match.

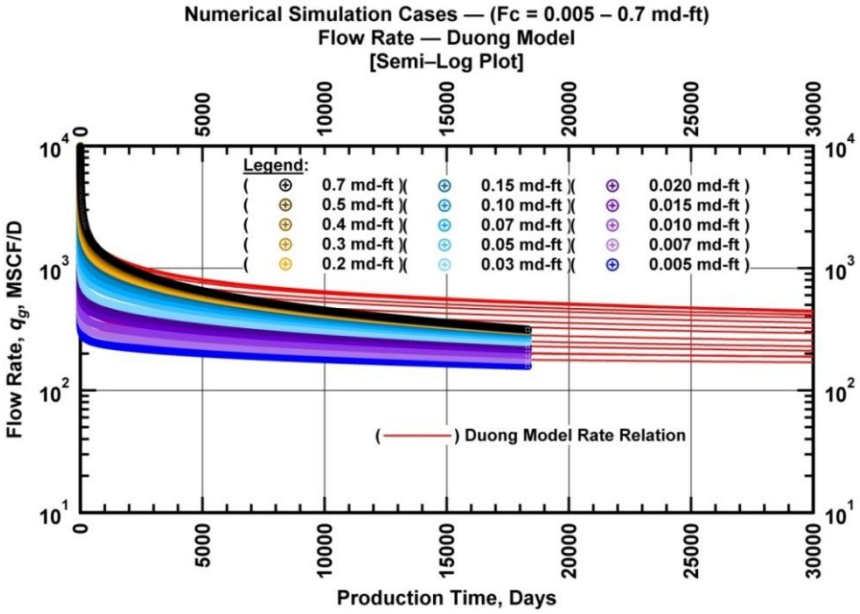

Figure E.2 — (Semi-log Plot): Flow rate (q_g) versus production time. Duong model match.

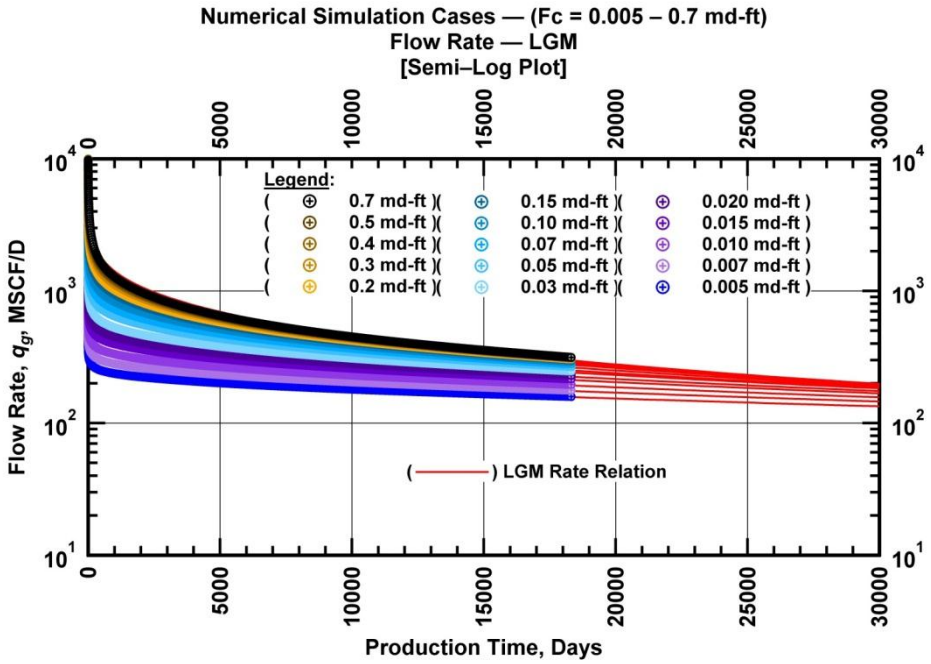

Figure E.3 — (Semi-log Plot): Flow rate (q_g) versus production time. Logistic growth model match.

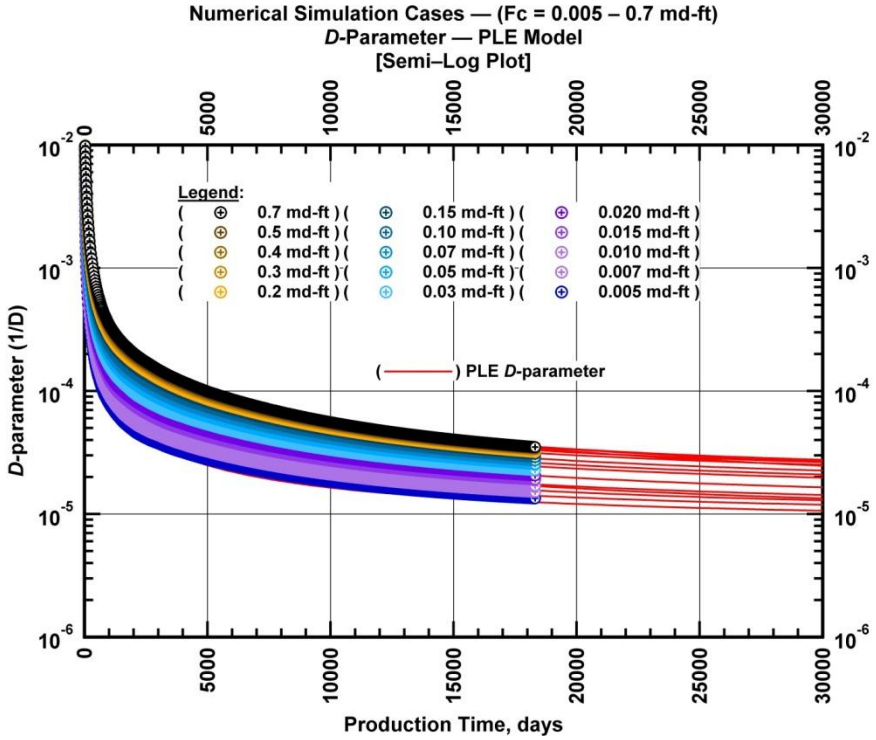

Figure E.4 — (Semi-log Plot): *D*-parameter versus production time. PLE model match.

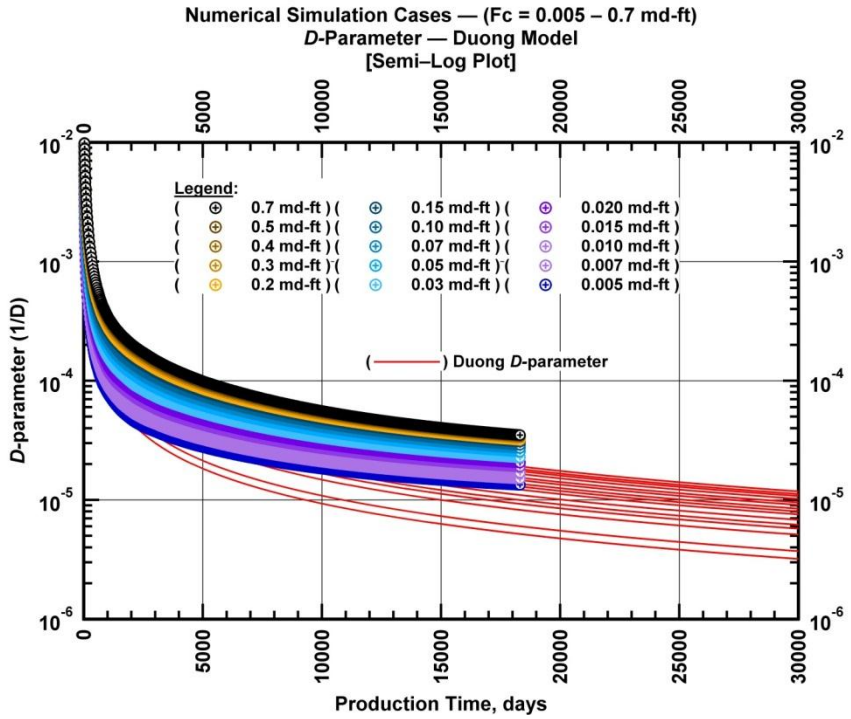

Figure E.5 — (Semi-log Plot): *D*-parameter versus production time. Duong model match.

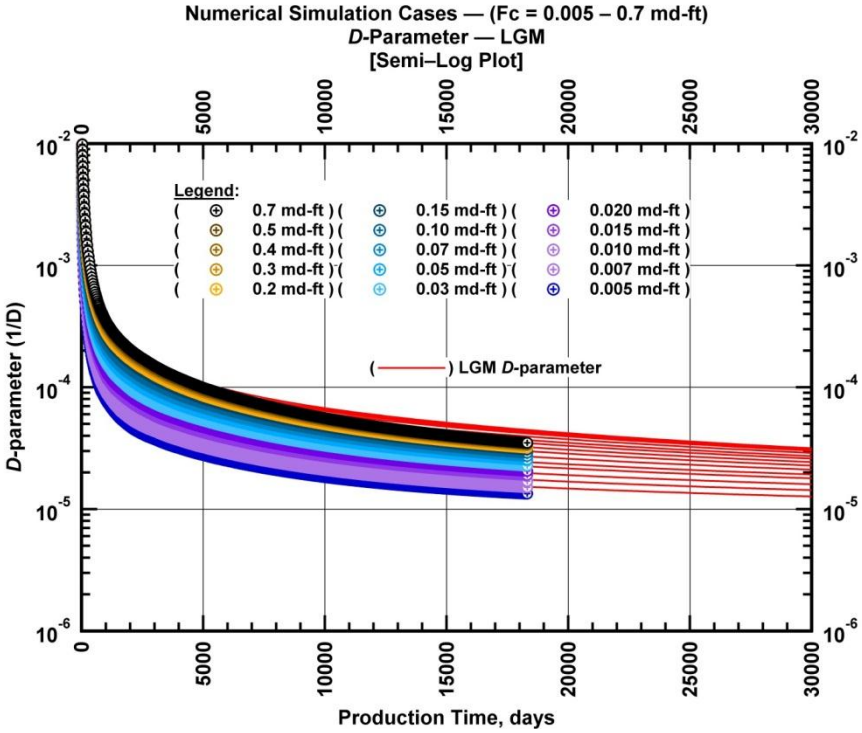

Figure E.6 — (Semi-log Plot): *D*-parameter versus production time. Logistic growth model match.

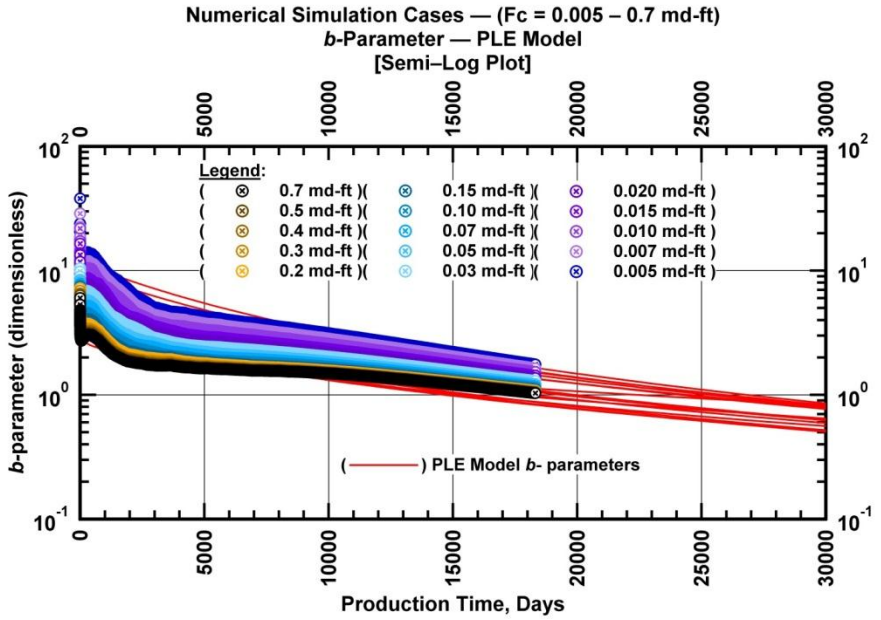

Figure E.7 — (Semi-log Plot): *b*-parameter versus production time. PLE model match.

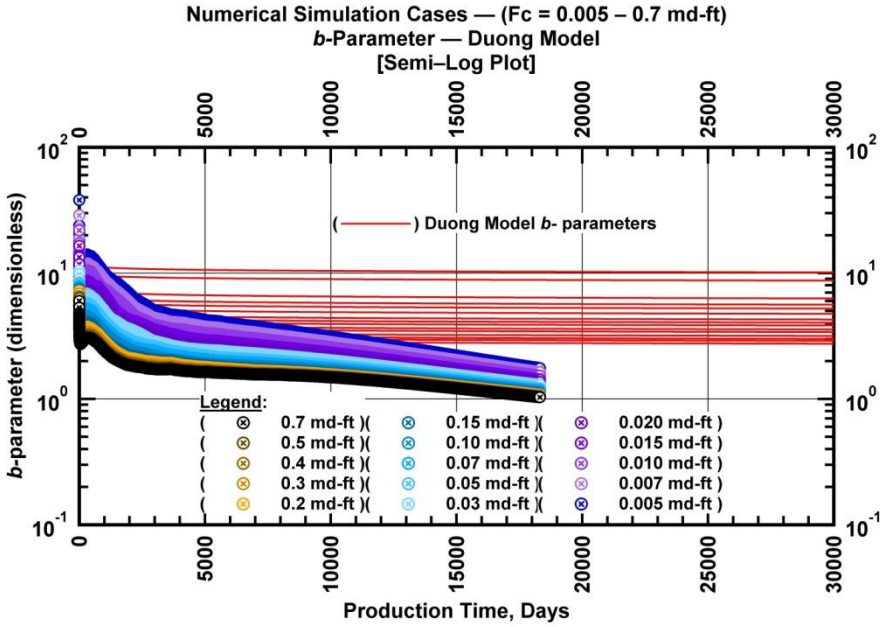

Figure E.8 — (Semi-log Plot): *b*-parameter versus production time. Duong model match.

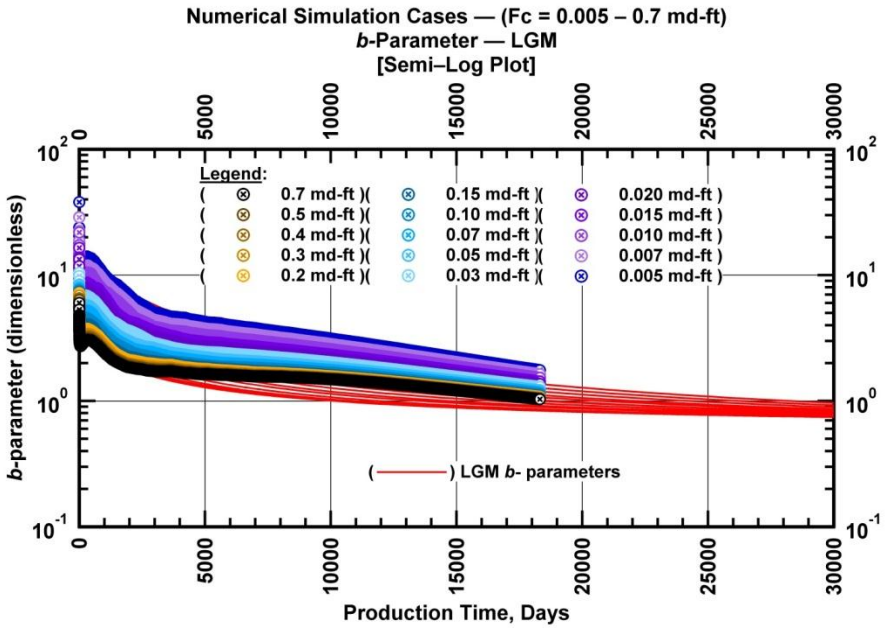

Figure E.9 — (Semi-log Plot): *b*-parameter versus production time. Logistic growth model match.

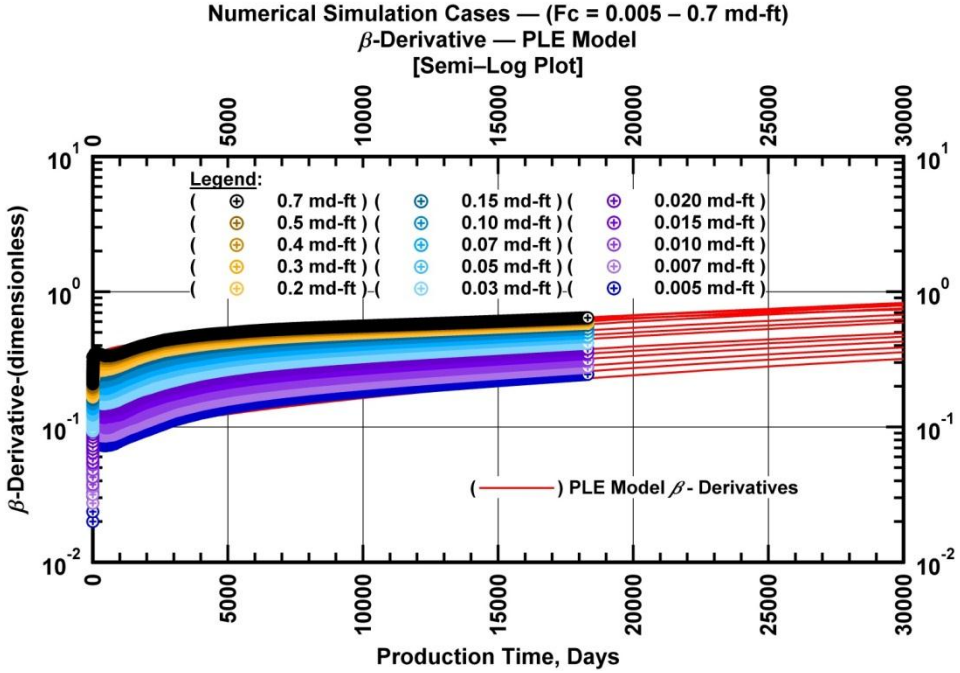

Figure E.10 — (Semi-log Plot): β-parameter versus production time. PLE model match.

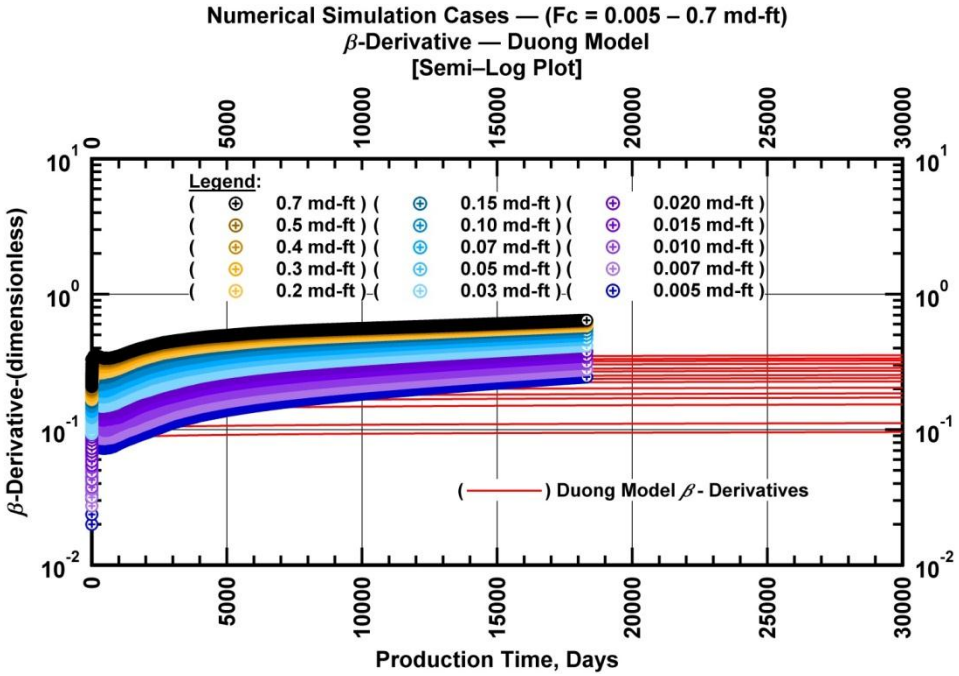

Figure E.11 ─ (Semi-log Plot): β-parameter versus production time. PLE model match.

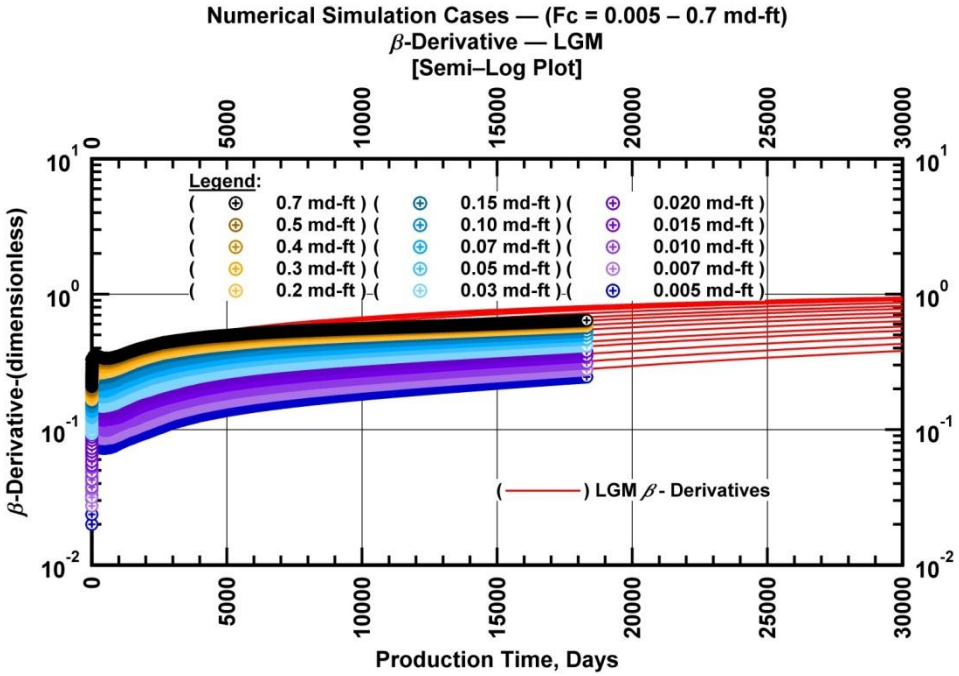

Figure E.12 ─ (Semi-log Plot): β-parameter versus production time. Logistic growth model match.